January 2013

A Wearable Motion Analysis System to Evaluate Gait Deviations

Amanda Lynn Martori
University of South Florida, martori@mail.usf.edu

A Wearable Motion Analysis System to Evaluate Gait Deviations

by

Amanda Lynn Martori

A thesis submitted in partial fulfillment
of the requirements for the degree of
Master of Science in Mechanical Engineering
Department of Mechanical Engineering
College of Engineering
University of South Florida

Major Professor: Stephanie L. Carey, Ph.D.
Rajiv Dubey, Ph.D.
Kevin Hufford, M.S.

Date of Approval:
July 3, 2013

Keywords: IMU, APDM, Sensors, Knee Angle, Quaternion

DEDICATION

I would like to dedicate this thesis to my parents, Sam and Debbie, my brother Scotty and my cousin Debra Marrano-Lucas.

ACKNOWLEDGMENTS

I would like to thank my advisor Stephanie Carey, as well as my committee members Rajiv Dubey and Kevin Hufford for their support and guidance. I would also like to thank all the members of the Rehabilitation Robotics and Prosthetics Testbed (RRT) for their participation in the study, as well as their help with many aspects of this project.

I would also like to thank my family for their continuous encouragement and support throughout this whole process. Without their constant love I would not have been able to complete this thesis. Mom, Dad, Scotty and Debbie, you guys were a major part of this accomplishment.

TABLE OF CONTENTS

LIST OF TABLES

LIST OF FIGURES

ABSTRACT

A Wearable Motion Analysis System (WMAS) was developed to evaluate gait, particularly parameters that are indicative of mild traumatic brain injury. The WMAS consisted on six Opal IMUs attached on the sternum, waist, left and right thigh and left and right shank. Algorithms were developed to calculate the knee flexion angle, stride length and cadence parameters during slow, normal and fast gait speeds. The WMAS was validated for repeatability using a robotic arm and accuracy using the Vicon motion capture system, the gold standard for gait analysis. The WMAS calculated the gait parameters to within a clinically acceptable range and is a powerful tool for gait analysis and potential concussion diagnosis outside of a laboratory setting.

CHAPTER 1: INTRODUCTION

Current methods of measuring gait parameters involve expensive optical motion capture systems, time intensive setup, wires, complicated filtering techniques, and a laboratory setting. A wearable and wireless motion analysis system would allow gait analysis to be performed outside of a laboratory setting during activities of daily living, in a clinical setting or on a football field or battlefield. Mild traumatic brain injury (mTBI), or concussion, and traumatic brain injury (TBI) have become a major problem in both the sports and military as well as the general population from car accidents and other traumatic events. There is a major need for a quick and accurate method to diagnose mTBI and TBI, and other gait deviations outside of a laboratory setting.

A review paper by Bergmann and McGregor investigated both clinicians and users' preferences about wearable sensors. Both clinicians and users stated that wearable sensors must be "compact (light and small), available alongside the work of health professionals, and simple to operate and maintain. User's also wanted wearable sensors that were "low-invasive and that did not affect normal daily behavior," while clinicians wanted sensors that "have real-time data function, minimal time to familiarize with the device, follow/monitor a patient's progress, low cost, simple interface, long battery life, large storage capacity and are not restricted to one location or room." [1] These preferences were considered in both the selection of a sensor and the development of the wearable motion analysis system (WMAS).

The Opal sensor by APDM (APDM Inc., Portland OR) is an inertial measurement unit (IMU) that consists of a tri-axial accelerometer, tri-axial gyroscope and tri-axial magnetometer. Each Opal sensor is about the size of a wristwatch and weighs less than 22 grams. One major benefit of the Opal sensor is it can collect data for an entire day (up to 16 hours) on one charge and store up to 28 days worth of data [2]. Therefore the Opal sensor is small and compact, has a long battery life and large storage capacity, and thus can be used outside of a motion analysis laboratory setting and during a person's activities of daily living. Wireless streaming, and visualization of real-time data is also possible with the Opal sensor. Since the Opal sensor meets both the user and clinician's preferences, it was selected as the wearable sensor for the WMAS.

The goal of this project was to continue to develop and validate a wearable motion analysis system (WMAS) that can provide clinically relevant information for researchers, physical therapists and physicians. The parameters stride length, cadence and knee flexion were collected. The WMAS knee flexion angles must have less than 5 degrees of error relative to the Vicon system. The stride length calculations also need to be improved from Simoes [3]. As a result, the WMAS could be used to detect gait deviations, particularly indicators of mild traumatic brain injury (mTBI); provide instant feedback on a person's gait; and as an evaluation tool for rehabilitation plans and outcomes.

Data were collected from ten healthy subjects. The WMAS consisted of six Opal IMU sensors located on the sternum, waist, right and left thigh and right and left shank. There was also simultaneous data collection with the Vicon motion analysis system using the Plug in Gait marker set [4]. The subjects performed a timed up and go test (TUG): sit in a chair, stand up, walk to the end, turn around, walk back to the chair and sit down. Each subject performed

fifteen trials: five at a normal (comfortable) speed, five at a very slow speed, and five at a fast speed.

The WMAS data from the Opal sensors were processed and analyzed in MATLAB, while the Vicon data were processed in Visual 3D. The parameters that were analyzed were stride length, cadence and knee flexion. The WMAS data was compared to the Vicon data in order to validate the WMAS. Root mean square error (RMSE), Pearson's R correlation and Bland Altman plots were used to compare the WMAS to the Vicon system.

CHAPTER 2: BACKGROUND

2.1 Gait

Gait is a cyclic, repetitive motion. There are many parameters that can affect a person's gait from a disease to their footwear. A gait cycle is the movement of one limb from heel-strike of one foot to successive heel strike of the same foot. The gait cycle is divided into two phases: stance and swing. The stance phase occurs when the foot is touching the ground and begins at heel-strike, while the swing phase begins at toe-off and occurs when the foot is moving forward not touching the ground. Double support is also part of the gait cycle and occurs when both feet are in contact with the ground [5]. Step length and stride length are gait parameters that are often confused or used interchangeable but are two different measurements. Step length is the distance between heel-strike of the one foot to the heel-strike of the opposite foot. Whereas stride length is the distance between heel-strikes of the same foot [5]. Cadence is another gait parameter that is the measure of the number of steps per minute. During gait analysis, kinematic parameters such as stride length; cadence and joint angles are calculated.

2.2 Traumatic Brain Injury

A traumatic brain injury (TBI) can occur from a battlefield trauma, fall, car accident, or other illnesses, and is one of the leading causes of disability [6, 7]. The Center for Disease Control (CDC) defines a traumatic brain injury (TBI) as:

> *"A TBI is caused by a bump, blow or jolt to the head or a penetrating injury that disrupts the function of the brain. The severity of a TBI may range from 'mild' (a brief change in mental status or consciousness) to 'severe' (an extended period of consciousness or amnesia after the injury)."* [8]

TBI can result in behavioral, cognitive and physical disabilities. A mild traumatic brain injury can also occur and may go undiagnosed [9].

2.2.1 Mild Traumatic Brain Injury

Mild traumatic brain injuries (mTBI), also known as concussions, are a major focus in both the military and sports communities. Similar to TBI, mTBI can result in behavioral, cognitive and physical disabilities. Furthermore, mTBI can affect a person's ability to walk or gait, as well as their activities of daily living [9].

2.2.2 Prevalence and Statistics of TBI and mTBI

According to the CDC, every year approximately 1.7 million people are diagnosed with TBI, of which 75% are classified as mild [10]. Sports-related brain injuries are also especially prevalent accounting for at least 1.6 million concussions annually [11]. In addition to having a major impact on the civilian population, TBI and mTBI are among the most common injuries to members of the military. The Department of Defense (DoD) reported that from 2000-2012 service members have sustained approximately 266,810 TBI, of which 82.4% were classified as mTBI. Last year alone, the DoD diagnosed 29,668 service members with TBI, of which 85.5% were classified as mTBI [12].

In order to address the growing number of mTBI, the National Football League (NFL) provided $30 million in funding for traumatic brain injury research to the National Institutes of Health [13]. Similarly, the Department of Defense and Veterans Affairs provided $100 million

to research new methods to identify and evaluate mTBI [14]. The military and NFL have also partnered together to combat mTBI in their players and soldiers [15]. Dr. Jonathan Woodson depicts the importance of mTBI research,

> *"PTSD and mTBI are two of the most-prevalent injuries suffered by our war fighters in Iraq and Afghanistan, and identifying better treatments for those impacted is critical."* -Dr. Jonathan Woodson, Assistant Secretary of Defense for Health Affairs [14]

2.2.3 Effect on Gait and Balance

Many researchers have shown there are several parameters that often occur during the gait of a person with TBI and mTBI when compared to a healthy individual. The most common abnormalities are reduced stride length and cadence [7, 9, 16-20] and slower gait speed [9, 16-19, 21-23]. Other gait parameters that affected by TBI include: wider base of support [16], stiff-legged gait [24-26] and increased double support time [19, 27]. TBI also has a significant effect on the trunk, pelvis and lower limbs [16, 28]. The center of mass (COM), hip, knee and ankle are the most affected parts of the body and these abnormalities are summarized in Figure 1.

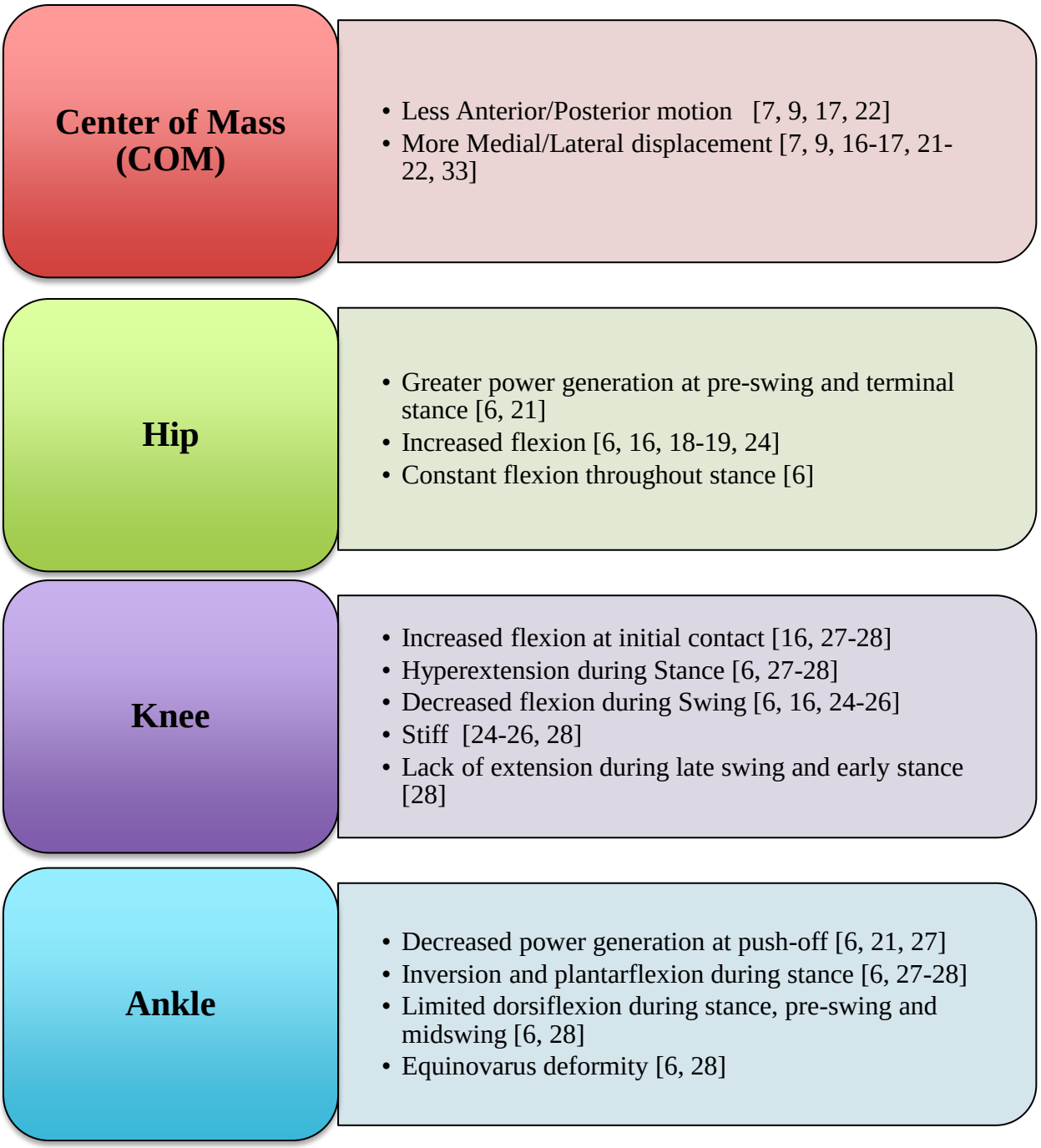

Figure 1 Abnormalities That Occur During the Gait of a Person with a TBI

The vestibular system, which is responsible for balance control, head movement and maintaining posture, can also be affected by TBI. Imbalance, dizziness, and vertigo can all be consequences of TBI [9, 22, 25, 29-33]. It has also been shown that at high head rotation speeds the vestibular-ocular reflex (VOR), used to stabilize gaze, does not work properly, causing issues with gait and balance in a person with TBI [3, 34].

2.2.4 Current Diagnostics

Several methods are used to diagnose and determine the severity of a TBI. The Glasgow Coma Scale (GCS) is one of the common diagnostic tests used to determine the severity of TBI and is particularly useful for determining the presence of a severe brain injury. The scale ranges from 3-15, where the low end of the scale represents a severe brain injury and 14-15 a mild brain injury. The GCS involves a combination of motor, eye and verbal tests to determine a person's consciousness [11]. The most common method for diagnosing sports-related mTBI is the Sports Concussion Assessment Tool (SCAT2), which involves motor and visual tests, a set of questions relating to memory or orientation, balance testing and a symptom checklist. However, the SCAT2 and other concussion tests are mostly subjective and rely on the evaluator (coach, trainer, etc.) to make the ultimate decision of whether to take the player or soldier off the field. The results are also often dependent on honest responses by the injured person, who is likely to represent their symptoms as better than they are in order to return to action [11]. Currently there is not a standardized test or method that is used universally to identify mTBI, especially in the field. There is a significant need for an accurate, simple, fast and objective method to identify and diagnose mTBI [11].

Current technology, such as the Vicon motion analysis system, used to evaluate gait parameters that are indicative of TBI is expensive, limited to a laboratory setting and time-consuming [9]. Previous work by Simoes analyzed parameters that are present during TBI including cadence, stride length, torso and head rotation using two systems: an industry standard optical tracking system and a wearable motion analysis system containing five inertial measurement units (IMUs) (APDM, Portland, OR). Correlations for cadence, head rate of rotation and torso rate of rotation were high between both systems [35].

2.2.5 What's Missing in TBI Research/Diagnosis?

TBI and mTBI research is lacking a quick, accurate and easy diagnostic test that can be performed outside of a laboratory setting. According to Dziemianowicz et al,

> *"While each test can be helpful in diagnosis or management, a single test that can reliably detect the presence of a concussion or complete recovery from a concussion has not been developed…There still is a need for further research into a quick and reliable test validated by scientific investigation."* [11]

There is a need for a test that can evaluate a TBI outside of a laboratory setting because someone may walk well in a confined environment where their only focus is on the task of walking, but when other factors are added such as a curb, lots of people around or other distractions the issues may arise [36].

2.3 Gait Analysis Methods

Gait analysis is the study of how a person walks. It can be as simple as how fast they walk or as complicated kinematic and kinetic parameters. There are two main methods of gait analysis: optical systems and inertial measurement units. Another method for gait analysis include the GAITRite mat, which uses pressure sensors in the walkway to determine gait parameters [37].

2.3.1 Optical System

The gold standard for gait analysis is optical motion capture systems. Optical motion capture systems use infrared cameras to track the motion of passive reflective or active light emitting markers in 3D space. While optical motion capture systems have high accuracy, they are very expensive and must be confined to a small laboratory setting.

2.3.2 Inertial Measurement Unit

In order to address the problems with optical motion capture systems for gait analysis, inertial measurement units (IMUs) have recently been a popular alternative for gait analysis. Gait parameters such as stride length, cadence, center of mass movement, range of motion, joint angles, and gait speed to name a few have been investigated [38-41].

An IMU typically consists of two sensors: an accelerometer, and a gyroscope. The accelerometer is used to measure acceleration or how fast something moves and the gyroscope is used to measure angular velocity rate of rotation. IMUs can also contain a magnetometer. The magnetometer is used to measure the orientation relative to the earth's magnetic field. These three components are combined to track the motion of an object [41, 42].

2.3.2.1 Previous Work

Many studies have used inertial measurement units (IMUs) or other sensors to measure knee, hip or ankle flexion angle, as well as other gait parameters such as stride length, gait speed, stance time, etc.

Guo et al. used two sets of IMUs on the thigh, shank and foot to calculate knee and foot flexion and differentiate between hemiplegia and healthy subjects. The subjects walked for five meters at their own comfortable pace and were recorded by a video camera. The angles were calculated using quaternions and a Kalman filter. The knee flexion angle was calculated using

the inverse of the quaternion from the shank sensor multiplied by the quaternion from the thigh sensor. While the results between the sets were accurate relative to a video camera based analysis, the data were not validated by an optical motion capture system [43].

Another study by Toffola et al. involved a wearable knee sleeve with an electrogoniometer and accelerometer to monitor knee flexion. This study involved one subject walking on a treadmill and compared the data from the sleeve to a Vicon system with a RMSE of 2.1 degrees [44].

Schiefer et al. used accelerometers and gyroscopes to calculate knee flexion during several activities of daily living, however not during gait, and compared the data to an optical camera system with a RMSE between 4.6 and 7.1 degrees [45].

Watanabe et al. used an IMU based system to calculate stride length and knee angles during treadmill and walking for several meters. This study used 7 IMUs with accelerometer and gyroscope components. Knee angles were calculated from the integration of the angular velocity from the thigh and shank gyroscopes. A Kalman filter was also applied to the data. An IMU on the foot was used to calculate the stride length using the accelerometer. An optical motion capture system was used to assess the accuracy of the data calculated from the IMUs. The data were reported with and without the Kalman filter. The average RMSE for the knee angle calculations was between 4 and 5 degrees. However, the average RMSE for the knee angle without the Kalman filter was 7 degrees and between 8 and 14 degrees for the several meter walking and treadmill walking respectively. The stride length calculations from the IMU on the foot were within 7% error relative to the optical system for slow walking, 8% error for normal walking and 5% error for fast walking [46].

Cloete and Scheffer evaluated the Xsens Moven full body inertial suit, which consisted of 16 IMUs. The IMUs have wires but communicate with a laptop via a wireless connection. The accuracy of the suit was validated using the Vicon motion capture system. The eight subjects walked and ran at several different speeds. The Xsens software, similar to the APDM software, exports a quaternion for each of the sensors. Knee angles were calculated by multiplying the quaternion from the shank by the complex conjugate of the quaternion from the thigh and then the resulting quaternion was converted to an Euler angle. Pearson's R correlations were 0.9 between the Xsens and Vicon systems for the knee flexion angle at normal speed. Even though the R correlation was high, the RMSE was 9.58 degrees for the right knee and 13.47 degrees for the left knee. The knee angles were also filtered and the bias was removed which resulted in knee flexion angle RMSE of 7.61 and 9.53 degrees for the right and left knees. The authors suggested that high RMSE may have been caused by movement of the suit during testing [47].

Another study by Pochappan et al. used 5 IMUs called Orient Specks, which contain accelerometers, gyroscopes and magnetometers. The IMUs were placed on the feet, shanks, thighs and the lower back. Knee flexions were calculated using a Latent Space Algorithm and the accelerometer data was used to identify gait events. The testing involved several trials in which the subjects walked 30 meters, however the analysis only looked at a few trials in which only one gait cycle was analyzed per trial. The data from the IMUs were compared to a Vicon system. The RMSE for the knee flexion angle was 9.12 degrees with a R correlation of 0.86. The error between the Vicon and IMU system for stride length was 0.17 meters. The authors suggested that the force plates on the floor may have interfered with the magnetometer signals and resulted in errors in the calculations [48].

Chen et al. used TEMPO inertial sensors, which contain an accelerometer and gyroscope component, to calculate the knee angle during treadmill walking. The tilt angle of the thigh and shank was calculated from the acceleration data. The angular velocity was integrated to calculate the knee angle during walking. Several different calibration methods and high pass filtering were used to remove error and drift. During slow, medium and fast walking on the treadmill the RMSE for the knee angle with the linear calibration method were 2.75, 3.03 and 3.15 degrees. The RMSE with the piecewise calibration method were 3.59, 3.88 and 4.01 degrees for the slow, medium and fast speeds [49].

Kun et al. and Lui et al. used a physical sensor and virtual sensor difference method in which the shank rotational acceleration was subtracted from the thigh rotational acceleration. This method did not involve integration of the accelerometer or gyroscope signals [50, 51]. The average RMSE reported by Kun et al. was 2.52 degrees [50]. Liu et al. reported an average RMSE of 3.07 degrees for the knee flexion angle during walking trials [51]. However, both of these studies used wired systems [50, 51].

Favre et al. conducted several studies that investigated the calibration, alignment and calculation of knee angles using IMUs [52-55]. The IMUs contained accelerometer and gyroscope components. The method used quaternions to calculate the knee angle and combined both the integration of the angular velocity from the gyroscope and the acceleration data from the accelerometer [53]. Several alignment procedures were also used to calibrate the IMUs and drift was filtered out [54]. The knee angle from the IMUs was compared to a magnetic tracking system during level walking with a RMSE less than 2 degrees and a high R correlation near 1 [52].

Dejnabadi et al. used filtered gyroscope and accelerometer data to calculate knee angles during treadmill walking. The IMUs were attached to metal plates and attached to the shank and thigh. The knee angle calculated by the IMUs was compared to an ultrasound motion capture system. At slow, medium and fast speeds the RMSE was 1.1, 1.25 and 1.6 degrees [56].

Bergmann et al. used Xsens MTx IMUs to investigate the knee flexion angle while walking up and down stairs. This is a wired system that calculates the knee angle using the rotation matrices from the thigh and shank IMUs. The data from the Xsens system was compared to an active marker Codamotion system with a RMSE of 4 degrees and a standard deviation of 3 degrees [57].

Schulze et al. calculated the knee angle by integrating the filtered angular velocity from the gyroscope. The IMUs were placed on the outer thigh and inner shank during treadmill walking at three different speeds. The knee angle calculated from the IMUs was compared to a video camera based analysis method. This study involved only one subject. The RMSE was 2.6 degrees for slow speed, 1 degree for normal speed and 6.3 degrees for fast speed [58].

Cooper et al used wired IMUs and a treadmill to calculate knee flexion angle from gyroscope and accelerometer signals. The IMU data were compared to an optical motion capture system. The authors reported a low RMSE of between 0.7 degrees for the slow speed and 4.1 degrees for the fast speed [59].

Takeda et al. used accelerometers and gyroscopes to calculate the knee flexion angle during gait. The system contained a data logger connected via wires to the IMUs. The inclination angle of the thigh and shank were calculated by the accelerometer, which was combined with the integrated angular velocity to calculate the knee angle. The average RMSE reported was 6.79 degrees, while the correlation coefficient was 0.93 [60].

Saito et al. also used accelerometers and gyroscopes to calculate the knee flexion angle during treadmill and 4-meter walk tests. In addition to using the accelerometer to determine inclination and the integrated angular velocity from the gyroscope, a Kalman filter was used. The data from the IMUs were compared to an optical motion capture system. The RMSE for the 4-meter walk tests with the Kalman filter was 2.98 degrees and without the Kalman filter was 5 degrees. The RMSE with the Kalman filter for the treadmill walking was 4.19 degrees [61].

Miyazaki et al. used a simplified gait model and a single gyroscope on the thigh to calculate the stride length and velocity during walking. The angular velocity from the gyroscope was integrated to get the angle of the thigh. The angle of the thigh and leg length was used to calculate the stride length. The error for the stride length calculation was 15% [62].

Aminian et al. compared spatio-temporal parameters from footswitches and a gyroscope system. The footswitches were placed under the heel and toe in order to detect heel-strike and toe-off gait events. The angular velocity measured by the gyroscope on the shank was used to identify the heel-strike and toe-off events. Sharp negative peaks in the angular velocity signal were shown to represent the heel-strike and toe-off events. A double pendulum and inverted double pendulum gait model was used to calculate the spatio-temporal parameters from the gyroscope system. The RMSE for stride length was 0.07 meters or 7.2% for the footswitch and gyroscope gait model [38].

Salarian et al. also used gyroscopes to calculate gait parameters. The gyroscope on the shank was used to calculate the gait events and temporal parameters. A data logger was connected with wires to the gyroscopes. The angular velocity signal was integrated to calculate the angle of the shank segment and the signal was filtered. The gait events were detected

similar to Aminian et al. [38]. However, a different peak detection algorithm was used to identify the maximum or mid-swing peaks and used and interval of 1.5 seconds to identify the local minimum peaks or gait events. A double and inverse pendulum model were used to calculate stride length, similar to Aminian et al [38]. A timed up and go (TUG) test was used for the gait trials. The error for the stride length calculations between the reference system and gyroscope algorithm was 3.5 centimeters [39].

Doheny et al. also used a single gyroscope to calculate gait parameters relative to the GAITRite electronic walkway. The angular velocity and detection of gait events were similar to Salarian et al [39]. The stride length was calculated using a scale factor, the height of the subject and the range of the shank angle. Data were collected at slow, normal and fast speeds. Stride length had a RMSE of 0.09 meters and an R correlation of 0.84 relative to the GAITRite walkway [63].

Previous work by Simoes analyzed cadence, stride length, torso and head rotation between two systems: an industry standard optical tracking system and a wearable motion analysis system containing five IMUs (APDM, Portland, OR). The gait parameters were calculated using APDM's iTUG plug in which is based on work by Aminian et al. [38] and Salarian et al. [39]. Cadence, head rate of rotation and torso rate of rotation had high Pearson's R correlation values. The R correlation values for stride length were 0.776, 0.8 and 0.817 for normal, fast and slow speeds, with an overall correlation of 0.86 [3, 35].

Shanshan et al. used IMUs to calculate stride length and gait speed. The angular velocity of the shank from the gyroscope signal was integrated to determine the angle of the shank. The angular velocity was low pass filtered and a peak detection algorithm was used to detect the gait events. The range of rotation of the shank during the gait cycle was used to

calculate stride length by a compass gait model. A refined model was also used, which added the range of rotation of the thigh in addition to the range of rotation of the shank [64].

Zexi et al. used gyroscopes to calculate step length and distance travelled. The angular velocity was integrated to determine the angle of the leg. The law of cosines was then used to calculate the step length based on the angle of the leg and the leg length. The distance travelled was calculated using three methods, the waist gyroscope, the thigh gyroscope, and the gyroscope on the foot. The error was lowest using the gyroscope on the thigh to calculate the step length and distance travelled [65].

CHAPTER 3: METHODS

3.1 WMAS Testing

3.1.1 Institutional Review Board Approval

This research study "Feasibility of Wearable Sensors to Determine Gait Parameters" was approved by the University of South Florida (USF) Institutional Review Board (IRB) as an adult minimal risk research study #Pro00003205 (see Appendix D). The principal investigator of the study was Dr. Stephanie Carey, and the research staff included Amanda Martori and Matt Wernke. Before participating in the study, each participant was briefed about the following using the IRB informed consent form: the purpose of the study, procedures, benefits, risks, disclosures, privacy, how the information will be used, their rights and how to withdraw from the study. After the briefing and participant's questions were answered, the participant and the research staff member both signed the informed consent form.

3.1.2 Participants

Ten participants, eight men and two women (average age 27) were recruited to participate in the study. All of the participants were over the age of 18 and healthy, with no known pathologies that would affect their gait. The subject identification number, age, height and weight of each subject is listed in Table 1.

Table 1 Subject Information

Subject ID	Age	Height (m)	Weight (kg)
WMAS01	22	1.815	76
WMAS02	22	1.81	83
WMAS03	25	1.845	102
WMAS04	28	1.79	74.5
WMAS05	22	1.86	72.4
WMAS06	21	1.695	59.5
WMAS07	54	1.74	92.3
WMAS08	24	1.83	85.2
WMAS09	25	1.63	76
WMAS10	22	1.89	95

3.1.3 WMAS Instrumentation

The Wearable Motion Analysis System (WMAS) was composed of six Opal inertial measurement units (APDM Inc., Portland, OR). Each wearable Opal IMU sensor includes a triaxial accelerometer, a triaxial gyroscope and a triaxial magnetometer. The Opal sensors also include precision temperature calibration and a docking station. Each sensor is about the size of a wristwatch and weighs 22 grams, has a battery life of 16 hours, wireless connectivity, latency recovery and 16 GB of on-board storage. The APDM system can utilize up to eight sensors transmitting data to a computer or the sensors can record data directly onboard. The real-time data can then be viewed once a wireless connection is detected and the on board data can be accessed once the sensors are connected to the docking station. In this study, the sensors transmitted real time data to a laptop via a wireless access point. Motion Studio software (APDM Inc., Portland, OR) was used to view the IMU data in real-time and save the data as comma separated value files (CSV).

The APDM instrumentation includes a Macbook Pro laptop, Motion Studio software, docking station, access point, two USB cables, an external power adapter, six Opal IMUs, a chest harness, belt, and two small Velcro straps. The external power adapter was used to plug the docking station into a power outlet. The access point and docking station were both plugged into the laptop. Each Opal IMU sensor was plugged into a separate dock on the docking station. The setup during sensor configuration (prior to data collection) is shown in Figure 2.

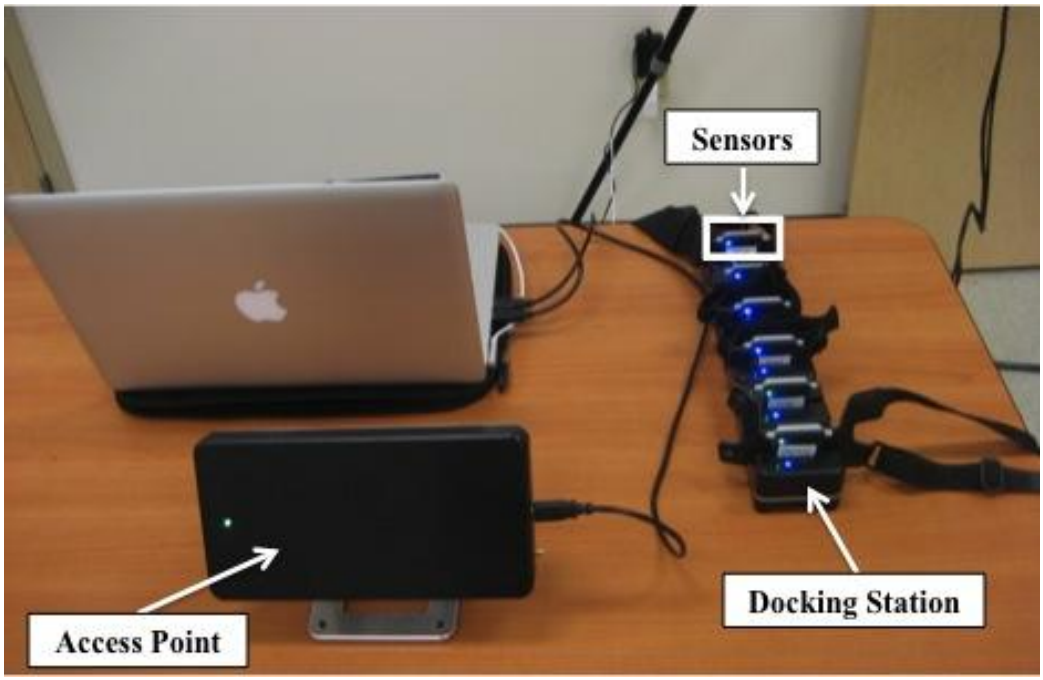

Figure 2 APDM Instrumentation Setup

The Motion Studio software was used to calibrate and configure the sensors. The sensors were calibrated according to the manufacturer's specifications. During configuration, the accelerometer with a range of ±6g, gyroscope and magnetometer sensors were enabled, the sampling rate was set to 128 Hertz and the recording configuration was "Robust Synchronized Streaming." After the configuration was complete, the sensors were removed from the docking station and attached to the subject.

3.1.3.1 Sensor Locations

The sensors were attached to the subject using the manufacturer's chest harness, belt, and small Velcro straps. In order to reduce the movement of the thigh sensors during walking, the sensors were attached with Velcro to two Neoprene sleeves that were then wrapped tightly around each thigh. The locations of the six sensors were the sternum, lower back, right thigh (RThigh), left thigh (LThigh), right shank (RShank) and left Shank (LShank) as shown in Figure 3.

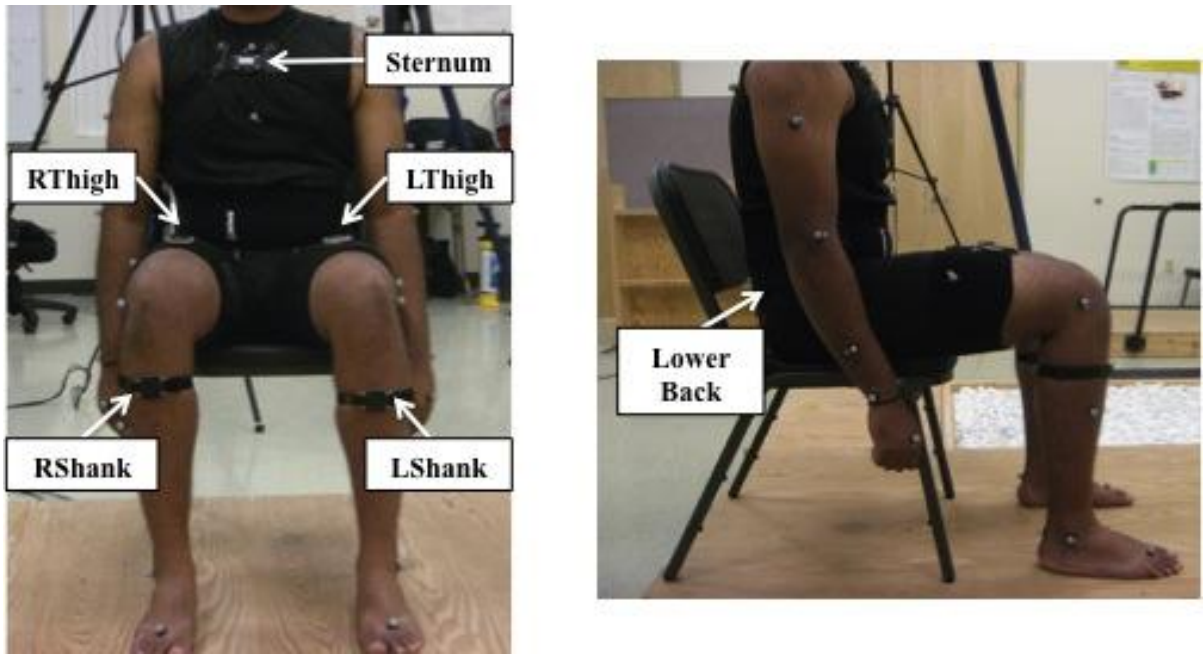

Figure 3 Sensor Locations

3.1.4 Vicon Instrumentation

A Vicon optical motion analysis system consisting of eight infrared cameras was used to track the motion of passive reflective markers placed on the subject. Vicon Workstation was used to calibrate the cameras, auto label the model, collect and check the gait trials. In addition, a Canon digital camcorder was used to simultaneously record each trial.

3.1.4.1 Reflective Marker Locations

Prior to data collection, thirty-five spherical reflective markers 14 millimeters in diameter were placed on subjects' skin at key bony landmarks, according to the Vicon Plug-In Gait marker set [4]. The marker labels, anatomical locations and descriptions for the Plug-In Gait marker set are listed in Table 2. Each body segment requires three markers to define its three-dimensional local coordinate system.

Table 2 Plug-In Gait Marker Set

Body Segment	Marker Label	Anatomical Location	Description of Location
Torso	C7	7th Cervical Vertebrae	Spinous process of the 7th cervical vertebrae on back of neck
	T10	10th Thoracic Vertebrae	Spinous process of the 10th thoracic vertebrae
	CLAV	Clavicle	Jugular notch where the clavicle meets the sternum, below base of neck and between the collar bones
	STRN	Sternum	On the bone above the Xiphoid process in the middle of the ribcage
	RBAK	Right Back	Right scapula, assymetrical, used for labeling purposes
Right Arm	RSHO	Right Shoulder	Right acromio-clavicular joint
	RUPA	Right Upper Arm	Right upper arm in between the shoulder and elbow markers
	RFRA	Right Forearm	Right forearm between the eblow and wrist markers
	RELB	Right Elbow	Right lateral epicondyle, approximating the elbow joint axis
	RWRA	Right Wrist A	Thumb side of the right wrist
	RWRB	Right Wrist B	Pinkie side of the right wrist
	RFIN	Right Finger	On the dorsum of the right hand below the third metacarpal
Left Arm	LSHO	Left Shoulder	Left acromio-clavicular joint
	LUPA	Left Upper Arm	Left upper arm in between the shoulder and elbow markers, assymetrical from the RUPA
	LFRA	Left Forearm	Left forearm between the elbow and wrist markers, assymetrical from the RFRA
	LELB	Left Elbow	Left lateral epicondyle, approximating the elbow joint axis
	LWRA	Left Wrist A	Thumb side of the left wrist
	LWRB	Left Wrist B	Pinkie side of the left wrist
	LFIN	Left Finger	On the dorsum of the left hand below the third metacarpal
Pelvis	RASI	Right Anterior Illiac Spine	On top of the anterior illiac spine
	LASI	Left Anterior Illiac Spine	
	RPSI	Right Posterior Illiac Spine	On top of the bony locations where the spine joins the pelvis
	LPSI	Left Posterior Illiac Spine	
Right Leg	RTHI	Right Thigh	Lower 1/3 of the lateral surface of right thigh
	RKNE	Right Knee	Lateral epicondyle of the right knee
	RTIB	Right Tibia	Lower 1/3 of the lateral surface of the right shank
	RANK	Right Ankle	Lateral malleolus on the right foot
	RTOE	Right Toe	Second metatarsal head on the right foot
	RHEE	Right Heel	Right calcaneous, height is level with the right toe marker
Left Leg	LTHI	Left Thigh	Lower 1/3 of the lateral surface of left thigh
	LKNE	Left Knee	Lateral epicondyle of the left knee
	LTIB	Left Tibia	Lower 1/3 of the lateral surface of left shank
	LANK	Left Ankle	Lateral malleolus on the left foot
	LTOE	Left Toe	Second metatarsal head on the left foot
	LHEE	Left Heel	Left calcaneous, height is level with the left toe marker

3.1.4.2 Subject Measurements

The Vicon Plug-In Gait model requires several anatomical measurements for each subject; these are listed in Table 3. The subject's height and weight was measured using a professional scale, in centimeters (cm) and kilograms (kg) respectively. The other measurements were taken by hand using a cloth measuring tape, and recorded in cm.

Table 3 Subject Measurements Required for Plug-In Gait

Measurement	Description	Units
Mass	Weight of the subject	kg
Height	Height of the subject	cm
ASIS Distance	Distance between RASI and LASI markers	cm
Leg Length	Distance from ASIS narker to medial malleolus	cm
Knee Width	Medio-lateral knee width about flexion axis	cm
Ankle Width	Distance between the lateral and medial malleolus	cm
Elbow Width	Distance between the lateral and medial epicondyle	cm
Wrist Width	Distance between the two wrist markers	cm
Hand Thickness	Thickness between the dorsum and palm of hand	cm
Shoulder Offset	Vertical distance between the SHO marker and shoulder joint center	cm

3.1.4.3 Camera Calibration

An L-frame with four passive reflective markers (shown in Figure 4) was used for calibration of the Vicon cameras. It was placed on the floor at the corner of the first force plate and was used to define the laboratory's global coordinate system, axes and the location of the origin. The data collection volume was also defined by moving a wand with two reflective markers (shown in Figure 4) in various directions over the entire walkway.

Figure 4 Vicon Calibration L-Frame and Wand

After the static and dynamic camera calibration was completed, a static trial was collected in which the participant was asked to stand still on the force plates in a T-pose (shown in Figure 5) in order to define and label the locations of the reflective markers.

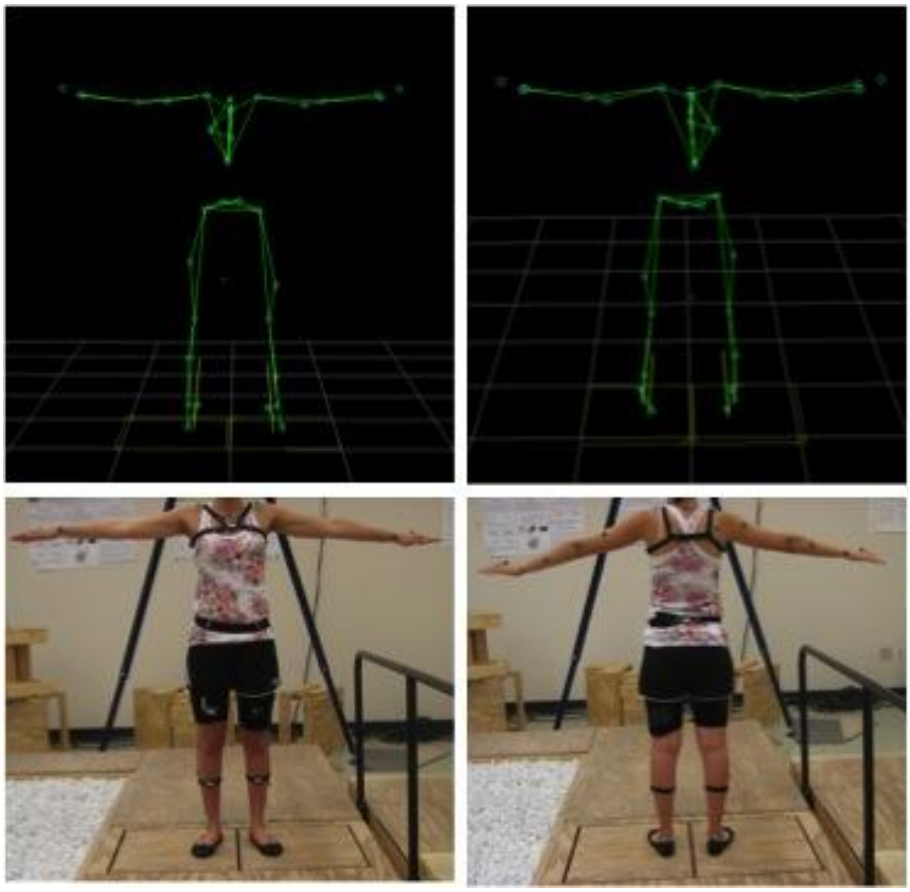

Figure 5 Vicon Static Trial T-Pose

3.1.5 Testing Protocol

This study was conducted in the Rehabilitation Robotics & Prosthetics Testbed (RRT) motion analysis laboratory at the University of South Florida. The eight Vicon cameras were focused on a 3-meter wooden walkway with two AMTI force platforms. A chair was placed at the beginning of the walkway. Both the WMAS and Vicon systems were configured and calibrated per the manufacturer's instructions prior to the beginning of the testing as described previously and in more detail in Appendix B. After the configuration of both systems, data were collected simultaneously from the WMAS and Vicon systems during the gait trials. One member of the research staff was needed to run the WMAS, and another staff member was needed to run the Vicon system. The start of the recording for each trial was coordinated verbally by one of the staff members.

3.1.5.1 WMAS

The Motion Studio software was used to record the data from the WMAS during the gait trials. After the sensors were configured in "Robust Synchronized Streaming Mode" at 128 hertz and removed from the docking stations, the stream button was pressed and a new window popped up on the screen as shown in Figure 6. The data from the WMAS was streamed to the laptop via the wireless access point and displayed in a real time strip chart from each of the sensors. The strip chart displayed the accelerometer, gyroscope and magnetometer readings, shown on the left hand side of Figure 6. Before each trial, the research staff member responsible for the WMAS was required to select the record duration as indeterminate, the file format as CSV and name the trial according to the format "Subject ID_Type of Trial_Trial Number." For each trial, the record button was pressed to begin the trial and the stop button

was pressed at the end of the trial. For detailed instructions on how the Motion Studio program was used see Appendix B.

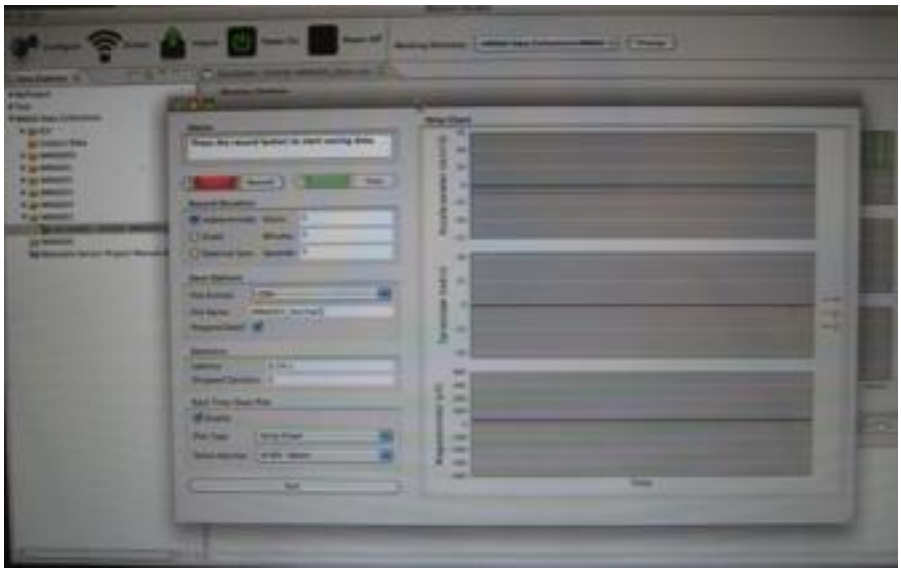

Figure 6 Motion Studio Screen During Streaming Prior to Data Collection

3.1.5.2 Vicon Motion Analysis System

The Vicon Workstation software was used to collect data from the Vicon optical motion analysis system. The static trial described previous was used to label each of the markers according the plug-in gait marker set (Table 2) and define an auto label pipeline. When the model was completed a stick figure of the subject was created based on the position of the markers and the defined segments (shown in Figure 5). The auto labeling was used to automatically define the stick figure for each of the trials, however due to occasional marker dropout it did not always work properly. As a result, after the data collection each trial needed to be checked to make sure all the markers were labeled properly and all the markers were present. Before the start of the each trial, the new trial icon was selected and named according to the WMAS data collection checklist (Appendix A). The start and stop buttons were used to

capture each trial. Each gait trial was checked briefly to make sure all the markers were present and there were no issues prior to the start of the next trial.

3.1.5.3 Timed Up and Go Test

A timed up and go (TUG) test [66] was used for all gait trials in this study. A TUG test is a common test used during gait analysis and physical therapy evaluation. The TUG test began with the subject sitting in a chair at one end of the walkway with their knees bent to approximately 90 degrees and hands on their lap. When asked to go, the subject stood up, walked to the other end of the walkway and when they reached a line on the floor, turned around, walked back to the chair and sat back down . The subjects were asked to walk at three different speeds: normal, slow and fast. Each subject completed five trials at each of the three speeds. The slow speed was used to correspond to mTBI patients.

3.2 Verification Testing

Three different verification tests were performed with the WMAS and APDM IMUs:

1. Movement analysis using a robotic motion.
2. Range of motion
3. Sit to stand

In the movement analysis testing, a wheelchair mounted robotic arm (WMRA) was used to provide a repeatable movement at varying speeds, with the sensors securely attached in order to investigate the accuracy of the APDM Opal IMUs for kinematic analysis relative to an optical motion analysis system without any filtering and to identify the sources of error. The range of motion and sit to stand movements were used to determine the accuracy of the knee angle calculation algorithm.

3.2.1 Movement Analysis Using a Programmed Robotic Motion

In order to verify the accuracy of the WMAS and its algorithms, the joint angles and velocities measured with the wearable IMU sensors were compared to measurements from a Vicon optical motion-tracking system while a robotic arm completed various predetermined paths. The robotic arm was used to test the repeatability of the measurements as it could provide the same movement over and over again for longer trials than is possible with human subject testing. The sensors were also running for a much longer period of time with the robotic arm testing than with the human subject testing. A 7 Degree of Freedom wheelchair mounted robotic arm (WMRA), developed at the University of South Florida was used. The robotic arm uses incremental encoders at each joint to measure and calculate its Cartesian motion relative to a reference frame using inverse kinematics [67]. Motion profiles of the robotic arm were tracked using an eight-camera Vicon motion-tracking system with passive retro-reflective markers, and four wearable APDM IMUs. In order to better isolate various types of contributing errors, linear, planar, and 3-dimensional robot motions were used. Data were collected from the sensors over several hours, which provided insight into time-based effects as well as management of large amounts of data for future long-term tracking applications. In addition, acquisition errors with high-speed gaits were found previously, thus robotic arm trajectories of varying velocities were used to provide further insight into these rate-based effects. Angular velocity and joint angles were compared for the Vicon and APDM systems and used to investigate the accuracy of the IMUs and algorithms during motion tracking. Effects on IMU performance due to the application of filtering algorithms were not investigated.

3.2.1.1 Instrumentation

The WMRA is shown in Figure 7, where the circles indicate the locations of the joints, the lines indicate the links or segments and the boxes indicate the locations of the sensors. The robotic arm was used to represent a person's leg, where joints 1 and 3 represent the "hip" joint, link 1 represents the "thigh" segment, joint 4 represents the "knee" joint and link 2 represents the "shank" segment. Two APDM sensors were placed on the "knee" joint, and one sensor was placed on each segment or link connected to the "knee" joint.

Figure 7 Wheelchair Mounted Robot Arm (WMRA)

Four Opal IMU units were placed on the robotic arm as shown by the red boxes in Figure 7 and Figure 8: one on link 1 (L1), one on link 2 (L2) and two on joint 4 coaxially.

Figure 8 Locations of IMUs on WMRA

An eight-camera Vicon optical motion analysis system was also used simultaneously to capture the movement of the robotic arm by tracking the position of passive reflective markers. A total of 16 spherical reflective markers were placed on the robotic arm (Figure 9). Each segment requires three markers to define its 3-dimensional local coordinate system. Redundant markers were used to avoid marker dropout due to the wheelchair blocking cameras from seeing markers.

Figure 9 Reflective Markers and IMUs on WMRA

3.2.1.2 Testing Protocol

The robotic arm was programmed to complete range of motion movements at particular joints and a 3-dimensional motion of all three joints. Data from each movement (trial) were collected from the APDM Opal sensors and the Vicon motion analysis system simultaneously. The following movements were recorded:

Joint 1: Hip flexion and extension

Joint 3: Hip internal and external rotation

Joint 4: Knee flexion and extension

The flexion and extension linear movements were collected at three different speeds, and the internal and external rotation movements were collected at two different speeds. The robotic arm was then programmed to continue simultaneous three-dimensional movement of all three joints for five complete cycles. A total of eighteen trials were recorded over the course of

several hours. The starting position of the WMRA for the flexion and internal rotation movements, and the ending position of the WMRA for the extension and external rotation movements was defined as zero degrees for the Vicon and APDM systems.

3.2.1.3 Data Analysis

The Vicon data were analyzed using Visual3D (C-Motion Inc., Germantown, MD). A model was created in Visual3D that used the positions of the reflective markers to define segments for link 1 ("thigh") and link 2 ("shank"). The joint angles were calculated from the model using the rotation of one segment relative to a reference segment (in some cases the laboratory coordinate frame) and followed by an X-Y-Z Euler sequence.

MATLAB was used to process and analyze the data from the APDM sensors. An algorithm was created to calculate the angle between link 1 and link 2 (joint 4) or "knee" angle between the two APDM sensors. Anatomically the knee angle is calculated using Equation 1 but an algorithm was used to calculate the knee angle from the sensors. This algorithm identified the quaternion "q" (Equation 2), which comes from the APDM sensors. The quaternion provides the orientation of the sensor and is calculated from a combination of the accelerometer, gyroscope and magnetometer readings as well as the temperature correction feature of the IMUs [68]. After the quaternion was identified, the norm of the quaternion was calculated (Equation 3). Next the quaternion was normalized using "w, x, y and z" (Equation 4). The knee angle quaternion was calculated by using Equation 5, in which the inverse of the shank quaternion was multiplied by the normalized thigh quaternion. Lastly, the knee angle quaternion was then converted into Y-X-Z Euler angles (Equation 6). This process was used to obtain the flexion angle for both the "thigh and "shank" sensors, which represent Link 1 and

Link 2 respectively. The Y-X-Z rotation is the sensor equivalent to the Vicon X-Y-Z rotation [10, 43, 69, 70].

$$\theta_{Knee} = \theta_{Thigh} - \theta_{Shank} \tag{1}$$

$$q = q_0 + q_1 + q_2 + q_3 \tag{2}$$

$$q_{norm} = \sqrt{q_0^2 + q_1^2 + q_2^2 + q_3^2} \tag{3}$$

$$w = \frac{q_0}{q_{norm}}; x = \frac{q_1}{q_{norm}}; y = \frac{q_2}{q_{norm}}; z = \frac{q_3}{q_{norm}}; \tag{4}$$

$$q_{Knee} = q_{Shank}^{-1} \otimes q_{Thigh} \tag{5}$$

$$q_{Knee}\ Euler\ Angles\ YXZ = \begin{bmatrix} atan2(-2xz + 2wy), z^2 - y^2 - x^2 + w^2 \\ \text{asin}(2yz + 2wx) \\ atan2(-2xy + 2wz, y^2 - z^2 + w^2 - x^2 \end{bmatrix} \tag{6}$$

For the two sensors located directly on joint 4 and to calculate joint angles 1 and 3, which represent the "hip" angle, Equation 1 and Equation 2 were used to identify and normalize the quaternion. Then the quaternion was converted directly to Euler angles. The joint angle calculated by the sensor located directly on the joint was compared to the joint angle calculated by the two-sensor algorithm (Equations 1-5).

In order to compare the Vicon and APDM systems, the joint angles were calculated from for each trial and were plotted in degrees versus time in seconds on the same graph. The Vicon and APDM systems collected data at 120 Hz and 128 Hz respectively. Therefore in order to compare the two systems, the data were down-sampled. The root mean square error (RMSE) and Pearson's R correlation were calculated in order to compare the joint angles from the Vicon and APDM sensors. The angles calculated by the two-sensor algorithm and the Vicon system were also compared to the angles calculated by the sensors located directly on joint 4 using the

RMSE. The average angular velocities for each trial were also compared in degrees per second for all three systems. The angular velocity measured by the APDM sensor's gyroscopes was compared to the calculated angular velocity from both the Vicon and WMRA systems.

3.2.2 Range of Motion

The range of motion tests were performed using the WMAS and Vicon motion analysis systems simultaneously in order to validate the knee angle algorithm created in Matlab for the WMAS. Both the WMAS and Vicon motion analysis systems were set up and calibrated according to methods previously discussed in sections 3.1.3 and 3.1.4. For all of the tests the subject was seated and asked to flex and extend their leg. Several tests were performed including knee extension from 90 degrees to 45 degrees (shown in the top two pictures of Figure 10), knee flexion from 45 degrees to 90 degrees, full knee flexion and extension (shown in the bottom two pictures of Figure 10).

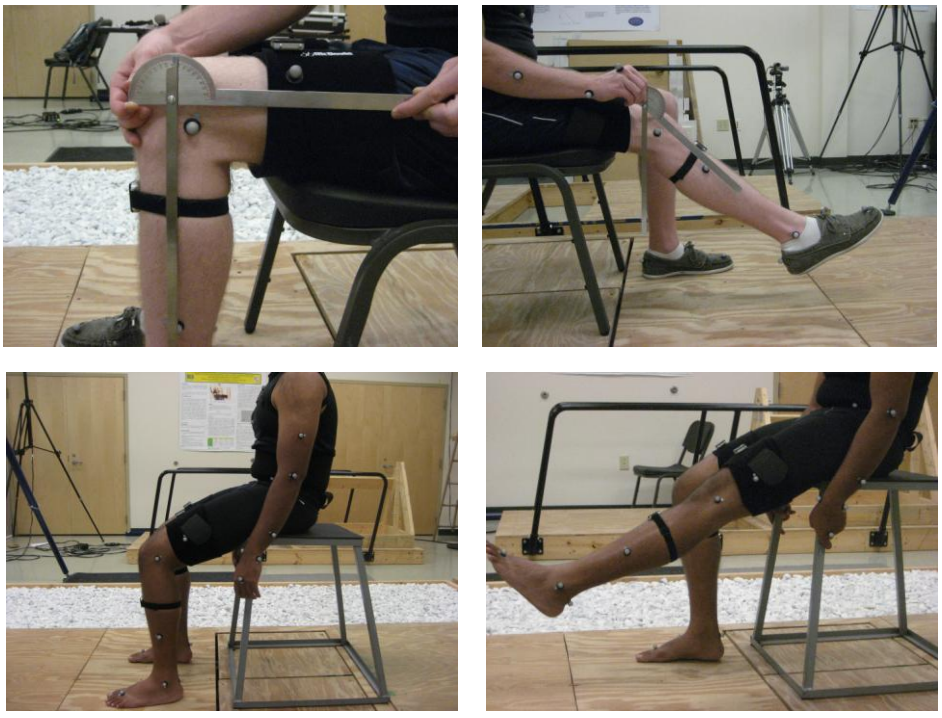

Figure 10 Range of Motion Tests

3.2.3 Sit to Stand

Sit to stand tests (shown in Figure 11) were performed using the same procedures as the range of motion testing. For these trials subject began in a seated position and was asked to stand up, and sit back down. These trials were also used to validate the knee angle calculation algorithm of the WMAS.

Figure 11 Sit to Stand Test

CHAPTER 4: DATA ANALYSIS

4.1 WMAS

The WMAS analysis was performed in Matlab. Algorithms were developed and adapted from previous work with quaternions [69, 70] to calculate knee flexion angle, stride length and cadence.

4.1.1 Knee Angle

The knee angle was calculated from the previously mentioned Equations 2-6 (also shown below) in Matlab. Before the calculations were performed, the csv file was imported into Matlab as column vectors with headings "RTQScalar, RTQX, RTQY, RTQZ, RSQScalar, RSQX, RSQY, RSQZ, LTQScalar, LTQX, LTQY, LTQZ, LSQScalar, LSQX, LSQY and LSQZ," representing the quaternion components of the right thigh, right shank, left thigh and left shank respectively. Equations 2-4 were performed for each of the four sensors: right thigh, right shank, left thigh and left shank. Equations 2-4 was used to define the quaternion calculate the norm of the quaternion, and to normalize the quaternion (Equation 4). Equation 5 was used to calculate the knee angle quaternion by multiplying the inverse of the shank quaternion by the thigh quaternion. Equation 6 was then used to convert the knee angle quaternion to Euler angles. The Y-X-Z rotation is the sensor equivalent to the Vicon X-Y-Z rotation, where angle 1 corresponds to flexion/extension, angle 2 corresponds to internal/external rotation and angle 3 corresponds to abduction/adduction [10, 43, 69-71].

$$q = q_0 + q_1 + q_2 + q_3 \tag{2}$$

$$q_{norm} = \sqrt{q_0^2 + q_1^2 + q_2^2 + q_3^2} \tag{3}$$

$$w = \frac{q_0}{q_{norm}}; x = \frac{q_1}{q_{norm}}; y = \frac{q_2}{q_{norm}}; z = \frac{q_3}{q_{norm}}; \tag{4}$$

$$q_{Knee} = q_{Shank}^{-1} \otimes q_{Thigh} \tag{5}$$

$$q_{Knee}\ Euler\ Angles\ YXZ = \begin{bmatrix} atan2(-2xz + 2wy), z^2 - y^2 - x^2 + w^2 \\ \text{asin}(2yz + 2wx) \\ atan2(-2xy + 2wz, y^2 - z^2 + w^2 - x^2 \end{bmatrix} \tag{6}$$

4.1.2 Stride Length

Aminian et al. found that the heel-strike and toe-off events can be identified using the angular velocity signal from the shank sensor. The toe-off and heel-strike events are evident in the minimum peaks of the shank angular velocity signal on either side of the maximum peaks (greater than 100 deg/s). The rectangles and circles in Figure 12 represent the toe-off and heel-strike gait events during one of the slow gait trials [38].

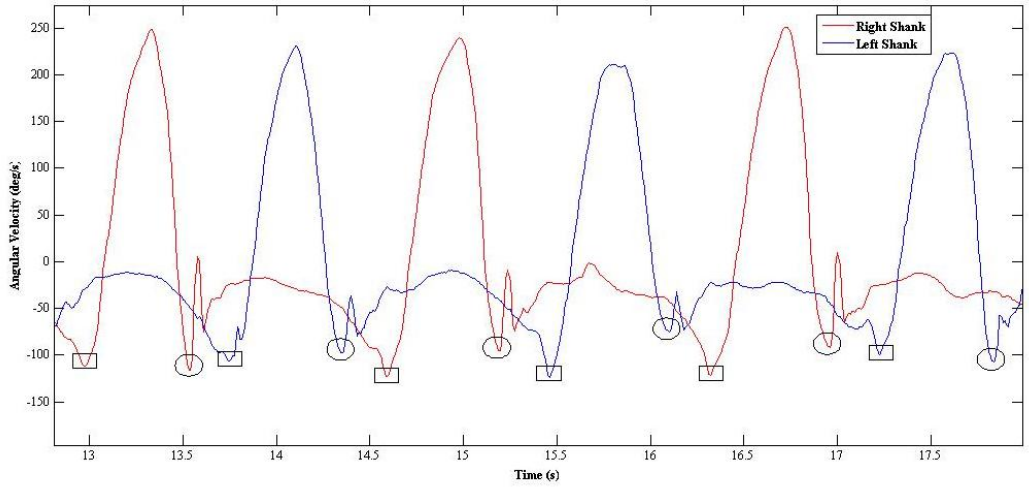

Figure 12 Shank Angular Velocity & Toe-Off (Rectangle) and Heel-Strike (Circle) Events

The toe-off and heel strike events were detected from the angular velocity signal using a peak detection algorithm in Matlab that located the minimum and maximum peaks of the signal [72]. Prior to stride length calculation the events were checked to make sure the points were the actual heel-strike and toe-off events and not a peak due to noise in the signal.

Stride length was calculated using the law of cosines, similar to the Zexi et al calculation of step length [65]. The stride length was equal to the sum of the right and left step. This consists of the sum of the distance from right heel-strike to left heel-strike and the distance from left heel-strike to subsequent right heel-strike. According to the law of cosines, if you have two sides of a triangle and the angle between them you can calculate the length of the third side [73]. As shown by s1 in Figure 13, the right step (RHS to LHS) includes the two sides or leg lengths and the angles of the right shank and left shank at heel-strike. These two angles are then added together to determine the angle between the right and left leg. The first step (s1) in Figure 13 is from right heel-strike to the left heel-strike, and the second step (s2) is from left heel-strike to the subsequent right heel-strike.

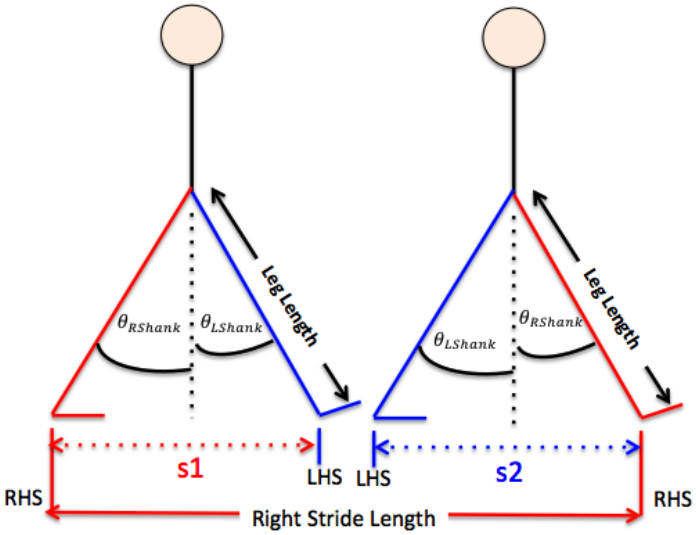

Figure 13 Parameters for Stride Length Calculation

Equation 7 was used to determine step length (s) based on the law of cosines [73]. Equation 8 was used to calculate the stride length by adding s1 and s2.

$$s = LegLength\sqrt{2 - (\cos(\theta_{RShank} + \theta_{LShank}))} \quad (7)$$

$$Stride\ Length = s_1 + s_2 \quad (8)$$

4.1.3 Cadence

Cadence or number of steps per minute was calculated using Equation 9. The heel-strike events were used to determine each step as defined previously. The number of steps before the turn and the total time from the beginning of the first step to the end of the last step was used in the calculation. This process was also repeated for the steps that occurred after the turn. The cadence before the turn and after the turn was averaged to determine the cadence for that trial.

$$Cadence = \frac{Steps}{Minute} = \#\ Steps \times \frac{60}{Total\ Time\ (s)} \quad (9)$$

4.1.4 Graphical User Interface Development

A graphical user interface was developed in Matlab using the GUIDE tool. The graphical user interface will allow the user to view the knee angle calculations and results by simply loading the CSV file from the sensors and running the program. The GUI needs to be easy to use and run by a clinician. The GUI was partially developed in this study, future work will involve adding the other gait parameters and the ability to collect and analyze the data directly rather than using another software program for data collection.

4.2 Vicon

The data from the Vicon system was first inspected using the BodyBuilder software, and was then exported into Visual 3D (C-Motion, Germantown, MD) software for further analysis.

4.2.1 Visual 3D Model

In Visual 3D, a model was created that identified the locations of the reflective markers and defined the bone segments based on the plug in gait marker set, static trial and subject measurements. The model was based on the C-Motion Visual 3D Tutorial: Building a Conventional Gait Model [74] and is shown in Figure 14.

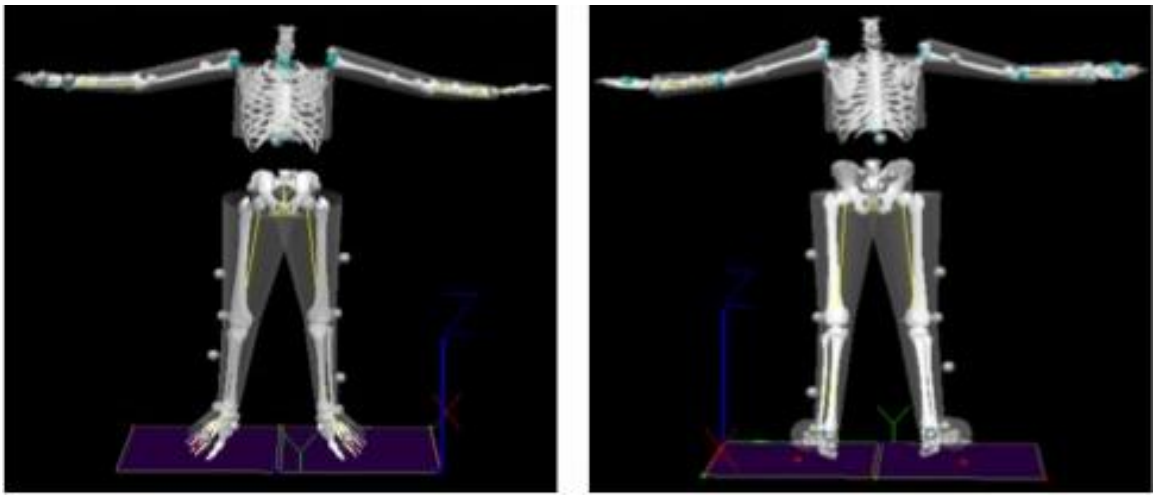

Figure 14 V3D Model

4.2.2 Visual 3D Pipeline

A pipeline was created in Visual 3D (V3D) to calculate the knee joint angle [75] and stride length [76, 77] (See Appendix C). The thigh and shank segments were used to calculate the angle of the shank relative to the thigh, or the knee flexion angle during the gait trials [75]. The position of the heel with respect to the pelvis was used to determine the heel-strike events.

4.3 Statistics

Three types of statistics were used to compare the WMAS and Vicon systems: Pearson's R Correlation, Root Mean Square Error (RMSE) and Bland Altman plots. Pearson's R Correlation was calculated using Equation 10 [78]. RMSE was calculated using Equation 11 [79]. In both Equations 10 and 11, X was the results from the WMAS system, Y was the results from the Vicon system and n is the number of samples.

$$R = \frac{n\sum XY - (\sum X)(\sum Y)}{\sqrt{[n\sum X^2 - (\sum X)^2][n\sum Y^2 - (\sum Y)^2]}} \quad (10)$$

$$RMSE = \sqrt{\frac{\sum (X-Y)^2}{n}} \quad (11)$$

Pearson's R Correlation is used to compare two variables by determining on a scale of positive to negative 1 the strength of their linear relationship. The closer the value is to 1, the stronger the correlation. If the value is close to zero, there is a weak linear relationship between the two variables [78]. Root mean square error (RMSE) is often used to compare two methods of measurement, or a model to a reference measurement. The RMSE is a measure of fit between two methods [79]. Another way to compare two measurement techniques is with a Bland Altman plot. The average of the two methods is the x-axis of the plot and the difference between the two methods is the y-axis of the plot. The center dashed line on the plot is the mean and the upper and lower dashed lines are the mean +/- two standard deviations. The upper and lower dashed lines are called the limits of agreement, and are used to determine if the two methods are similar. If the limits of agreement are within an acceptable range of error then the two methods are similar. The advantage of a Bland Altman plot is the outliers, bias and similarities between the two methods are easy to identify [80, 81]. Bland Altman plots were

used in addition to R correlation values because an R correlation assumes a linear relationship, and it is possible for two methods to have a linear relationship but not be similar.

CHAPTER 5: RESULTS

5.1 Verification Tests

5.1.1 Movement Analysis Using a Robotic Motion

There were six trials recorded during the movement of joint 1. The hip flexion and hip extension angles calculated by the Vicon and APDM systems at speeds A, B and C are shown in the following graphs in degrees versus time in seconds. The Vicon system is shown in the plots by the blue lines and the red lines show the APDM system. Figure 15 shows the angles for both the Vicon and APDM system during the movement of joint 1, representative of hip flexion at speed A. Joint 1 hip flexion B and joint 1 hip flexion C are shown in Figure 16 and Figure 17.

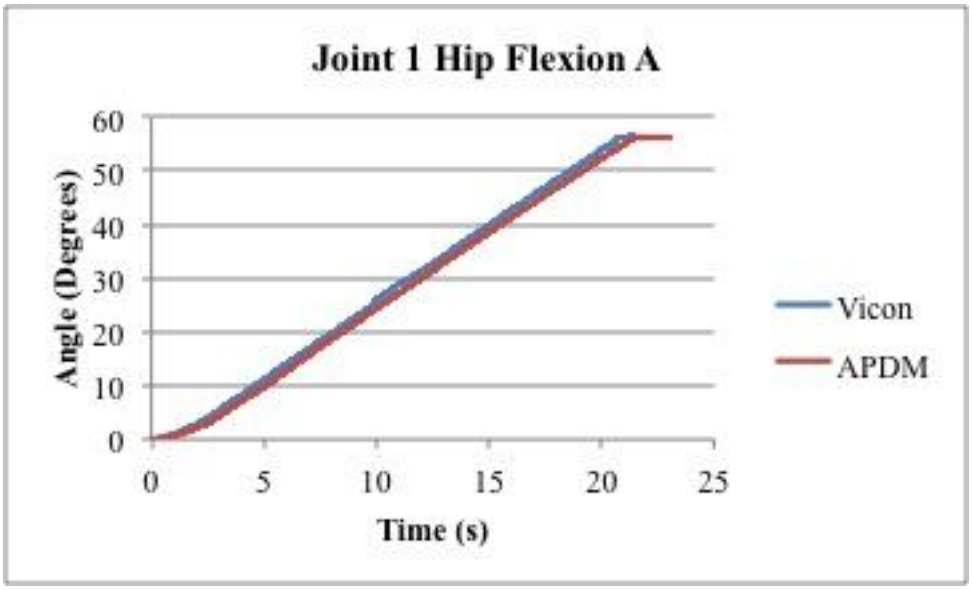

Figure 15 Joint 1 Hip Flexion A

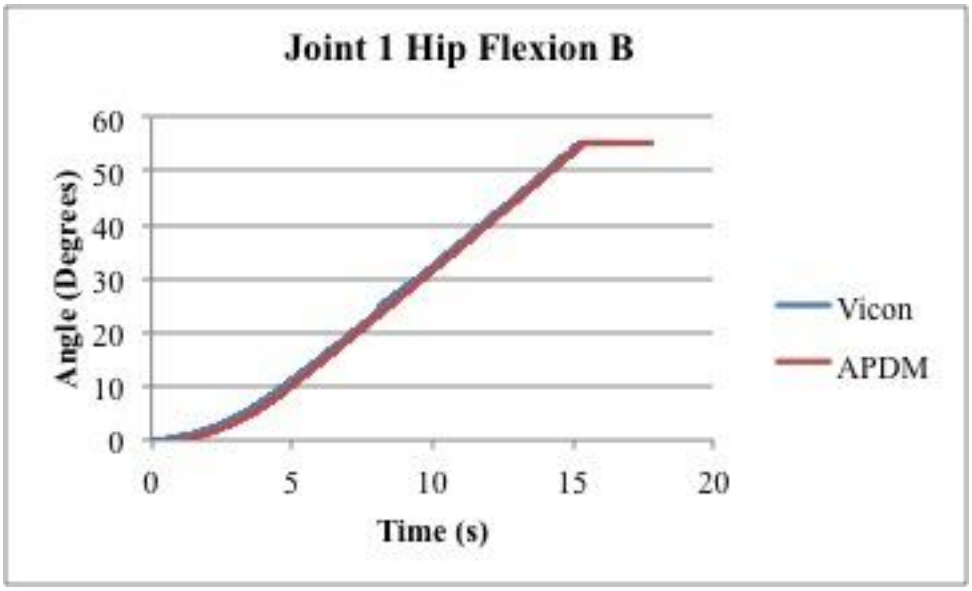

Figure 16 Joint 1 Hip Flexion B

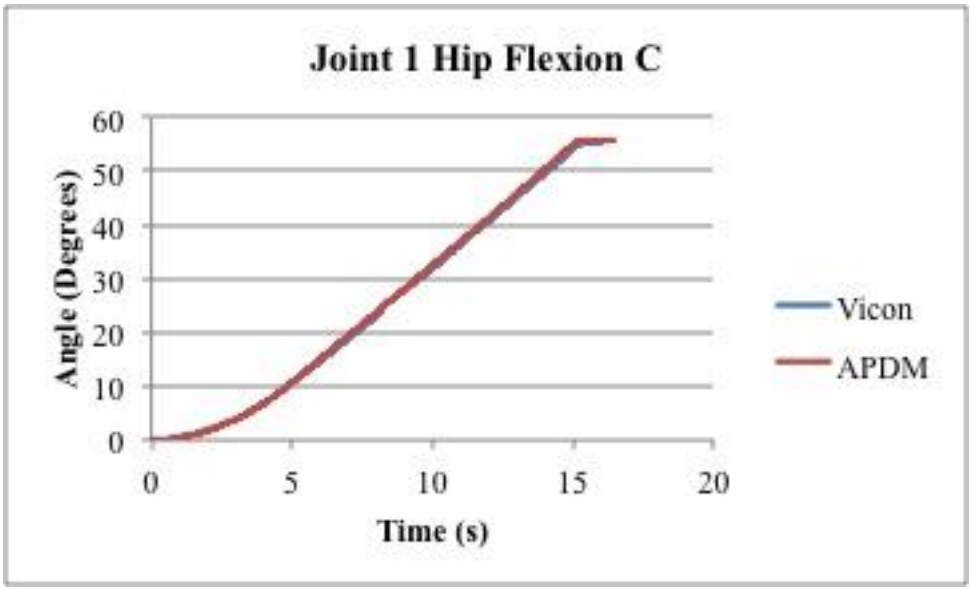

Figure 17 Joint 1 Hip Flexion C

The comparison of the angle measured by the Vicon system and the APDM system for joint 1 hip extension A is shown in Figure 18. The movement of joint 1 hip extension B is shown in Figure 19. The movement of joint 1 hip extension at speed C is shown in Figure 20.

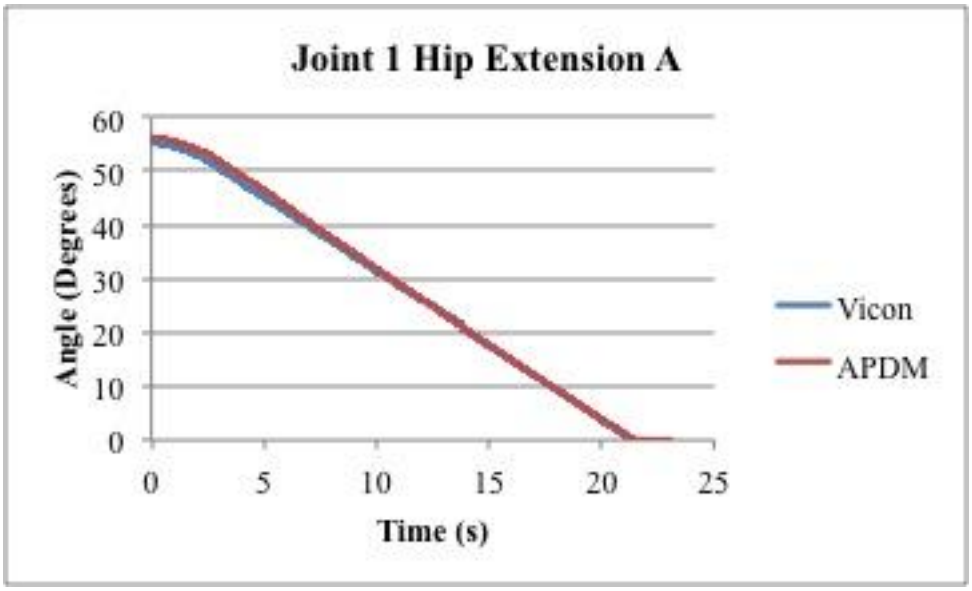

Figure 18 Joint 1 Hip Extension A

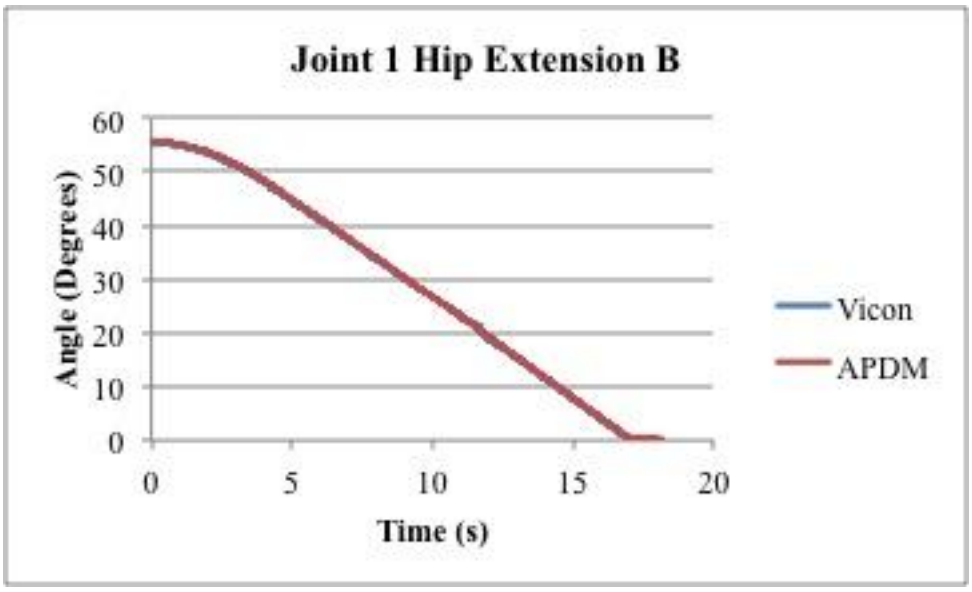

Figure 19 Joint 1 Hip Extension B

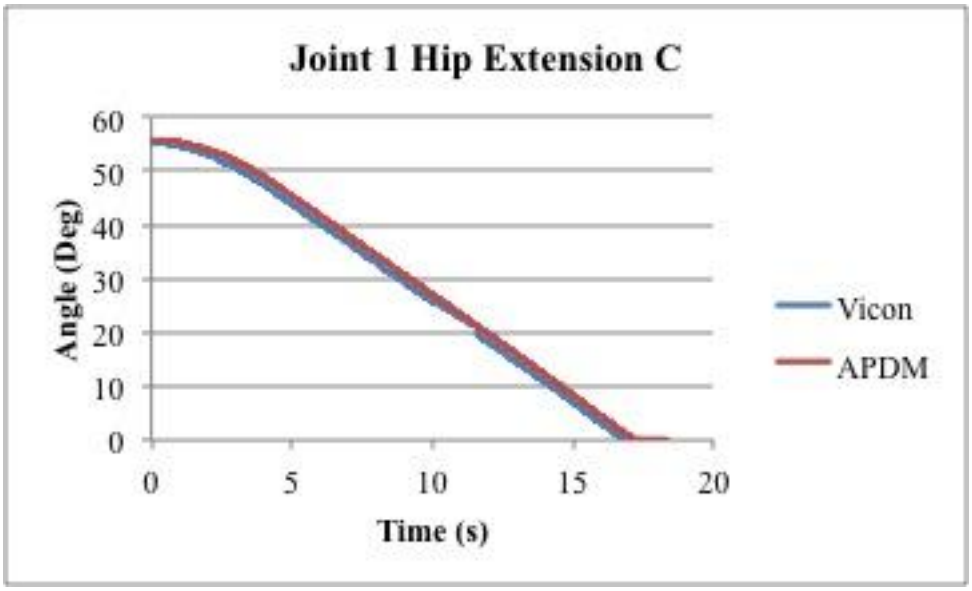

Figure 20 Joint 1 Hip Extension C

Four trials were recorded during the movement of joint 3, representative of internal and external rotation, at speeds A and B. Figure 21 and Figure 22 shows the movement of joint 3 hip internal rotation at speeds A and B respectively.

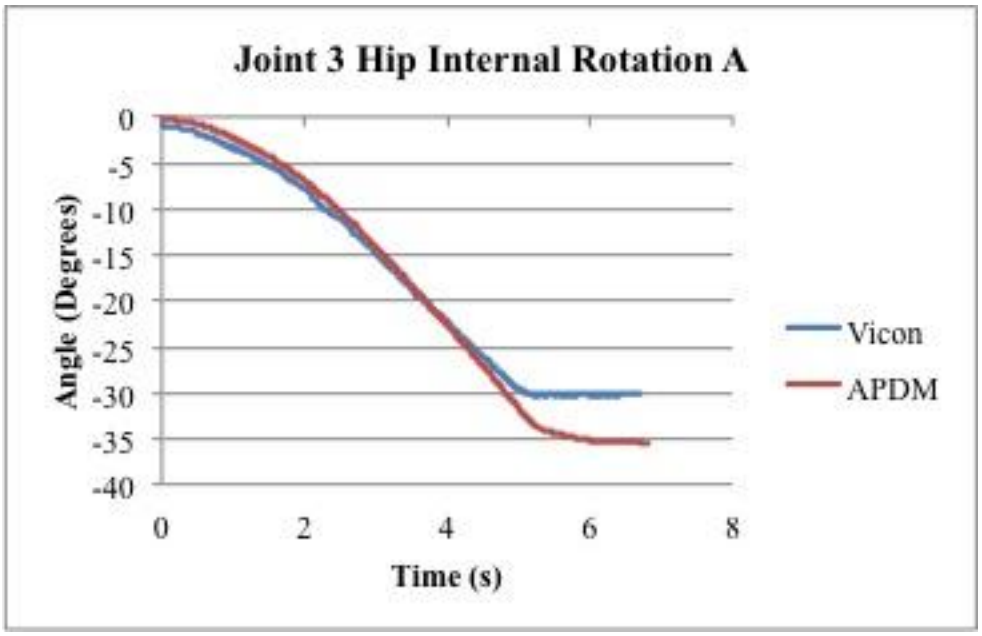

Figure 21 Joint 3 Hip Internal Rotation A

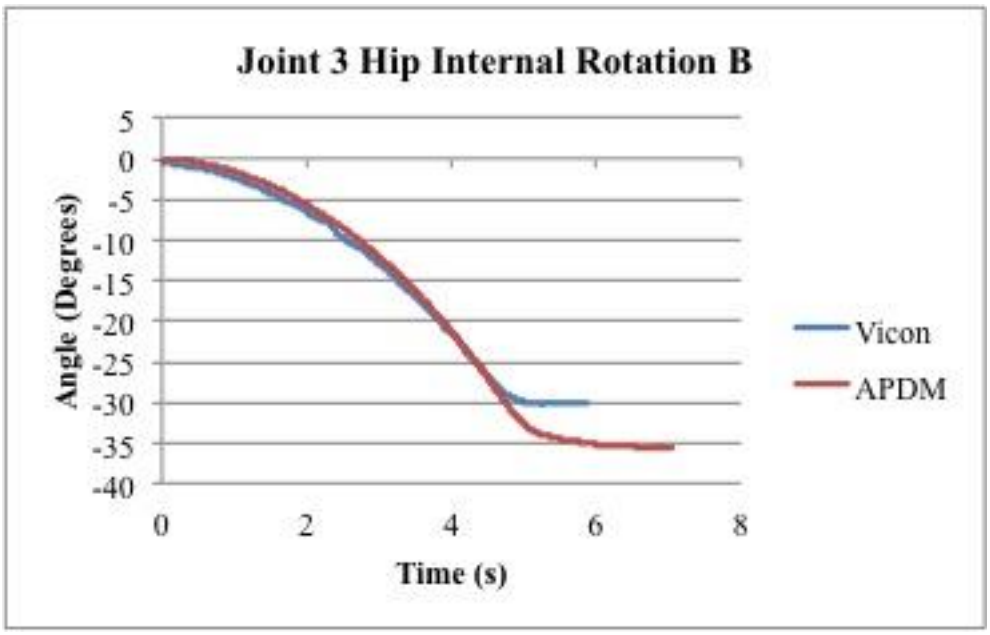

Figure 22 Joint 3 Hip Internal Rotation B

The movement of joint 3 hip external rotation at speeds A and B is shown in Figure 23 and Figure 24.

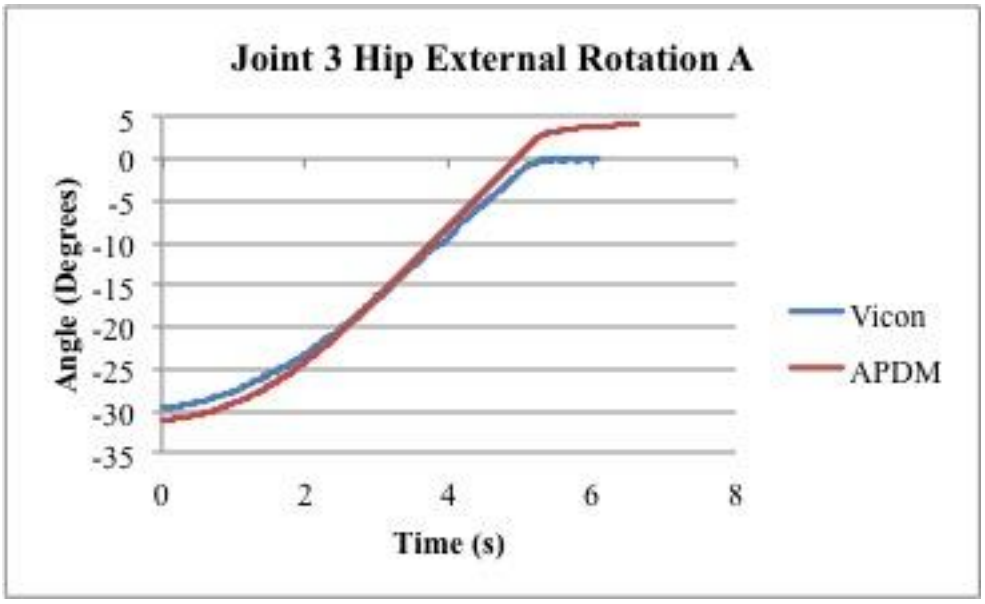

Figure 23 Joint 3 Hip External Rotation A

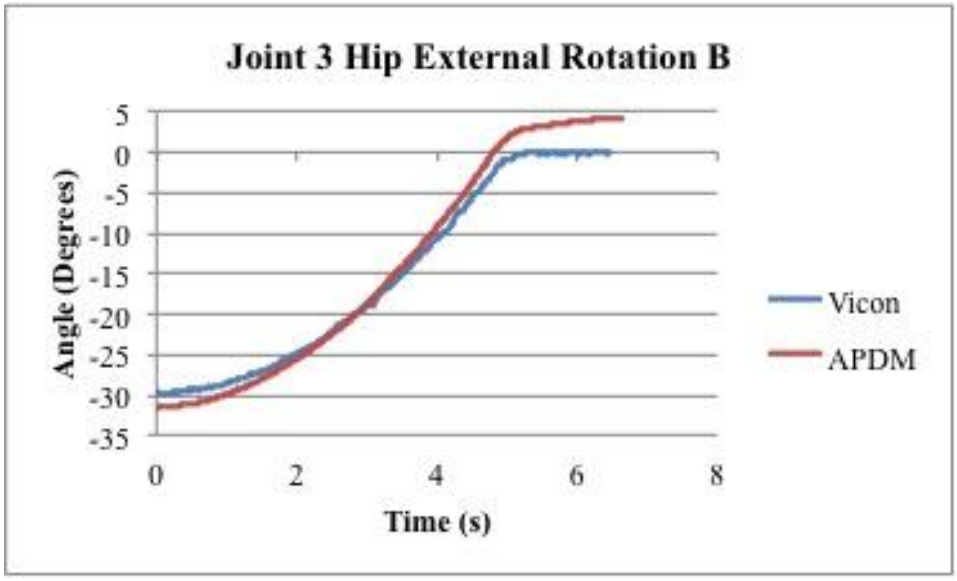

Figure 24 Joint 3 Hip External Rotation B

There were six trials recorded for joint 4, representative of knee flexion and extension at speeds A, B and C. The Vicon and systems are shown in the plots by the blue and red lines respectively. Figure 25, Figure 26 and Figure 27 show joint 4 knee flexion at speeds A, B and C.

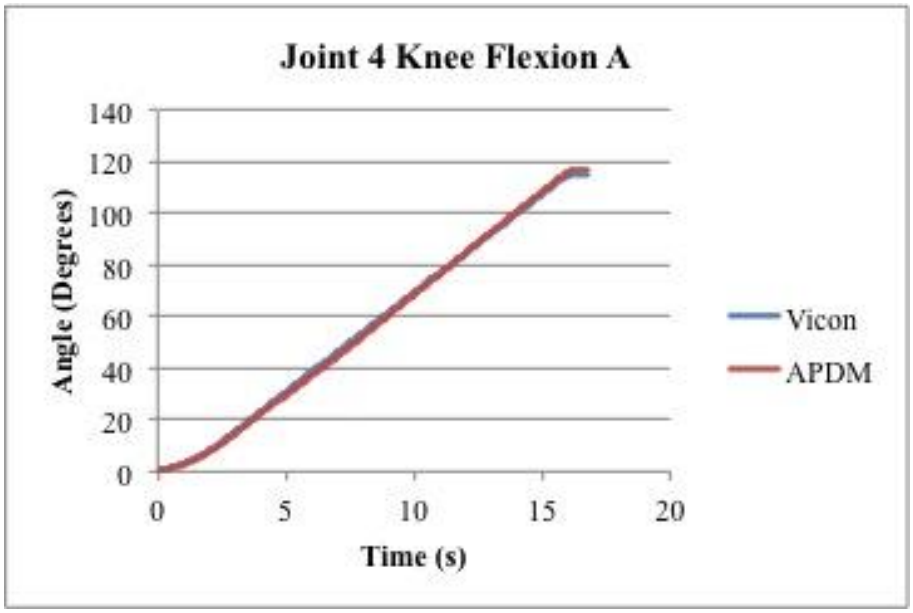

Figure 25 Joint 4 Knee Flexion A

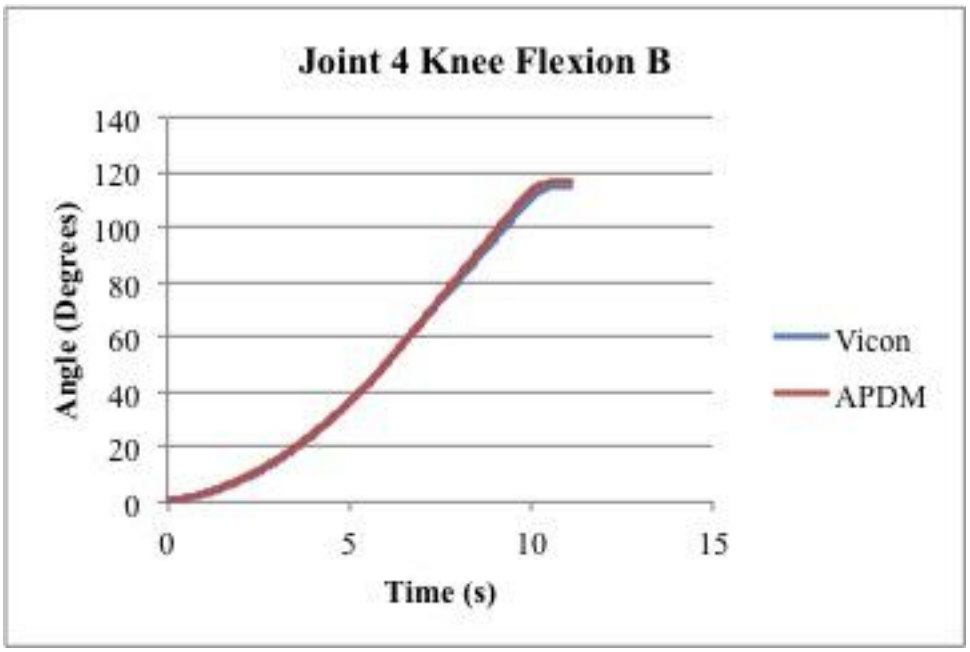

Figure 26 Joint 4 Knee Flexion B

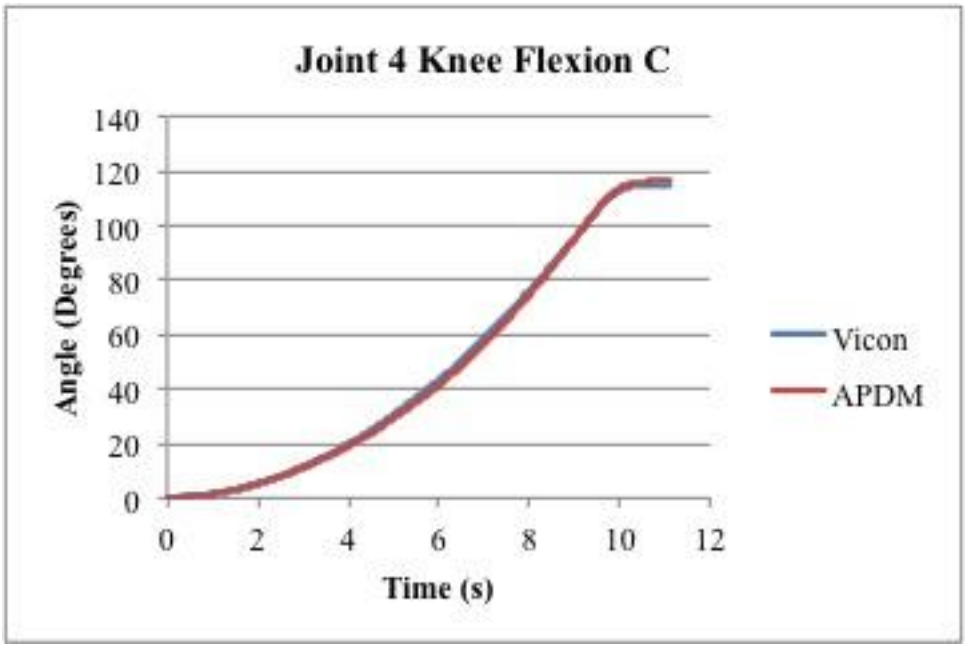

Figure 27 Joint 4 Knee Flexion C

Joint 4, representative of knee extension, at speeds A, B and C are shown in Figure 28, Figure 29 and Figure 30.

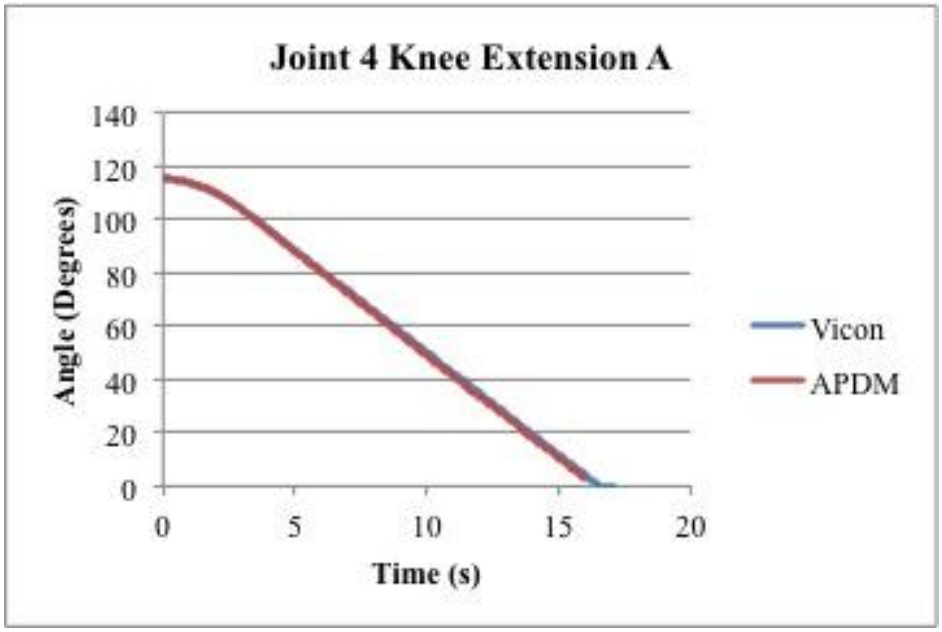

Figure 28 Joint 4 Knee Extension A

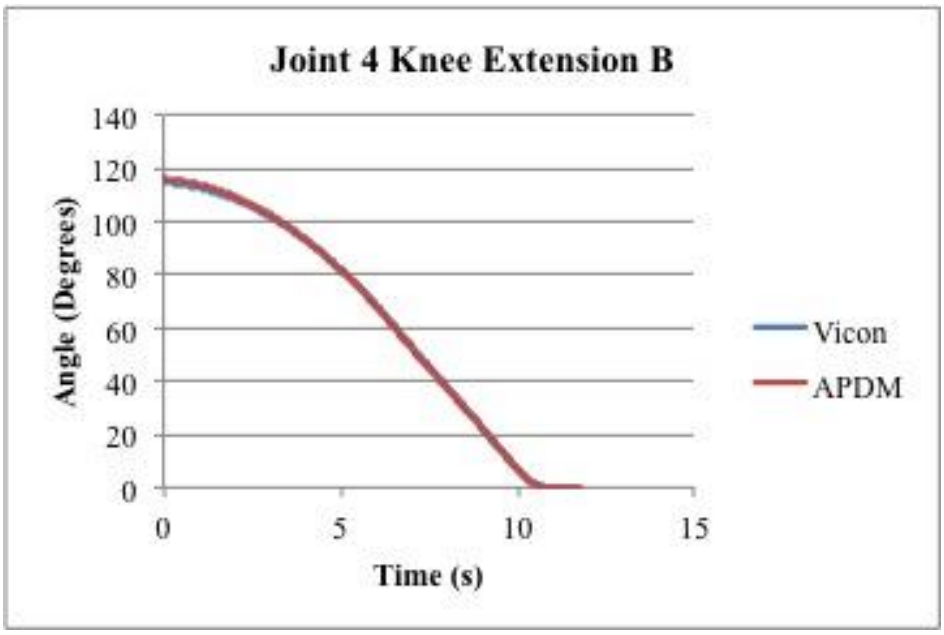

Figure 29 Joint 4 Knee Extension B

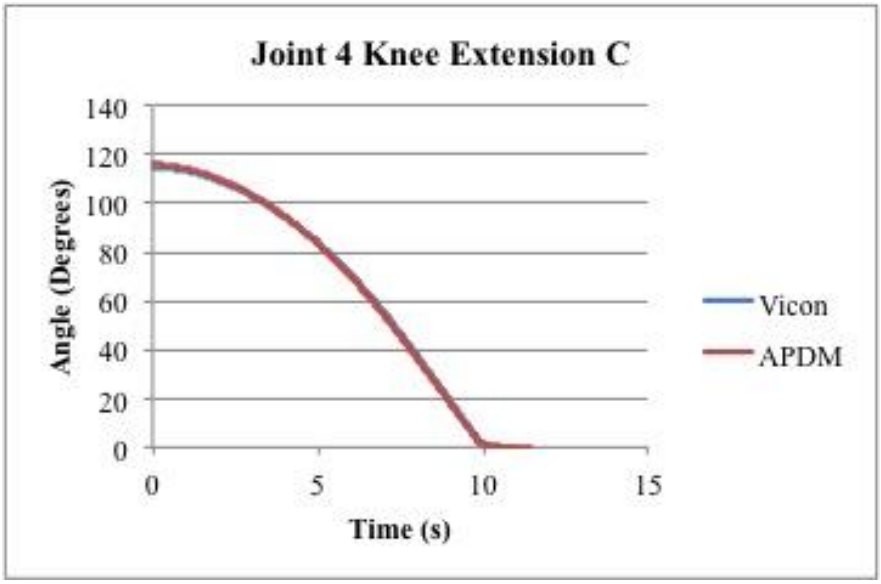

Figure 30 Joint 4 Knee Extension C

Table 4 shows the RMSE in degrees between the Vicon and APDM joint angle calculations for the single joint movements. The joint 4 "knee" angles for the APDM sensors were calculated using the two-sensor algorithm (Equations 2-6). The Pearson's R correlation values were all 0.999 except joint 3 hip internal rotation B which was 0.996.

Table 4 RMSE Between Vicon and APDM Sensors

Joint	Movement	RMSE (Degrees)
Joint 1	Hip Extension A	0.8
	Hip Extension B	0.4
	Hip Extension C	1.4
	Hip Flexion A	1.3
	Hip Flexion B	0.9
	Hip Flexion C	0.5
Joint 3	Hip External Rotation A	2.1
	Hip External Rotation B	2.1
	Hip Internal Rotation A	2.4
	Hip Internal Rotation B	1.8
Joint 4	Knee Extension A	1.0
	Knee Extension B	0.8
	Knee Extension C	0.9
	Knee Flexion A	1.0
	Knee Flexion B	1.4
	Knee Flexion C	1.1

The knee angle or joint 4 angle was calculated three different ways: the Vicon system, with the two-sensor algorithm and the sensor directly on the joint. An example of the comparison between the angles calculated by the Vicon system, two-sensor algorithm and the sensor on joint 4 are shown in Figure 31. The blue line represents the Vicon system, the red line is the two-sensor algorithm and the orange line is the sensor directly on joint 4.

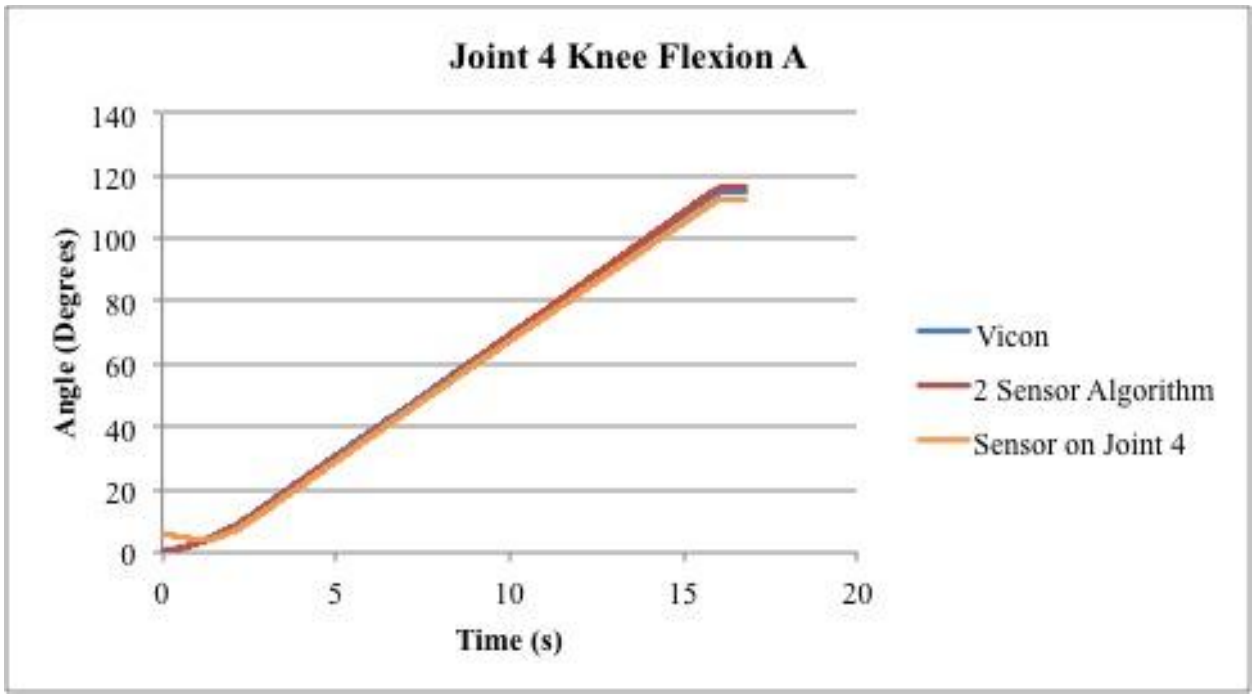

Figure 31 Comparison Between Algorithm and Sensor On Joint 4

The RMSE between the Vicon and the two-sensor algorithm, between the Vicon and the sensor on joint 4 and the two-sensor algorithm and the sensor directly on the joint 4 is shown in Table 5. The Pearson's R correlation values were all 0.999.

Table 5 RMSE for 3 Methods of Knee Angle Calculation

	Movement	RMSE (Degrees)		
		Vicon and 2 Sensor Algorithm	Vicon and Sensor on Joint	2 Sensor Algorithm and Sensor on Joint
Joint 4	Knee Flexion A	1.0	2.0	2.2
	Knee Flexion B	1.4	1.2	1.9
	Knee Flexion C	1.1	2.2	2.2
	Knee Extension A	1.0	2.3	2.5
	Knee Extension B	0.8	3.9	4.2
	Knee Extension C	0.9	2.1	2.7

Table 6 shows the angular velocity in degrees per second for each of the three systems: Vicon, APDM and WMRA.

Table 6 Angular Velocity

Link	Movement	Angular Velocity (deg/s)		
		Vicon	APDM	WMRA
Link 1	Hip Flexion A	2.6	2.7	2.6
	Hip Flexion B	3.4	3.3	3.5
	Hip Flexion C	3.5	3.6	3.6
	Hip Extension A	-2.5	-2.0	-2.5
	Hip Extension B	-3.1	-2.8	-3.2
	Hip Extension C	-3.2	-2.9	-3.2
Link 2	Hip Internal Rotation A	-4.3	-4.1	-5.2
	Hip Internal Rotation B	-4.5	-4.4	-5.7
	Hip External Rotation A	4.9	4.5	5.2
	Hip External Rotation B	4.7	4.7	6.0
	Knee Flexion A	6.8	6.3	6.8
	Knee Flexion B	10.3	9.7	10.2
	Knee Flexion C	10.2	10.1	10.8
	Knee Extension A	-6.7	-6.7	-6.8
	Knee Extension B	-9.6	-9.5	-10.1
	Knee Extension C	-10.2	-10.1	-10.7

All three joints were moved simultaneously during the 3-dimensional motion for five cycles, and two separate trials. The two trials for joint 1 are shown in Figure 32 and Figure 33.

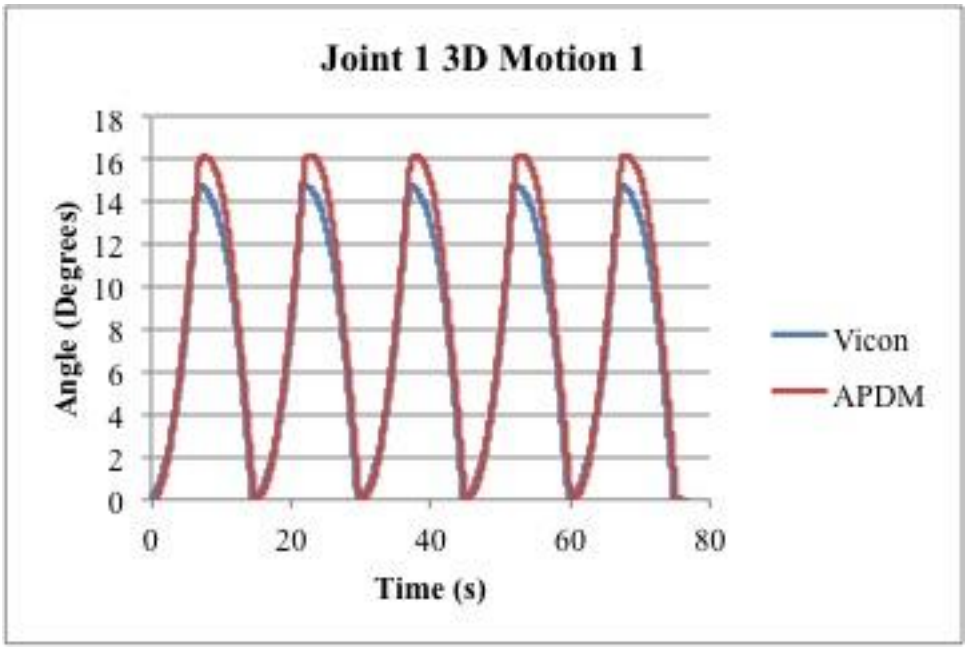

Figure 32 Joint 1 3D Motion 1

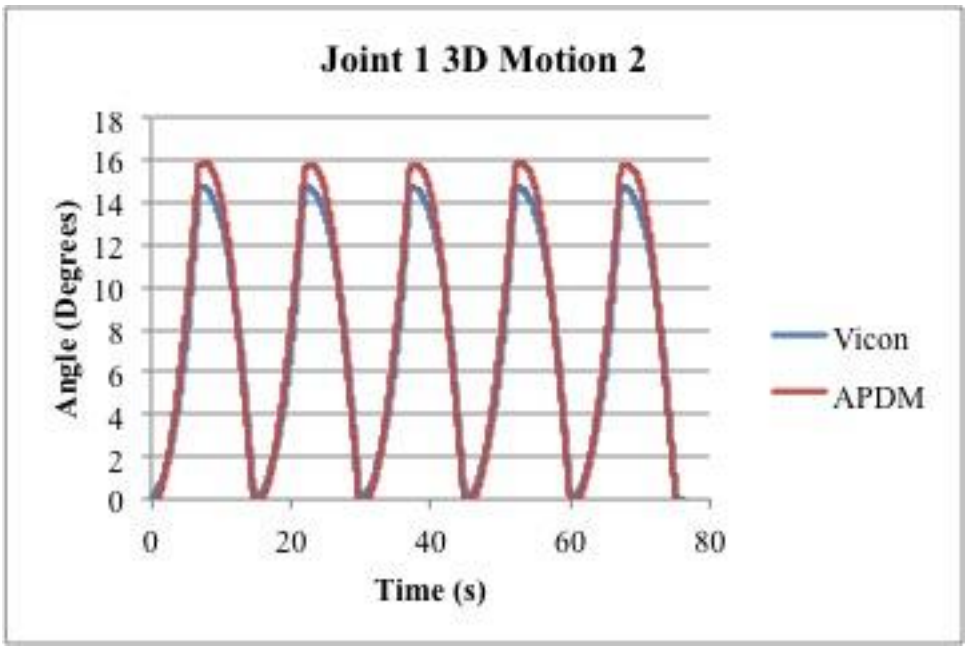

Figure 33 Joint 1 3D Motion

The movement of joint 3 during the 3-D trials is shown in Figure 34 and Figure 35.

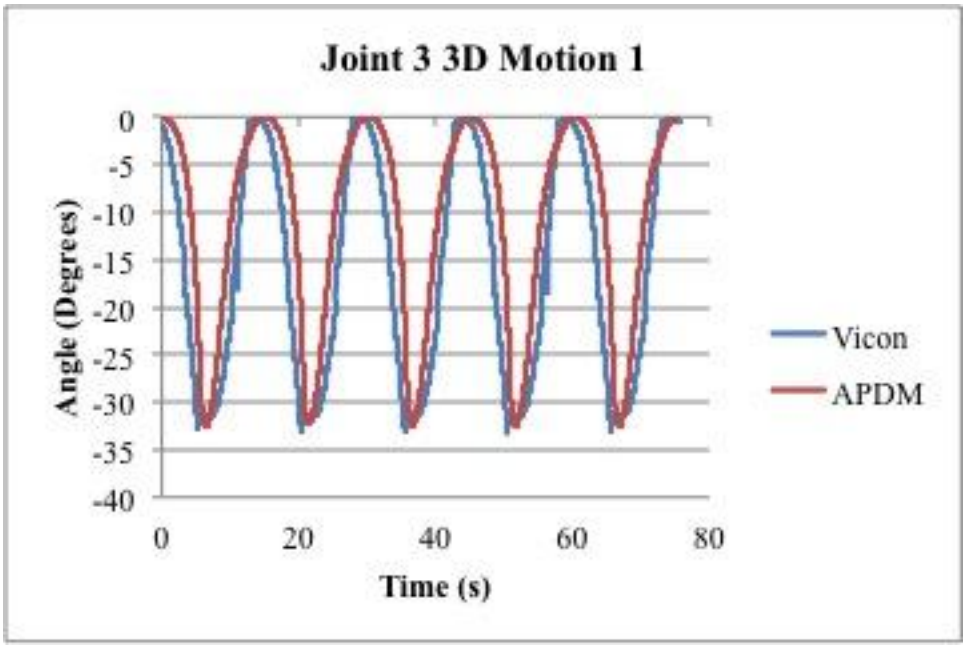

Figure 34 Joint 3 3D Motion 1

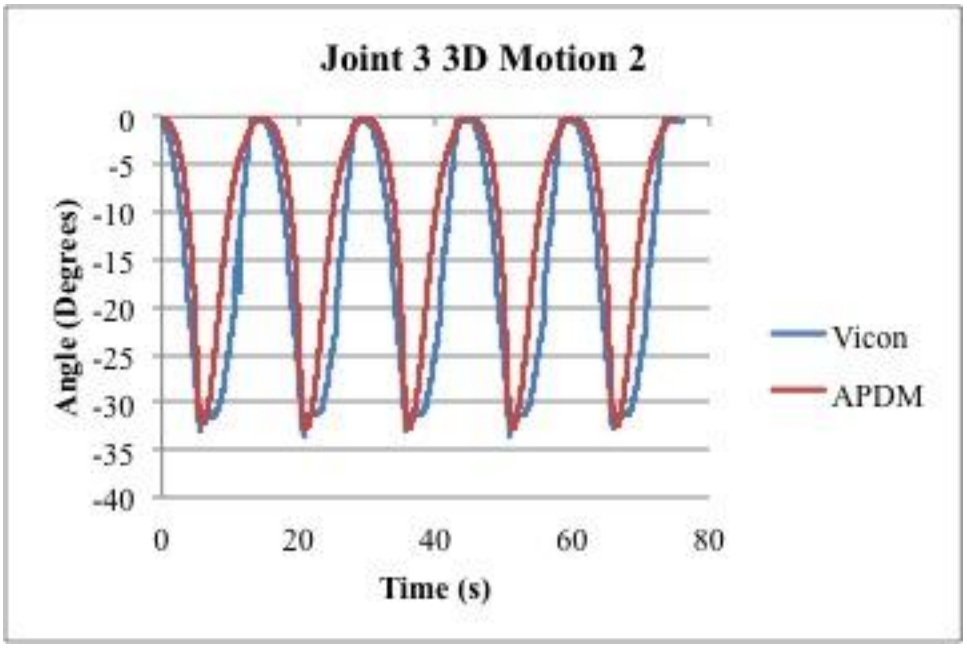

Figure 35 Joint 3 3D Motion 2

The movement of joint 4 during the 3-D trials is shown in Figure 36 and Figure 37.

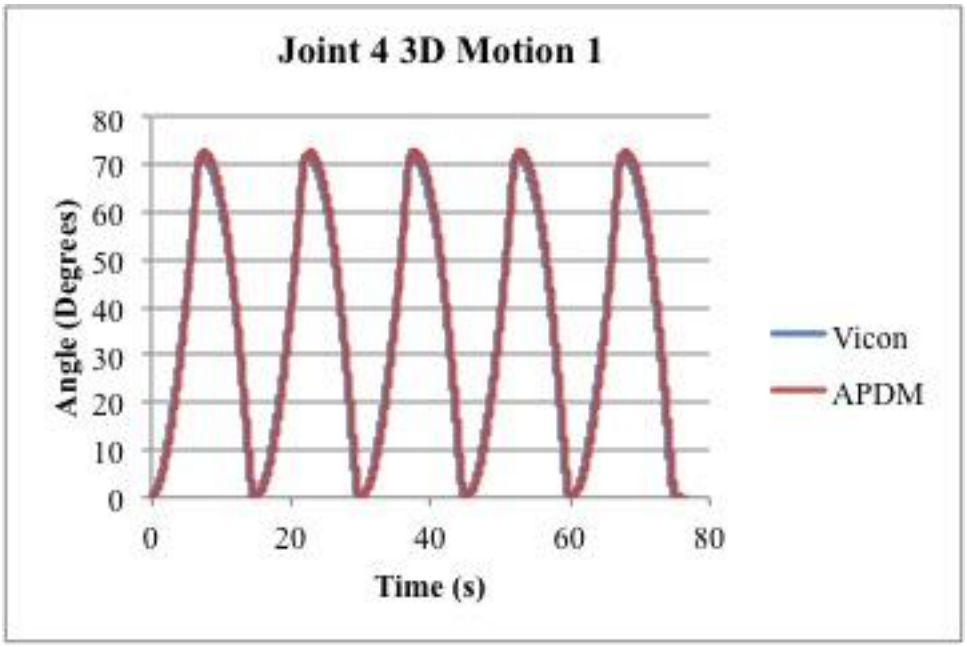

Figure 36 Joint 4 3D Motion 1

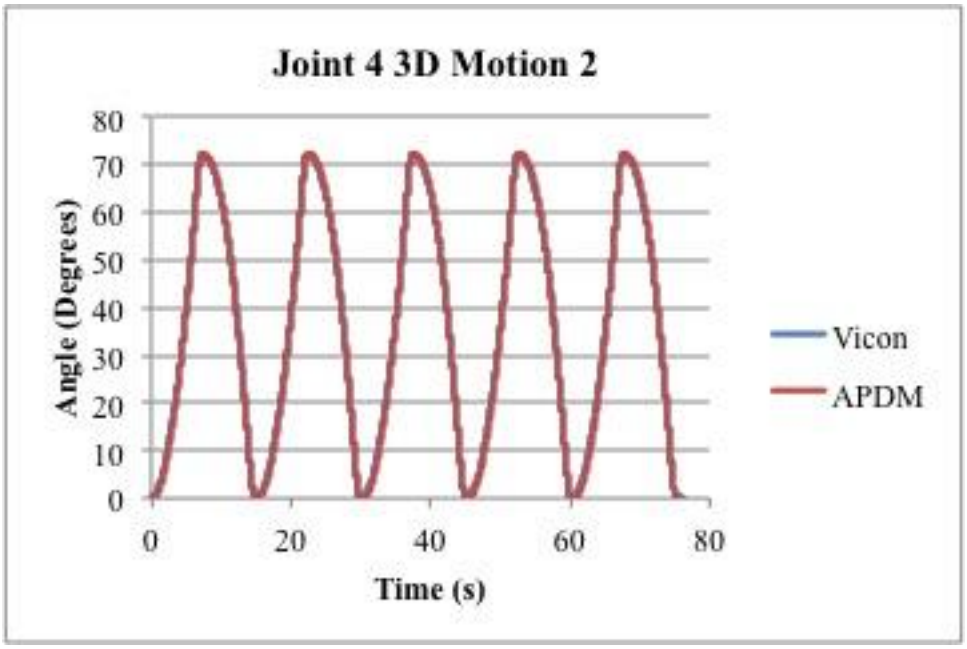

Figure 37 Joint 4 3D Motion 2

The RMSE and Pearson's R correlation between the APDM and Vicon calculations for 3D motion trials 1 and 2 are shown in Table 7.

Table 7 RMSE and R Values for 3D Motion Trials 1 & 2

APDM vs Vicon				
Joint	**3D Motion 1**		**3D Motion 2**	
	RMSE (Deg)	**Pearson's R**	**RMSE (Deg)**	**Pearson's R**
Joint 1	1.1	1.0	0.8	1.0
Joint 3	7.0	0.9	6.8	0.9
Joint 4	4.0	1.0	0.8	1.0

5.1.2 Range of Motion Tests

Figure 38 shows the range of motion test during the Vicon data collection.

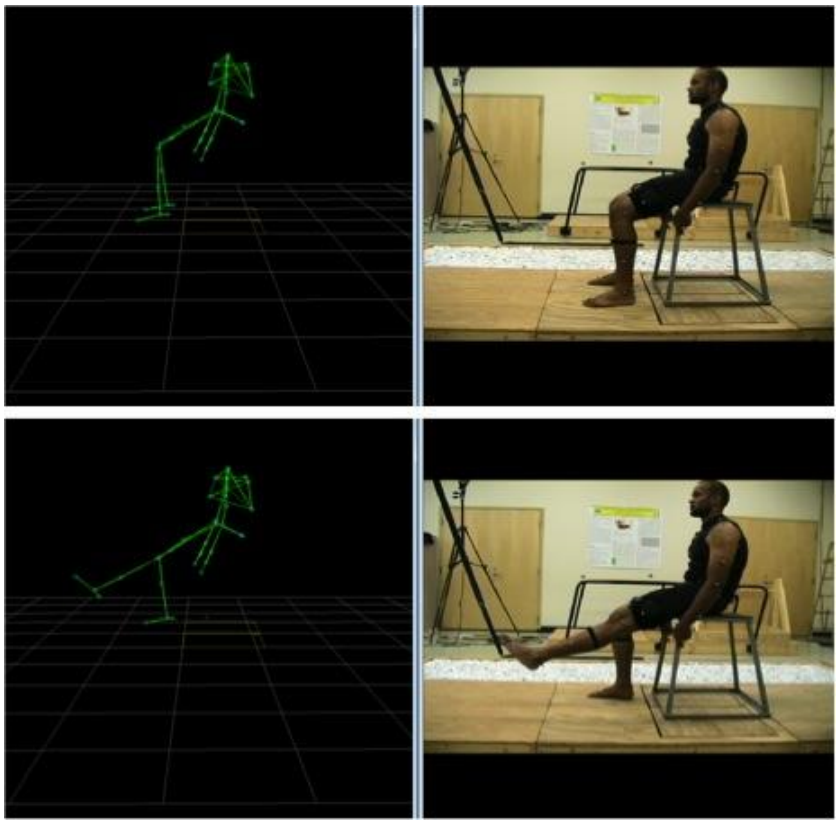

Figure 38 Range of Motion Test

The comparison between the knee flexion angle calculated by the WMAS and the Vicon system during the range of motion test is shown in Figure 39.

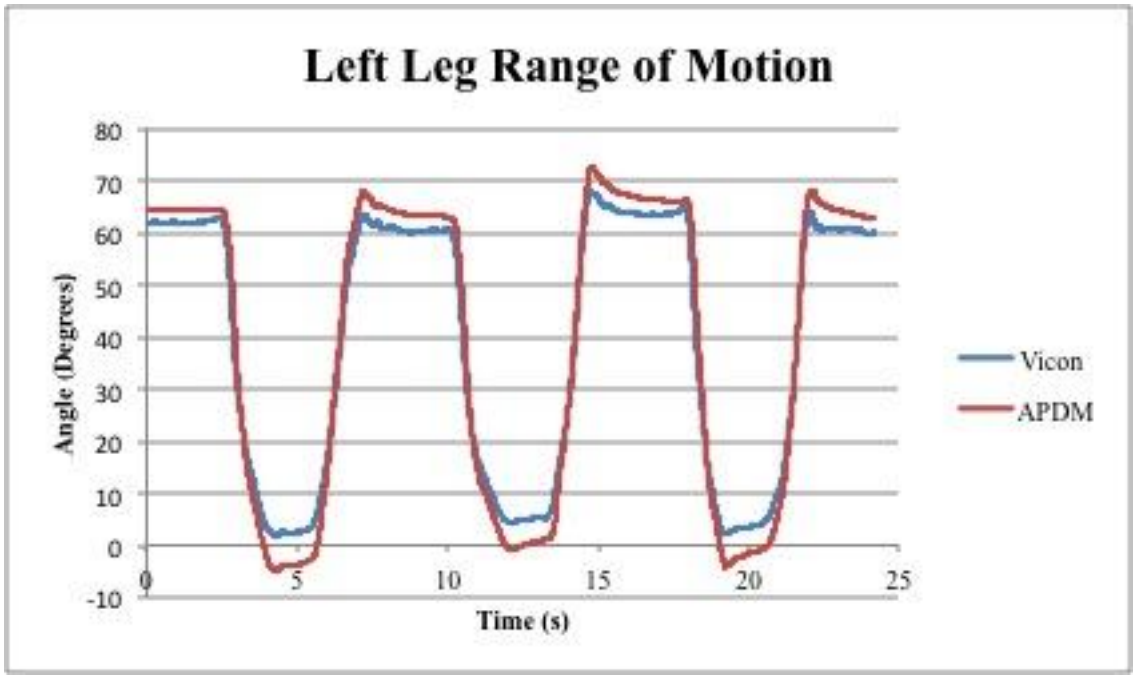

Figure 39 Left Knee Angle Range of Motion WMAS and Vicon

The RMSE and R Correlation for the range of motion tests are shown in Table 8.

Table 8 RMSE and R Values For Range of Motion Tests

	Left Knee Angle	
Trial	**RMSE (Degrees)**	**R**
ROM L1	4.0	0.998
ROM L2	4.1	0.998
ROM L3	4.3	0.998
Overall	**4.1**	**0.998**

5.1.3 Sit to Stand Tests

The sit and stand positions, as well as the Vicon plug in gait model and autolabel are shown in Figure 40. Figure 41 shows the comparison between the WMAS and Vicon calculated right knee angles during the sit to stand test.

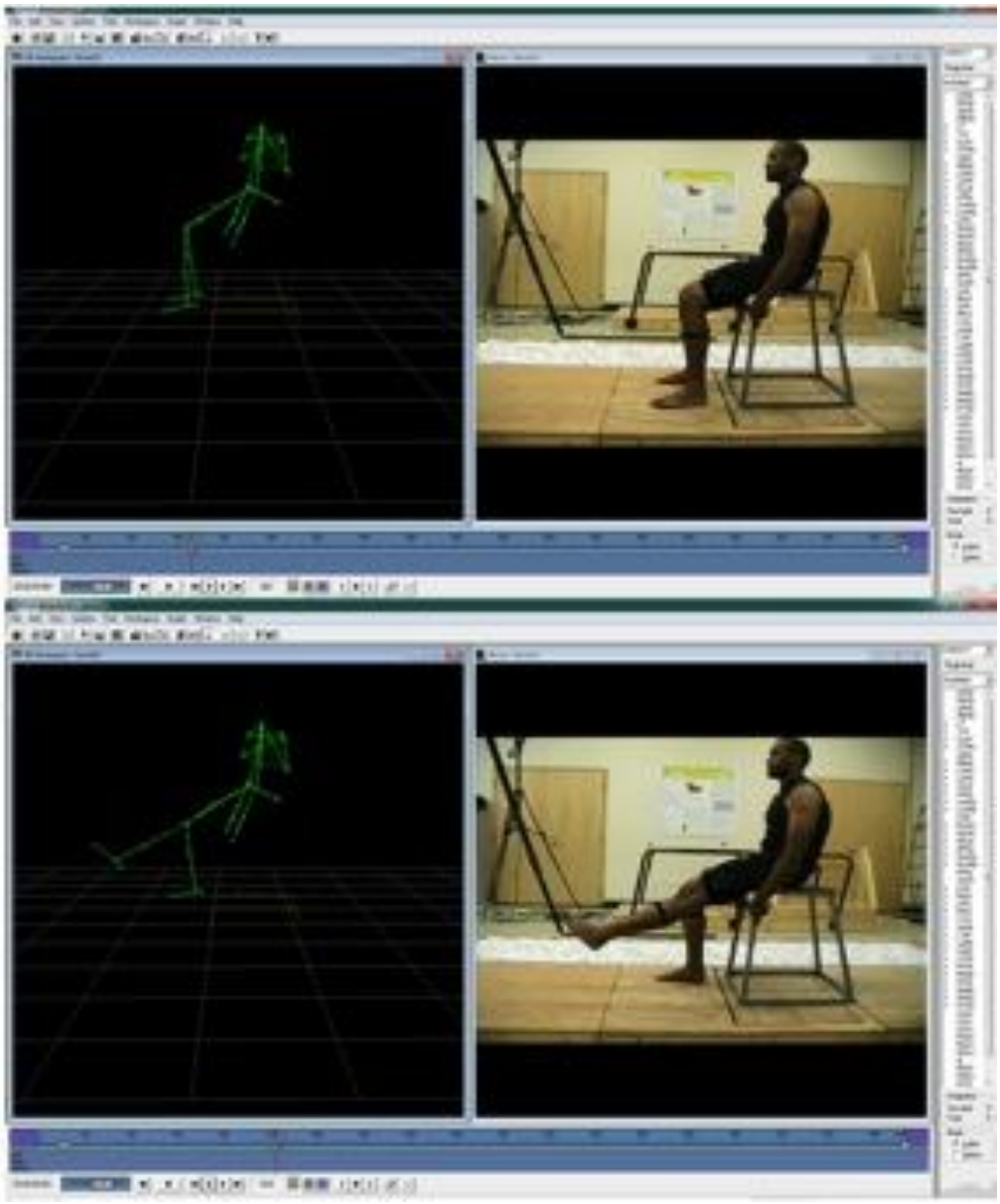

Figure 40 Sit To Stand Test in Vicon Workstation

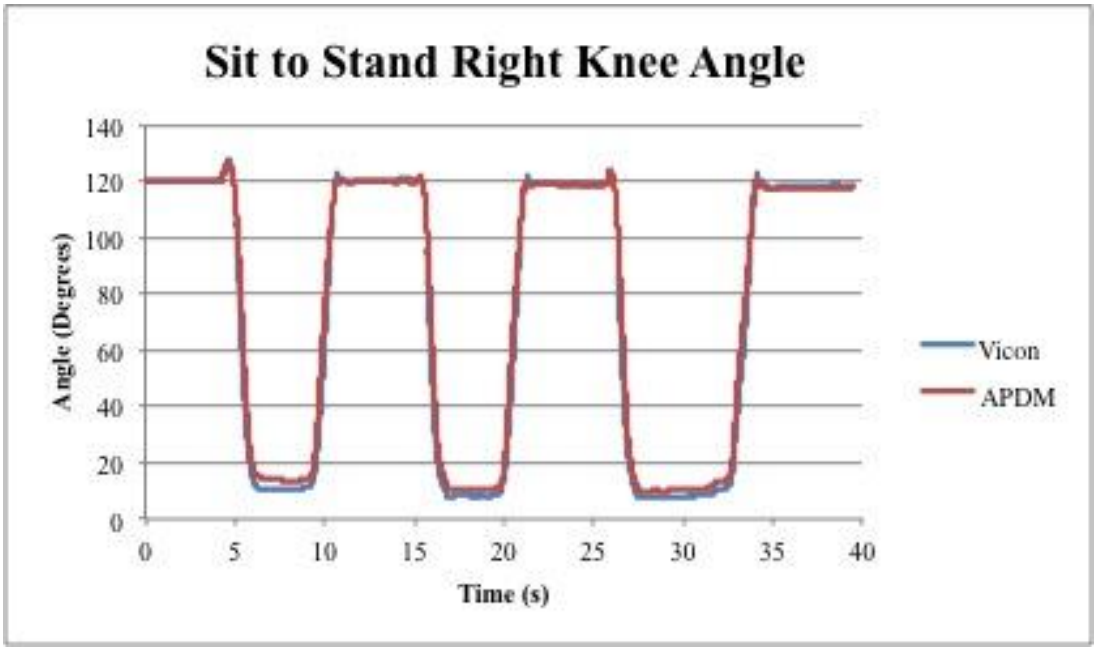

Figure 41 Right Knee Angle During Sit To Stand

The RMSE and R Values are shown in Table 9.

Table 9 RMSE and R Values For Sit To Stand Testing

	Right Knee Angle		Left Knee Angle	
Trial	**RMSE (Degrees)**	**R**	**RMSE (Degrees)**	**R**
STS 2	4.0	0.999	4.0	0.998
STS 4	5.2	0.999	5.4	0.999
STS 5	4.1	0.998	4.2	0.998
Overall	**4.4**	**0.999**	**4.5**	**0.998**

5.2 WMAS

The WMAS calculates knee flexion angle, stride length, and cadence. The results for each of these parameters are in sections 5.2.1, 5.2.2 and 5.2.3 respectively. The graphical user interface is also shown in section 5.2.4.

5.2.1 Knee Angle

Examples of the right knee flexion angle with the WMAS and Vicon system overlayed are shown in the following figures. An example of the right knee flexion angle during one slow gait cycle is shown in Figure 42. The knee flexion angle in degrees is shown as percent gait cycle. The WMAS angle is shown in red and the Vicon angle is shown in blue.

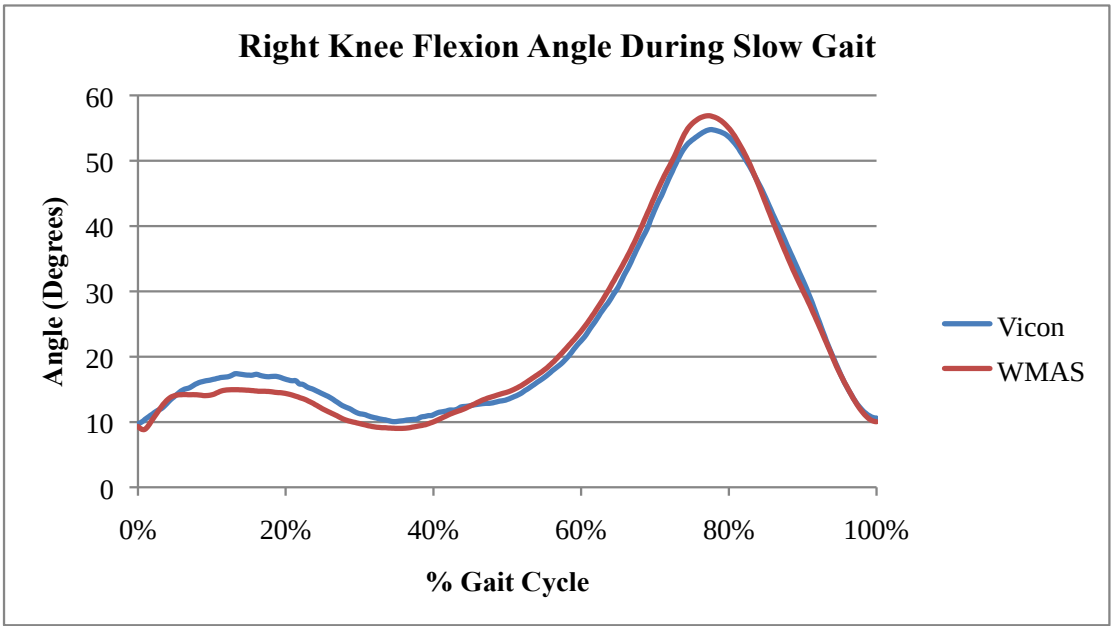

Figure 42 Right Knee Flexion Angle During One Slow Gait Cycle

An example of the right knee flexion angle during one normal gait cycle is shown in Figure 43. The blue line represents the knee flexion angle in degrees calculated by the Vicon system and the red line is the knee flexion angle calculated by the WMAS.

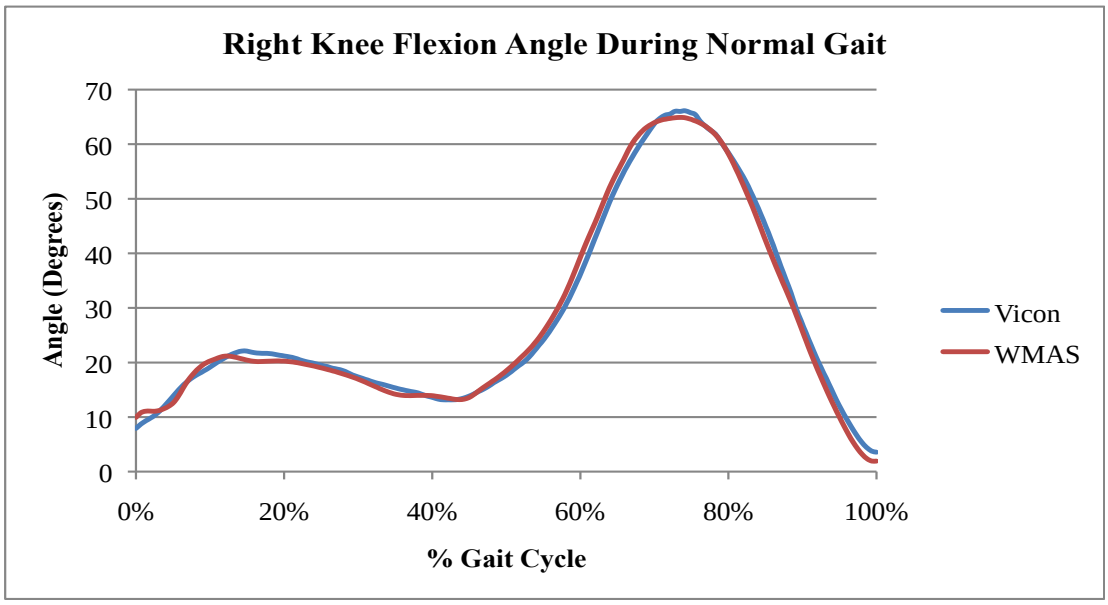

Figure 43 Right Knee Flexion Angle During One Normal Gait Cycle

Figure 44 shows an example of the right knee flexion angle calculated by both the WMAS and Vicon systems during one fast gait cycle.

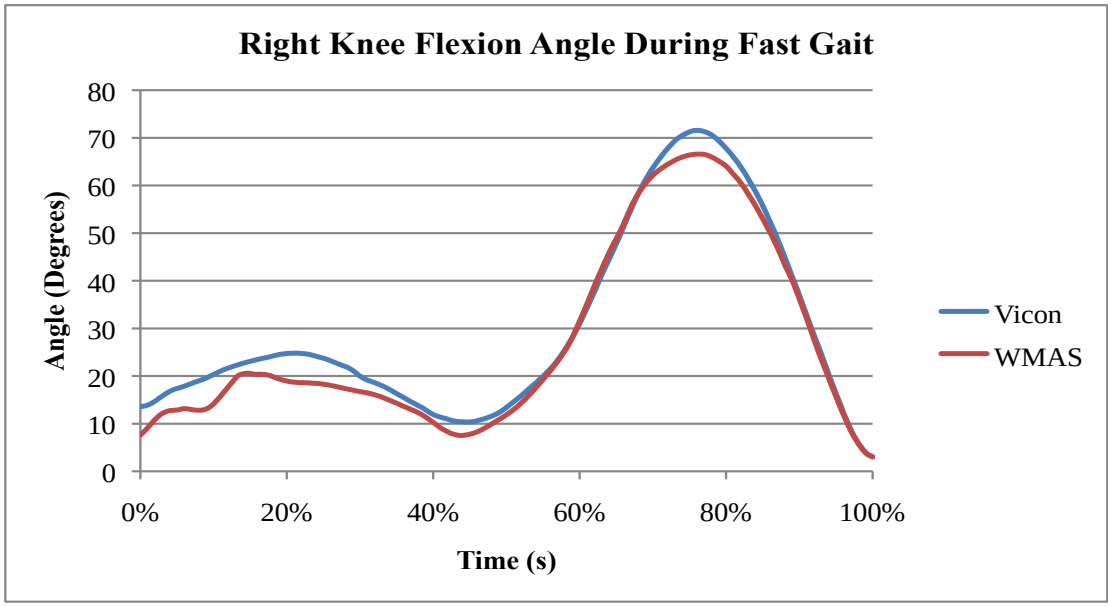

Figure 44 Right Knee Flexion Angle During One Fast Gait Cycle

The WMAS and Vicon knee flexion angles were compared for the all of the gait trials. The RMSE and R correlations values the knee flexion angle for the slow, normal and fast speeds is shown in Table 10.

Table 10 RMSE and R Values For Knee Flexion Angle

Speed	RMSE Right Knee Flexion (Degrees)	Pearson's R Right Knee Flexion	RMSE Left Knee Flexion (Degrees)	Pearson's R Left Knee Flexion
Slow	3.3	0.992	3.9	0.983
Normal	3.3	0.989	3.9	0.988
Fast	4.1	0.978	4.4	0.987
Overall	3.5	0.988	3.3	0.986

Each gait trial was separated in gait cycles and the maximum knee flexion angle was identified. The maximum knee flexion angle from the WMAS compared to the Vicon maximum knee flexion for each gait cycle. The RMSE for both the right and left knees at each of the three speeds is shown in Table 11.

Table 11 RMSE For Maximum Knee Flexion

Speed	RMSE Right Knee Max Flexion (Degrees)	RMSE Left Knee Max Flexion (Degrees)
Slow	2.6	2.3
Normal	2.6	2.8
Fast	3.5	3.4
Overall	**2.8**	**2.8**

The maximum knee flexion angle for one subject during slow gait as calculated by the WMAS and Vicon systems are compared in the Bland Altman plots shown in Figure 45. The top dashed line represents the mean of the APDM angle (degrees) minus the Vicon Angle (degrees) plus two standard deviations. The bottom dashed line represents the mean minus two

standard deviations. The upper and lower dashed lines are the limits of agreement. The center dashed line represents the mean for the maximum knee flexion angle in degrees. The Bland Altman plot for the maximum knee flexion during normal gait is Figure 46. The Bland Altman plot for the maximum knee flexion during fast gait is Figure 47.

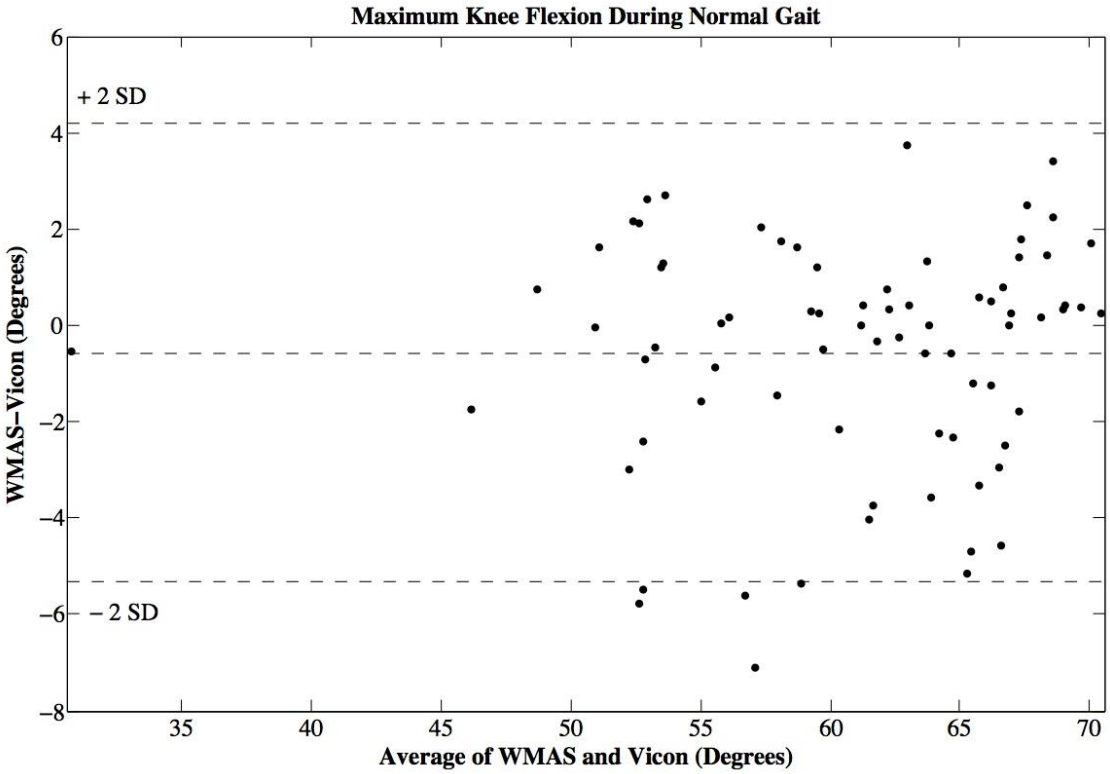

Figure 45 Bland Altman Plot: Maximum Knee Flexion During Slow Gait

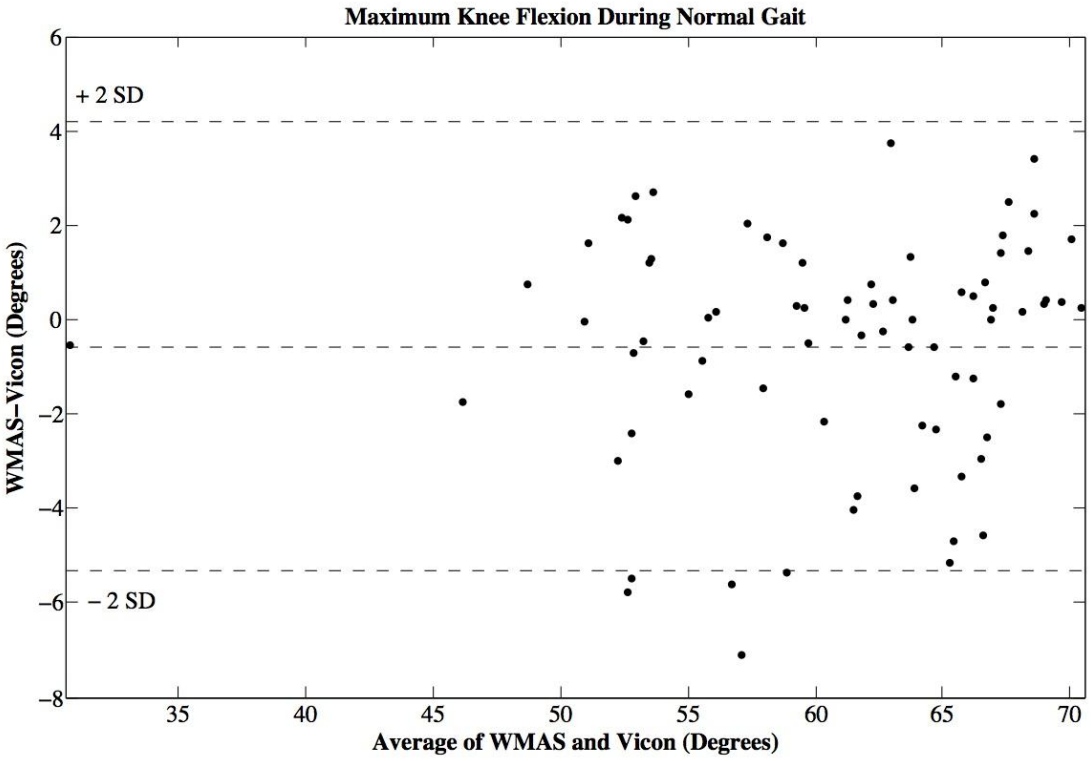

Figure 46 Bland Altman Plot: Maximum Knee Flexion During Normal Gait

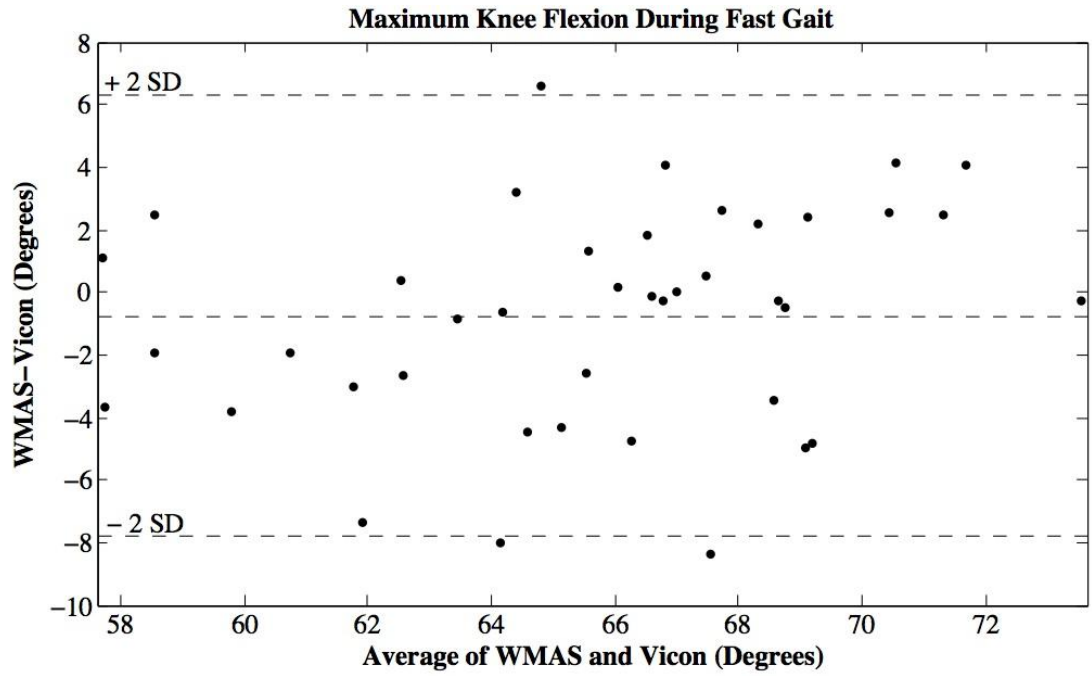

Figure 47 Bland Altman Plot: Maximum Knee Flexion During Fast Gait

5.2.2 Stride Length

The average stride length in meters at the slow, normal and fast speeds is shown in Table 12. The Pearson's R correlation values, RMSE and percent difference for stride length between the WMAS and Vicon system is shown in Table 13.

Table 12 Average Stride Length

Average Stride Length (m)		
Speed	**Vicon**	**APDM**
Slow	1.08	1.11
Normal	1.29	1.25
Fast	1.54	1.48
Overall	**1.30**	**1.27**

Table 13 Stride Length Statistics

Speed	Pearson's R	RMSE (m)	Percent Difference
Slow	0.91	0.056	1.96%
Normal	0.88	0.067	0.37%
Fast	0.87	0.136	5.31%
Overall	**0.89**	**0.091**	2.11%

Bland Altman plots for stride length are shown for the slow, normal and fast gait speeds for one subject in Figure 48, Figure 49 and Figure 50.

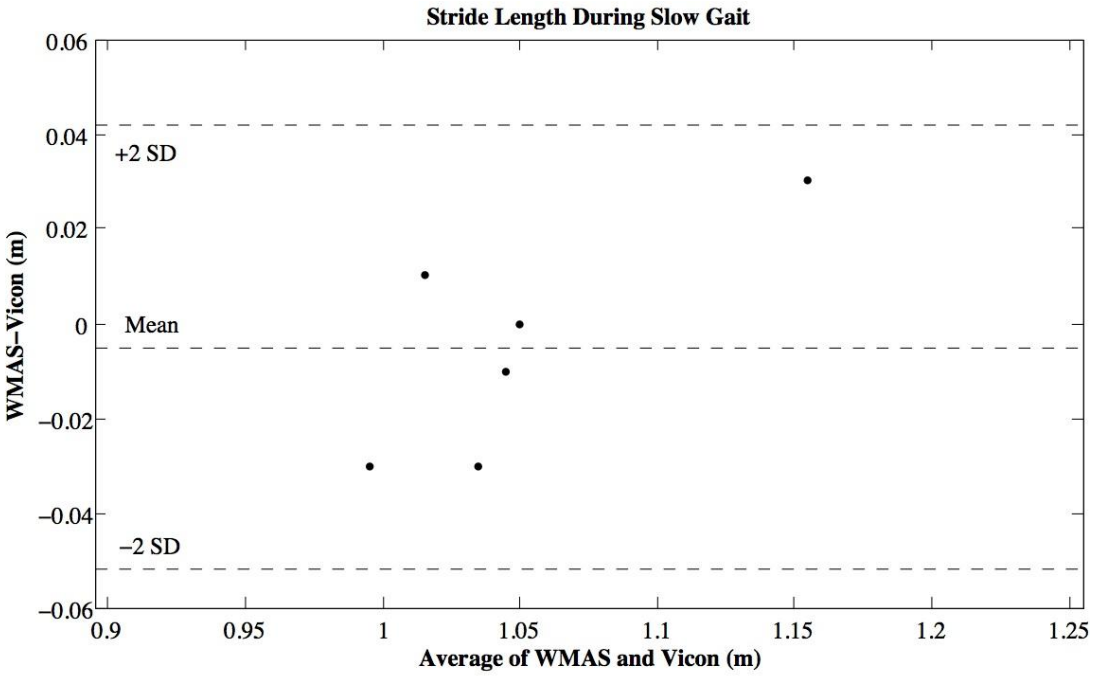

Figure 48 Bland Altman Plot: Stride Length During Slow Gait

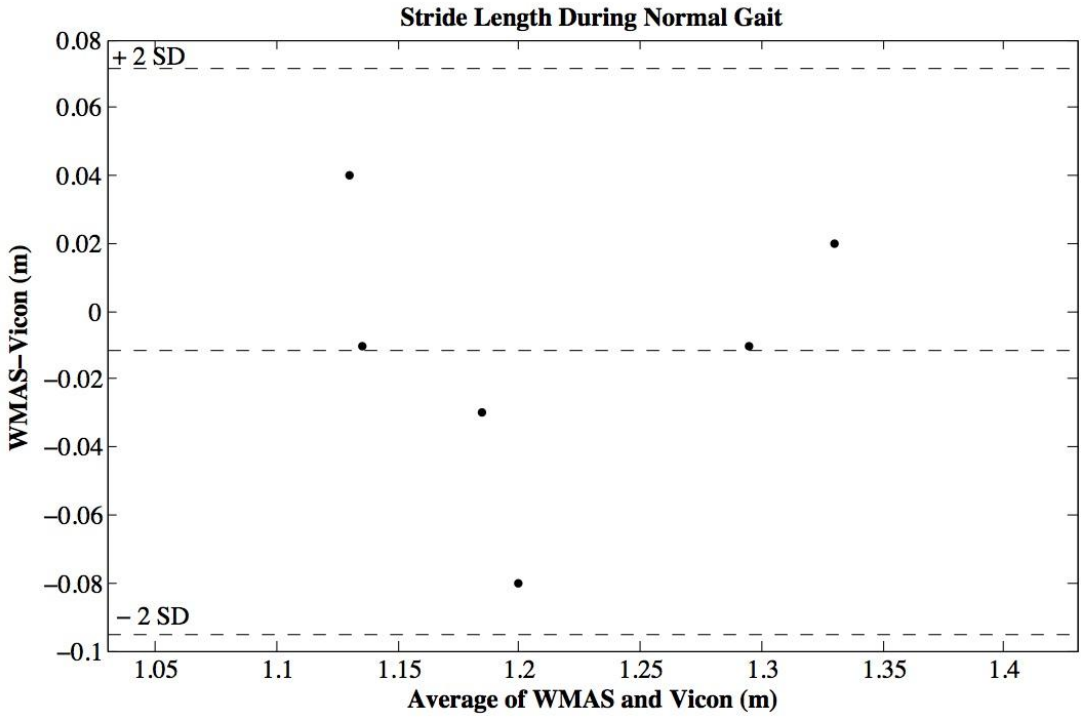

Figure 49 Bland Altman Plot: Stride Length During Normal Gait

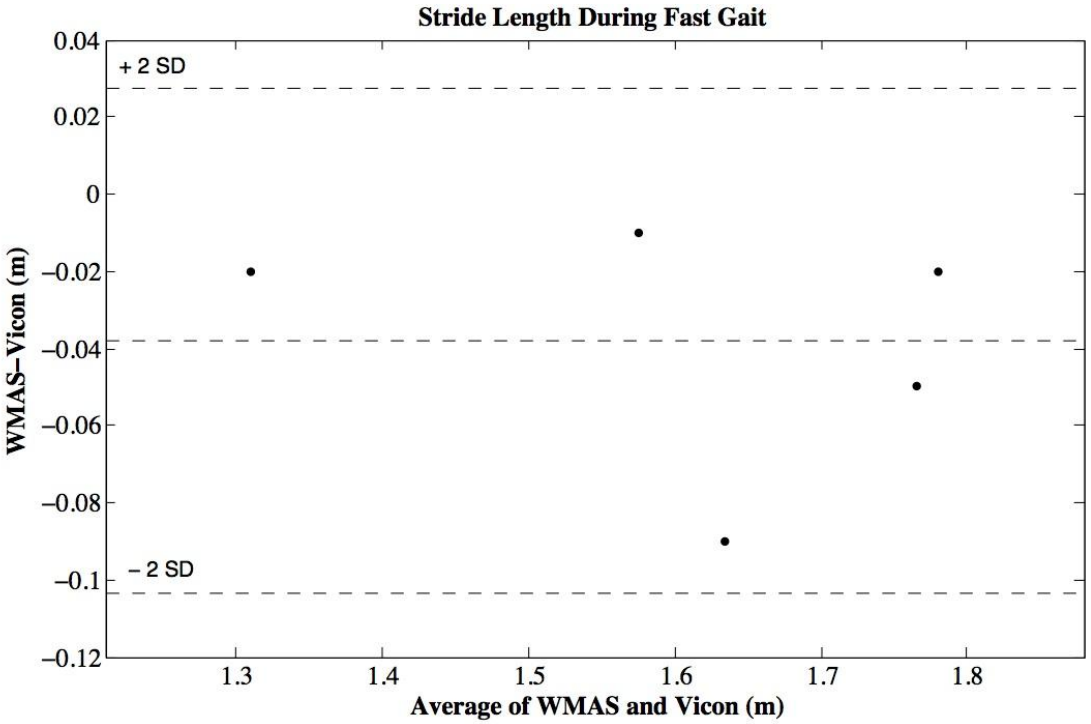

Figure 50 Bland Altman Plot: Stride Length During Fast Gait

5.2.3 Cadence

Cadence was calculated from the WMAS and Vicon system and the results are shown in Table 14. The average cadence is reported in steps per minute at each of the three speeds.

Table 14 Average Cadence

Speed	WMAS (steps/min)	Vicon (steps/min)	Pearson's R
Slow	70	71	0.951
Normal	96	94	0.933
Fast	123	120	0.908
Overall	96	95	0.931

5.2.4 Graphical User Interface

A graphical user interface (GUI) was created in Matlab to display the knee angle analysis as shown in Figure 51. The GUI has a drop down menu to select which trial to plot.

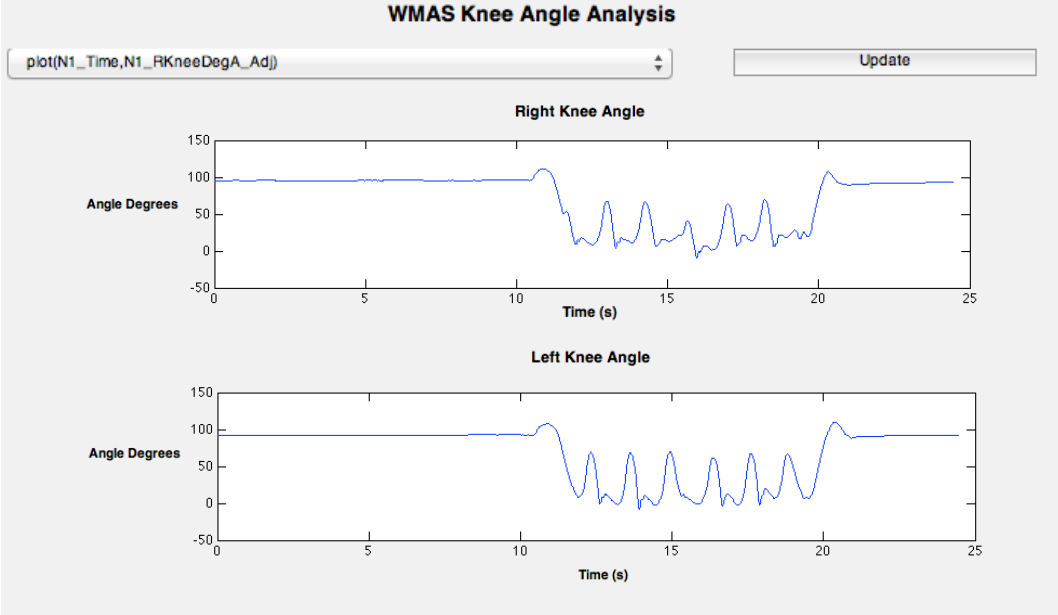

Figure 51 Knee Angle GUI

The GUI can also display two knee angle trials on top of each other as shown in Figure 52. This is a useful feature if you want to compare two separate trials, or a new to a baseline trial.

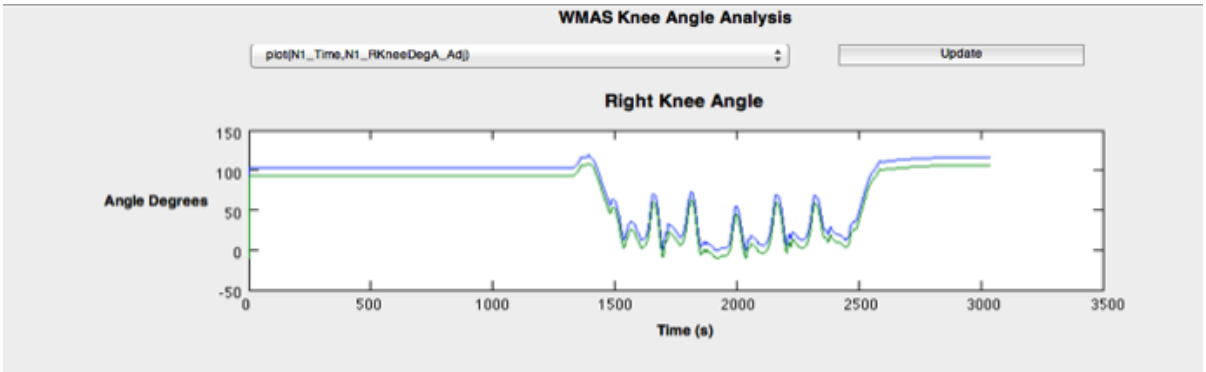

Figure 52 Knee Angle GUI Comparing Two Knee Angles

CHAPTER 6: DISCUSSION

6.1 Verification Tests

The purpose of the verification tests was to show that the WMAS algorithm calculated the knee flexion angle within 5 degrees of error relative to the gold standard Vicon motion capture system.

The first step of the verification testing used a robotic arm to provide a repeatable movement. These movements allowed for the comparison between the Vicon optical motion capture system and the APDM Opal IMU system in terms of joint angle calculation, angular velocity and trajectory recognition.

During the linear or single joint movements, the calculated joint angles from the Vicon, APDM and WMRA systems shown in Figures 4-6 were very similar. The three speeds did not seem to have a significant effect on the joint angle calculations. The joint angles calculated by the Vicon and APDM systems for the linear movements had an average RMSE of 1.2 degrees. The Vicon and APDM systems were also strongly correlated with a Pearson's R correlation value of 0.998. According to manufacturer, the APDM Opal sensors have a static roll/pitch orientation accuracy of 1.15 degrees, a static heading orientation accuracy of 1.50 degrees and dynamic orientation accuracy of 2.80 degrees [82]. Therefore, the quaternion-based algorithm improved the accuracy of the APDM sensors. The largest deviations in joint angle between the three systems were most apparent in the joint 3 hip internal and external rotation movements.

The APDM sensor begins to drift towards the end of each trial. Joint 3 hip internal and external rotation trials have an average RMSE between the Vicon and APDM sensors of 2.1 degrees; nearly double the average RMSE for all linear movements. This is because the APDM sensors begin to drift at the end of each trial.

When the Vicon system and two-sensor algorithm was compared the average RMSE for the knee flexion angle was 1.0 degree. Since the Vicon system is considered the gold standard for gait analysis, this shows that the two-sensor algorithm accurately calculates the knee flexion angle within a clinically acceptable range. The RMSE was less than the results reported by Schiefer et al. and Toffola et al [44, 45] and the manufacturer's specifications. The comparison between the Vicon system and sensor directly on joint 4 had a RMSE of 2.3, which was nearly double the error calculated by the two-sensor algorithm. The RMSE between the two-sensor algorithm and the sensor directly on the joint was 2.6 degrees.

The angular velocity measurements from the APDM sensors came directly from the data from the gyroscope sensor and the manufacturer's calibration, whereas the Vicon and WMRA angular velocities were calculated using the time and angle measurements. The correlation between the Vicon system and APDM average angular velocities was the highest with a Pearson's R-value of 0.999 and RMSE of 0.29 degrees per second. The WMRA and Vicon had a correlation value of 0.997 and an average RMSE of 0.57 degrees per second. The WMRA and Vicon systems had an R-value of 0.997 and an average RMSE of 0.69 degrees per second. Since the APDM sensor directly measures the angular velocity, it makes sense that the APDM and Vicon comparison has the highest correlation and lowest RMSE, followed by the APDM and WMRA comparison. The APDM angular velocity towards the end of each trial the measurements did not drift significantly, the signals were a little noisy but remained relatively

constant. This is likely due to the calibration of the gyroscope data. The raw gyroscope data was noisier than the calibrated data, and contained some drift. When the joint angles were calculated by integrating the gyroscope signal, the drift continually increased and the error was compounded over time. However, the manufacturer's calibration seems to correct the gyroscope drift, so drift was not a significant problem in this study.

The last trials collected were the two three-dimensional trials where all three joints moved simultaneously for five complete cycles. All three systems had been running for several hours and the calibration files were not reset for any of the systems. The largest differences between the three systems joint angles, particularly the WMRA, were evident in the 3-dimensional motion trials. These trials also had some of the highest RMSE, particularly for joint 3. Before beginning the study, time-based effects were expected to be a factor and source of error. Knee angle calculations using the two-sensor algorithm for both 3-D trials 1 and 2 were still within a clinically acceptable range, even after several hours of data collection.

The management of several hours of IMU data in this study was possible due to the MATLAB (Mathworks, Natick, MA) algorithm and the ability to save each trial separately in the Motion Studio program. However, the APDM Opal sensors are capable of on board data storage, which would allow for continuous data collection outside of a laboratory setting during activities of daily living. The calculations of the joint angles would be similar to having separate trials, however the processing time of the MATLAB algorithm would be increased. The problems with data management would arise when attempting to separate different activities.

The manufacturer's calibration of the APDM sensor gyroscopes limited the drift and time-based effects. As a result, the APDM sensor algorithm accurately calculated the joint angles well within a clinically acceptable range relative to the gold standard Vicon gait analysis system.

The range of motion and sit to stand tests were an additional method used to verify the WMAS knee angle calculation algorithm. Both the range of motion and sit to stand tests had a RMSE of less than 5 degrees when compared to the Vicon system. A potential source of error in these tests was the height of the stool that the subject sat on. The stool did not allow the subject to begin with their legs at a 90-degree angle and it was difficult for the subject to sit completely upright. However, the stool was used rather than the chair used during the rest of the gait trials because the RPSI and LPSI markers were blocked from the view of the cameras by the back of the chair. Since three markers are needed to define a segment, the pelvis could not be defined at the start of the trials due to drop out of two of the four pelvis markers. The pelvis is used as a reference segment for the legs, and as a result the knee angles could not be calculated using the chair. Another potential source of error was movement of the pelvis markers during the trial. The pelvis markers were attached to the elastic belt on the APDM strap, and moved slightly during the trials. However, these tests showed that WMAS was able to accurately measure the knee flexion angle within the goal of 5 degrees error relative to the Vicon system and within clinically acceptable range.

6.2 Comparison Between Vicon and WMAS

The Vicon and WMAS were compared for three gait parameters: knee flexion angle, stride length and cadence. The three verification tests were the first methods that were used to compare the WMAS and Vicon system. As mentioned previously, the Vicon motion analysis

system is the gold standard for gait analysis and was used to validate the algorithms and accuracy of the WMAS.

The goal of the WMAS knee angle calculations was to have less than 5 degrees of error relative to the Vicon system. The RMSE for the WMAS was less than 5 degrees for both the entire trial comparisons and the maximum knee flexion angle comparison. For the entire gait trial comparisons, the RMSE for the right knee during the slow, normal and fast speeds was 3.3 degrees, 3.3 degrees and 4.1 degrees respectively. The left knee flexion RMSE were slightly higher than those calculated for the right knee. Slow, normal and fast RMSE for the left knee were 3.9 degrees, 3.9 degrees and 4.4 degrees. For both the left and right knee flexion angles, the R correlation values were between 0.983 and 0.992. The overall RMSE and Pearson's R correlation values for the right knee were 3.5 degrees and 0.988, whereas the left knee was 3.3 degrees and 0.986.

The maximum knee flexion angles were also well within under the goal of 5 degrees of error with an overall RMSE of 2.8 degrees. Analysis of the bland altman plot shows that the maximum flexion angles were well with an error of 5 degrees, with the exception of a few outliers. The bland altman plot was used to show a comparison between the Vicon and WMAS measurements, and to validate if the WMAS is an acceptable alternative to the gold standard. Unlike Pearson's R correlation, the bland altman plot does not assume a linear relationship between the values. The limits of agreement are the top and bottom dashed lines in the figure representing the mean +/- two standard deviations. Since the limits of agreement fall within a clinically acceptable range, it can be assumed that the WMAS is a reliable alternative to the Vicon system.

There are several potential sources of error for the knee angle calculations. The potential error sources related to the Vicon system include misplacement of the knee markers. These markers are difficult to locate properly, and a slight offset could affect the location of the knee joint center. An additional source of error related to the Vicon system is the movement of the pelvis markers during the trials due to their placement on an elastic belt on the waist and the movement of the subjects shirt and in turn the reflective markers. The potential error sources related to the WMAS include misalignment of the APDM sensor with the axes of the thigh and shank, magnetic interference and movement of the sensors during the trials. Magnetic interference may have occurred due to the force platforms, solo step, cameras and computer system, but did not seem to have a major effect on the results. Lastly, the sensors were not calibrated before each data collection. The Motion Studio software has been updated since the collections for this study were completed and now includes a calibration feature that can recalibrate the gyroscopes and magnetometers before beginning data collection. It is expected that recalibrating the sensors before every data collection would improve the results.

Another goal of this study was to improve the stride length calculations in a previous study using the APDM sensors by Simoes. Simoes reported stride length R correlations of 0.776, 0.8 and 0.817, which correspond to normal, fast and slow speeds, and an overall correlation of 0.861 [3, 35]. In this study the stride length calculations were improved at all three speeds as well as in the overall correlation. The highest correlation value for stride length in this study was 0.91 at slow speed. The normal and fast correlation values were 0.88 and 0.87 respectively. Overall the stride length correlation was 0.89. In addition to the correlation values, the overall average RMSE was 0.091m, with the slow speed having the lowest RMSE at 0.056m. The limits of agreement from the stride length Bland Altman plot for slow gait also

show that the error between the two methods at slow speed was approximate 0.05m. Since the literature has shown that subjects with TBI tend to walk slower, so the WMAS will be able to calculate the TBI parameters accurately. The overall percentage difference between the WMAS and Vicon stride length calculations was 2.11%.

In the WMAS, a peak detection method was used to identify the heel-strike and toe-off gait events from the angular velocity signal. However, manual inspection was necessary to avoid selection of noise in the signal rather than a peak or gait event. A filtering technique should be used in the future to eliminate the need for manual inspection of the locations of the gait events.

The WMAS was able to achieve the goals of 5 degrees or less of error in the knee flexion measurements and improve upon previous stride length results.

6.3 Comparison Between WMAS and Previous Work

There are several differences between the WMAS and the previous work with IMUs mentioned in Chapter 2. One significant difference is a lot of the systems contain wires connected to a data logger, and are not small or practical for a person to wear during their activities of daily living. Another difference between previous work and the WMAS is the gait parameters were calculated directly not from integrating gyroscope or accelerometer signals. This resulted in a smaller error due to the elimination of error propagation and drift accumulation during integration. The WMAS was also validated against a gold-standard, industry leading, Vicon optical motion capture system rather than a video camera based, magnetic or ultrasound system. No extensive filtering, such as Kalman filtering, was used in the WMAS but was popular in previous work. The WMAS is different from the iTUG plug-in used by Simoes because the data is based off individual subject measurements rather than a

normative database, the data is output into columns and graphs that are editable rather than a standard template report that cannot be edited, and the equations and calculations are known to the user rather than a "black box" type software. The other major advantage to the WMAS is the gait parameters and knee angles are calculated directly from the orientation data rather than the integration of the sensor data. In addition the WMAS can be used for other activities and gait tests, other than just the TUG test, which is the only test Simoes was able to perform [3, 35].

The WMAS RMSE for knee flexion angle was 3.3 degrees for the normal and slow speeds and 4.1 degrees for the fast speed during gait, which were lower than those reported in the literature. For example, Schiefer et al. used accelerometers and gyroscopes to calculate knee flexion during several activities of daily living compared the data to an optical camera system with a RMSE between 4.6 and 7.1 degrees [46]. Watanabe reported RMSE of 4-5 degrees, and 7 degrees without a Kalman filter, which are also higher than those from the WMAS [46]. Pochappan reported a RMSE of 9.12 degrees, nearly triple the error calculated by the WMAS [48]. The Xsens MTx sensors are a similar product to the APDM Opal sensors, however Cloete and Scheffer reported RMSE of 7.6 degrees for the knee flexion angle using the Xsens software [47]. RMSE from the WMAS were not as small as Dejnabadi [83] or Cooper [59], however, these systems were not validated with an optical motion capture system. Lastly, Favre reported lower average RMSE for knee flexion angle but used several calibration and alignment procedures prior to data collection [52, 54, 55], which were not used with the WMAS.

The work by Aminian [38] and Salarian [39] was used in the WMAS to identify the gait events or heel-strike and toe-off from the angular velocity signal from the shank IMU. However, unlike Aminian [38] and Salarian [39], the gyroscope data was not integrated to get

the segment angles that are necessary to calculate parameters such as stride length. The WMAS calculations for stride length were similar to Zexi, however their equations were used to calculate step length and the segment angles were calculated by integrating the angular velocity [65]. Aminian reported RMSE of 0.07 meters and 7.2% error for stride length calculations [38], which are slightly higher than the WMAS. The WMAS has a RMSE of 0.056 meters and 0.067 meters for slow and normal gait speeds, and an average error of 2.11%. Salarian reported lower stride length RMSE than the WMAS with 3.5 centimeters, however Salarian used filtering and a more complex gait double pendulum and inverse double pendulum gait model [39]. Doheny reported a RMSE of 0.09 meters and an R correlation of 0.84 for stride length calculations [63]. The WMAS performed better during slow and normal speeds, and had about the same average RMSE for all three speeds (0.091 meters) with an R correlation of 0.89. Lastly, as previously mentioned the stride length calculations were improved with the WMAS relative to the work by Simoes with the APDM Opal sensors [3].

6.4 Graphical User Interface

A graphical user interface was also created in Matlab for use with the knee angle analysis during gait. The user is able to select the data which they have previously collected and plot both the right and left knee flexion angles, or compare a knee flexion angle to one collected previously as a baseline. This will allow for visual analysis of the knee angle during gait. A future improvement includes adding the values for maximum knee flexion. Future work could also involve adding the stride length parameters. The GUI could also be programmed to collect the data directly from the sensors rather than from Motion Studio. This would allow for collection and analysis in one easy to use tool.

6.5 Limitations of this Research

There are several limitations of this research in addition to the previously discussed sources of error. The main limitation is a small sample size of only healthy; generally young subjects participated in the study. Ten healthy individuals with an average age of 27 participated in the study. The ultimate application of the study is for mTBI and TBI research, as well as concussion or return to duty diagnosis, which would require an additional validation study. Another limitation is the use of a short gait lane in a defined laboratory setting. However, despite these limitations the WMAS showed it was able to calculate gait parameters within a clinically acceptable range to the gold standard Vicon motion capture system.

6.6 Applications of WMAS

The WMAS has several applications including use in a physical therapy or rehabilitation clinic, data collection outside of a laboratory setting during a person's normal activities of daily living, on the sidelines at sporting events or in the battlefield to analyze concussion injuries, and to determine return to duty or return to play after a head injury.

CHAPTER 7: CONCLUSION

The purpose of this study was to develop a wearable motion analysis system to evaluate gait parameters that are indicative of gait deviations, particular those relevant to mTBI and TBI. In addition to developing the WMAS, one of the goals of this project was to calculate knee flexion angle within 5 degrees of error of the Vicon optical motion capture system. The other goal was to improve the stride length calculations from Simoes [3]. Both of these goals were met as the RMSE of the knee flexion angle was 3.5 degrees relative to the Vicon system and the stride length correlations were increased to strong correlation values of 0.91, 0.88 and 0.87 corresponding to slow, normal and fast speeds. The WMAS is a powerful clinical tool for gait analysis, especially outside of a laboratory setting. A future study will include mTBI patients, and test the validity of the WMAS for evaluating and rehabilitating mTBI.

CHAPTER 8: FUTURE WORK

8.1 Use with mTBI and TBI Subjects

The next phase of this project should involve testing the validity and accuracy of the WMAS with mTBI and TBI subjects. Similar testing to this study could be used, with an addition of treadmill walking. The data from the mTBI and TBI subjects can be compared to the data collected in this study from healthy subjects.

8.2 Robotic Arm

Future work with the robotic arm will also include the development of algorithms to detect gait abnormalities such as those seen in patients with mild traumatic brain injury (mTBI). To complement human subject testing with gait pathology, controlled introduction of gait deviations into this robotic testing framework will allow for well-characterized unit testing, providing more robust algorithm development.

8.3 Testing Outside of Laboratory

Future studies will involve collecting data continuously on board the sensors outside of a laboratory setting. After the data collection, there would be a large amount of data to process, and would test the ability to extract only the relevant parameters.

8.4 CAREN

The CAREN or Computer Assisted Rehabilitation Environment and WMAS system could be used together for return to duty testing for subjects with mTBI or PTSD. The testing could begin in the gait laboratory with the WMAS and Vicon motion capture system for analysis of level walking, stairs and gravel. The testing framework could also include noises and visual distractions during the gait trials. The next phase would involve testing on the CAREN for several weeks with visual distractions, varying terrain and noises. The final phase would involve retesting in the gait laboratory to determine if the rehabilitation training improved the gait and could result in return to duty. A benefit of using the WMAS and the CAREN would be the ability to control the environment and the movement of the platform. The CAREN could provide perturbations and obstacles, as well as distractions that cannot be provided during gait analysis on a flat walkway in a laboratory setting. Someone may walk well when the only focus is walking, but when other factors are introduced gait deviations may occur. This would allow the WMAS to be tested with closer to real life situations than the traditional gait lane testing, but still in a controlled and known environment.

8.5 Sports Concussion

The WMAS has the potential to identify the growing number of concussion and mTBIs that occur during sports such as football, hockey and baseball. As mentioned previously, the current on field diagnostic tools for concussions are subjective. There is a major need for an objective, portable method to determine whether a player can return to play or has suffered a concussion on the field. Baseline gait measurements with the WMAS could be collected prior to the start of the season for each player, and used to compare to the gait measurements after a potential concussion. Treadmill walking should be tested, in addition to the regular gait trials

because if there is a correlation between slow speed and concussion players may be able to outsmart the system by walking slower. If a treadmill was used, the speed would be controlled, and the gait deviations would be evident and not dependent on gait speed.

REFERENCES

[1] Bergmann, J. H., and McGregor, A. H., 2011, "Body-worn sensor design: what do patients and clinicians want?," Ann Biomed Eng, 39(9), pp. 2299-2312.

[2] APDM, 2010, "Opal Technical Specifications," http://apdm.com/products/movement-monitors/opal/.

[3] Simoes, M. A., 2011, "Feasibility of Wearable Sensors to Determine Gait Parameters," Master of Science, University of South Florida, Graduate School Theses and Dissertations.

[4] 2010, "Plug-In Gait Product Guide Foundation Notes (Rev. 2.0)," http://www.vicon.com/support/downloads/cef70cc8dbcc7149988652bf7dff8ff84cc6bc77302948.73654482/Plugin_Nexus_PluginGait_ProductGuide_Foundation_Rev2.0_2010April.pdf.

[5] Perry, J., and Burnfield, J. M., 2010, Gait Analysis: Normal and Pathological Function, SLACK Incorporated, Thorofare, NJ.

[6] Esquenazi, A., 2004, "Evaluation and management of spastic gait in patients with traumatic brain injury," J Head Trauma Rehabil, 19(2), pp. 109-118.

[7] Williams, G., Galna, B., Morris, M. E., and Oliver, J., 2010, "Spatiotemporal Deficits and Kinematic Classification of Gait Following a Traumatic Brain Injury: A Systematic Review," The Journal of Head Trauma Rehabilitation, 25(5), pp. 366-374.

[8] Faul, M., Xu, L., Wald, M., and Coronado, V., 2010, "Traumatic Brain Injury in the United States: emergency department visits, hospitalizations, and deaths," Center for Disease Control and Prevention, National Center for Injury Prevention, Atlanta, GA.

[9] Basford, J. R., Chou, L. S., Kaufman, K. R., Brey, R. H., Walker, A., Malec, J. F., Moessner, A. M., and Brown, A. W., 2003, "An assessment of gait and balance deficits after traumatic brain injury," Arch Phys Med Rehabil, 84(3), pp. 343-349.

[10] Stevens, B. L., and Lewis, F. L., 2003, Aircraft Control and Simulation, Wiley.

[11] Dziemianowicz, M., Kirschen, M., Pukenas, B., Laudano, E., Balcer, L., and Galetta, S., 2012, "Sports-Related Concussion Testing," Current Neurology and Neuroscience Reports, 12(5), pp. 547-559.

[12] Center, D. a. V. B. I., 2013, "DoD Worldwide Numbers for TBI," http://www.dvbic.org/dod-worldwide-numbers-tbi.

[13] 2012, "The National Football League Commits $30 Million Donation to the Foundation for the National Institutes of Health to Support Medical Research."

[14] 2012, "VA, DOD to Fund $100 Million PTSD and TBI Study," Department of Veterans Affairs Washington, DC.

[15] Lopez, C. T., "Army, NFL report to Congress on brain-injury initiatives," http://www.army.mil/article/87297.

[16] Williams, G., Morris, M. E., Schache, A., and McCrory, P. R., 2009, "Incidence of Gait Abnormailities After Traumatic Brain Injury," Archives of Physical Medicine and Rehabilitation, 90, pp. 587-593.

[17] Chou, L. S., Kaufman, K. R., Walker-Rabatin, A. E., Brey, R. H., and Basford, J. R., 2004, "Dynamic instability during obstacle crossing following traumatic brain injury," Gait Posture, 20(3), pp. 245-254.

[18] McFadyen, B. J., Swaine, B., Dumas, D., and Durand, A., 2003, "Residual Effects of a Traumatic Brain Injury on Locomotor Capacity: A First Study of Spatiotemporal Patterns During Unobstructed and Obstructed Walking," The Journal of Head Trauma Rehabilitation, 18(6), pp. 512-525.

[19] Ochi, F., Esquenazi, A., Hirai, B., and Talaty, M., 1999, "Temporal-spatial feature of gait after traumatic brain injury," J Head Trauma Rehabil, 14(2), pp. 105-115.

[20] Scherer, M. R., and Schubert, M. C., 2009, "Traumatic brain injury and vestibular pathology as a comorbidity after blast exposure," Phys Ther, 89(9), pp. 980-992.

[21] Williams, G., Morris, M. E., Schache, A., and McCrory, P. R., 2010, "People Preferentially Increase Hip Joint Power Generation to Walk Faster Following Traumatic Brain Injury," Neurorehabilitation and Neural Repair, 24(6), pp. 550-558.

[22] Kaufman, K. R., Brey, R. H., Chou, L.-S., Rabatin, A., Brown, A. W., and Basford, J. R., 2006, "Comparison of subjective and objective measurements of balance disorders following traumatic brain injury," Medical Engineering & Physics, 28(3), pp. 234-239.

[23] Paul F. Pasquina, M. D., Cooper, R. A., United States. Dept. of the Army. Office of the Surgeon, G., and Borden, I., 2009, Care of the combat amputee, Office of the Surgeon General, United States Army.

[24] Horn, L. J., and Zasler, N. D., 1996, Medical rehabilitation of traumatic brain injury, Hanley & Belfus.

[25] Hutin, E., Pradon, D., Barbier, F., Gracies, J.-M., Bussel, B., and Roche, N., 2011, "Lower limb coordination patterns in hemiparetic gait: Factors of knee flexion impairment," Clinical Biomechanics, 26(3), pp. 304-311.

[26] Kerrigan, D. C., Bang, M. S., and Burke, D. T., 1999, "An algorithm to assess stiff-legged gait in traumatic brain injury," J Head Trauma Rehabil, 14(2), pp. 136-145.

[27] Williams, G. P., and Schache, A. G., 2010, "Evaluation of a Conceptual Framework for Retraining High-Level Mobility Following Traumatic Brain Injury: Two Case Reports," The Journal of Head Trauma Rehabilitation, 25(3), pp. 164-172 110.1097/HTR.1090b1013e3181dc1120b.

[28] Hsu, J. D., Michael, J. W., Fisk, J. R., and Surgeons, A. A. o. O., 2008, AAOS atlas of orthoses and assistive devices, C V MOSBY Company.

[29] Fausti, S. A., Wilmington, D. J., Gallun, F. J., Myers, P. J., and Henry, J. A., 2009, "Auditory and vestibular dysfunction associated with blast-related traumatic brain injury," J Rehabil Res Dev, 46(6), pp. 797-810.

[30] Sosnoff, J., Broglio, S., and Ferrara, M., 2008, "Cognitive and motor function are associated following mild traumatic brain injury," Experimental Brain Research, 187(4), pp. 563-571.

[31] Bland, D. C., Zampieri, C., and Damiano, D. L., 2011, "Effectiveness of physical therapy for improving gait and balance in individuals with traumatic brain injury: a systematic review," Brain Inj, 25(7-8), pp. 664-679.

[32] Gottshall, K. R., Sessoms, P. H., and Bartlett, J. L., 2012, "Vestibular physical therapy intervention: utilizing a computer assisted rehabilitation environment in lieu of traditional physical therapy," Engineering in Medicine and Biology Society (EMBC), 2012 Annual International Conference of the IEEE, pp. 6141-6144.

[33] Clark, R. A., Williams, G., Fini, N., Moore, L., and Bryant, A. L., 2012, "Coordination of Dynamic Balance During Gait Training in People With Acquired Brain Injury," Archives of Physical Medicine and Rehabilitation, 93(4), pp. 636-640.

[34] Whitney, S. L., Marchetti, G. F., Pritcher, M., and Furman, J. M., 2009, "Gaze stabilization and gait performance in vestibular dysfunction," Gait Posture, 29(2), pp. 194-198.

[35] Carey, S., Hufford, K., Martori, A., Simoes, M., Sinatra, F., and Dubey, R., "Development of a Wearable Motion Analysis System for Evaluation and Rehabilitation of Mild Traumatic Brain Injury (mTBI)," Proc. ASME Summer Bioengineering Conference.

[36] Moseley, A. M., Lanzarone, S., Bosman, J. M., van Loo, M. A., de Bie, R. A., Hassett, L., and Caplan, B., 2004, "Ecological validity of walking speed assessment after traumatic brain injury: a pilot study," J Head Trauma Rehabil, 19(4), pp. 341-348.

[37] Greene, B. R., Foran, T. G., McGrath, D., Doheny, E. P., Burns, A., and Caulfield, B., 2012, "A Comparison of Algorithms for Body-Worn Sensor-Based Spatiotemporal Gait Parameters to the GAITRite Electronic Walkway," J Appl Biomech, 28(3), pp. 349-355.

[38] Aminian, K., Najafi, B., Bula, C., Leyvraz, P. F., and Robert, P., 2002, "Spatio-temporal parameters of gait measured by an ambulatory system using miniature gyroscopes," J Biomech, 35(5), pp. 689-699.

[39] Salarian, A., Russmann, H., Vingerhoets, F. J., Dehollain, C., Blanc, Y., Burkhard, P. R., and Aminian, K., 2004, "Gait assessment in Parkinson's disease: toward an ambulatory system for long-term monitoring," IEEE Trans Biomed Eng, 51(8), pp. 1434-1443.

[40] Bonato, P., 2009, "Clinical applications of wearable technology," Engineering in Medicine and Biology Society, 2009. EMBC 2009. Annual International Conference of the IEEE, pp. 6580-6583.

[41] Zeng, H., and Zhao, Y., 2011, "Sensing Movement: Microsensors for Body Motion Measurement," Sensors, 11(1), pp. 638-660.

[42] Madgwick, S. O. H., Harrison, A. J. L., and Vaidyanathan, R., 2011, "Estimation of IMU and MARG orientation using a gradient descent algorithm," Rehabilitation Robotics (ICORR), 2011 IEEE International Conference on, pp. 1-7.

[43] Guo, Y., Wu, D., Liu, G., Zhao, G., Huang, B., and Wang, L., 2012, "A Low-Cost Body Inertial-Sensing Network for Practical Gait Discrimination of Hemiplegia Patients," Telemed J E Health.

[44] Toffola, L. D., Patel, S., Ozsecen, M. Y., Ramachandran, R., and Bonato, P., 2012, "A wearable system for long-term monitoring of knee kinematics," Biomedical and Health Informatics (BHI), 2012 IEEE-EMBS International Conference on, pp. 188-191.

[45] Schiefer, C., Kraus, T., Ochsmann, E., Hermanns, I., Ellegast, R., and Duffy, V., 2011, "3D Human Motion Capturing Based Only on Acceleration and Angular Rate Measurement for Low Extremities Digital Human Modeling," Springer Berlin / Heidelberg, pp. 195-203.

[46] Watanabe, T., Saito, H., Koike, E., and Nitta, K., 2011, "A preliminary test of measurement of joint angles and stride length with wireless inertial sensors for wearable gait evaluation system," Comput Intell Neurosci, 2011, p. 975193.

[47] Cloete, T., and Scheffer, C., 2008, "Benchmarking of a full-body inertial motion capture system for clinical gait analysis," Engineering in Medicine and Biology Society, 2008. EMBS 2008. 30th Annual International Conference of the IEEE, pp. 4579-4582.

[48] Pochappan, S. S., Arvind, D. K., Walsh, J., Richardson, A. M., and Herman, J., 2012, "Mobile Clinical Gait Analysis Using Orient Specks," Wearable and Implantable Body Sensor Networks (BSN), 2012 Ninth International Conference on, pp. 172-177.

[49] Chen, S., Brantley, J. S., Kim, T., and Lach, J., "Characterizing and minimizing synchronization and calibration errors in inertial body sensor networks," Proc. Proceedings of the Fifth International Conference on Body Area Networks, ACM, pp. 138-144.

[50] Kun, L., Tao, L., Shibata, K., and Inoue, Y., 2009, "Ambulatory measurement and analysis of the lower limb 3D posture using wearable sensor system," Mechatronics and Automation, 2009. ICMA 2009. International Conference on, pp. 3065-3069.

[51] Kun, L., Yoshio, I., and Kyoko, S., 2010, "Visual and quantitative analysis of lower limb 3D gait posture using accelerometers and magnetometers," Mechatronics and Automation (ICMA), 2010 International Conference on, pp. 1420-1425.

[52] Favre, J., Jolles, B. M., Aissaoui, R., and Aminian, K., 2008, "Ambulatory measurement of 3D knee joint angle," J Biomech, 41(5), pp. 1029-1035.

[53] Favre, J., Jolles, B. M., Siegrist, O., and Aminian, K., 2006, "Quaternion-based fusion of gyroscopes and accelerometers to improve 3D angle measurement," Electronics Letters, 42(11), pp. 612-614.

[54] Favre, J., Aissaoui, R., Jolles, B. M., Siegrist, O., de Guise, J. A., and Aminian, K., 2006, "3D joint rotation measurement using MEMs inertial sensors: Application to the knee joint," Ninth International Symposium on the 3D Analysis of Human Movement, International Society of Biomechanics (ISB) Technical Group on the 3-D Analysis of Human Movement, France.

[55] Favre, J., Aissaoui, R., Jolles, B. M., de Guise, J. A., and Aminian, K., 2009, "Functional calibration procedure for 3D knee joint angle description using inertial sensors," Journal of Biomechanics, 42(14), pp. 2330-2335.

[56] Dejnabadi, H., Jolles, B. M., and Aminian, K., 2005, "A new approach to accurate measurement of uniaxial joint angles based on a combination of accelerometers and gyroscopes," Biomedical Engineering, IEEE Transactions on, 52(8), pp. 1478-1484.

[57] Bergmann, J. H., Mayagoitia, R. E., and Smith, I. C., 2009, "A portable system for collecting anatomical joint angles during stair ascent: a comparison with an optical tracking device," Dyn Med, 8, p. 3.

[58] Schulze, M., Liu, T.-H., Xie, J., Zhang, W., Wolf, K.-H., Calliess, T., Windhagen, H., and Marschollek, M., 2012, "Unobtrusive ambulatory estimation of knee joint angles during walking using gyroscope and accelerometer data - a preliminary evaluation study," Biomedical and Health Informatics (BHI), 2012 IEEE-EMBS International Conference on, pp. 559-562.

[59] Cooper, G., Sheret, I., McMillian, L., Siliverdis, K., Sha, N., Hodgins, D., Kenney, L., and Howard, D., 2009, "Inertial sensor-based knee flexion/extension angle estimation," Journal of Biomechanics, 42(16), pp. 2678-2685.

[60] Takeda, R., Tadano, S., Todoh, M., Morikawa, M., Nakayasu, M., and Yoshinari, S., 2009, "Gait analysis using gravitational acceleration measured by wearable sensors," J Biomech, 42(3), pp. 223-233.

[61] Saito, H., Watanabe, T., Arifin, A., Dössel, O., and Schlegel, W. C., 2009, "Ankle and Knee Joint Angle Measurements during Gait with Wearable Sensor System for RehabilitationWorld Congress on Medical Physics and Biomedical Engineering, September 7 - 12, 2009, Munich, Germany," R. Magjarevic, ed., Springer Berlin Heidelberg, pp. 506-509.

[62] Miyazaki, S., 1997, "Long-Term Unrestrained Measurement of Stride Length and Walking Velocity Utilizing a Piezoelectric Gyroscope," IEEE Transactions on Biomedical Engineering, 44(8), pp. 753-759.

[63] Doheny, E. P., Foran, T. G., and Greene, B. R., 2010, "A single gyroscope method for spatial gait analysis," Engineering in Medicine and Biology Society (EMBC), 2010 Annual International Conference of the IEEE, pp. 1300-1303.

[64] Shanshan, C., Cunningham, C. L., Lach, J., and Bennett, B. C., 2011, "Extracting Spatio-Temporal Information from Inertial Body Sensor Networks for Gait Speed Estimation," Body Sensor Networks (BSN), 2011 International Conference on, pp. 71-76.

[65] Zexi, L., and Won, C.-H., 2010, "Knee and waist attached gyroscopes for personal navigation: Comparison of knee, waist and foot attached inertial sensors," Position Location and Navigation Symposium (PLANS), 2010 IEEE/ION, pp. 375-381.

[66] Salarian, A., Horak, F. B., Zampieri, C., Carlson-Kuhta, P., Nutt, J. G., and Aminian, K., 2010, "iTUG, a sensitive and reliable measure of mobility," IEEE Trans Neural Syst Rehabil Eng, 18(3), pp. 303-310.

[67] Schrock, P., Farelo, F., Alqasemi, R., and Dubey, R., 2009, "Design, simulation and testing of a new modular wheelchair mounted robotic arm to perform activities of daily living," Rehabilitation Robotics, 2009. ICORR 2009. IEEE International Conference on, pp. 518-523.

[68] Almeida, E. C. V. d., 2012, "Development of a wearable sensor system for real-time control of knee prostheses," Linköping.

[69] Isenberg, D. R., 2009, "Quaternion and Euler-angle based approaches to the dynamical modeling, position control, and tracking control of a space robot," Ph.D, The University of North Carolina at Charlotte.

[70] Tincknell, M., 2013, "Matlab quaternion class."

[71] Diebel, J., 2006, "Representing Attitude: Euler Angles, Unit Quaternions, and Rotation Vectors."

[72] Billauer, E., 2012, "peakdet: Peak detection using MATLAB," http://www.billauer.co.il/peakdet.html.

[73] Stewart, J., Redlin, L., and Watson, S., 2011, Trigonometry, 2nd ed, Brooks Cole Publishing Company.

[74] C-Motion, 2013, "Tutorial: Building a Conventional Gait Model," http://www.c-motion.com/v3dwiki/index.php?title=Tutorial:_Building_a_Conventional_Gait_Model.

[75] C-Motion, 2013, "V3D Wiki: Joint Angle," http://www.c-motion.com/v3dwiki/index.php?title=Joint_Angle.

[76] C-Motion, 2012, "V3D Wiki: Events Example 6," http://www.c-motion.com/v3dwiki/index.php?title=Events:Example_6.

[77] C-Motion, 2012, "V3D Wiki: Metric Vector Between Events," http://www.c-motion.com/v3dwiki/index.php?title=Metric_Vector_Between_Events.

[78] Randolph, K. A., and Myers, L. L., 2013, Basic Statistics in Multivariate Analysis, Oxford University Press, USA.

[79] Mould, R. F., 2010, Introductory Medical Statistics, 3rd edition, Taylor & Francis.

[80] Bland, J. M., and Altman, D. G., 1999, "Measuring agreement in method comparison studies," Statistical Methods in Medical Research, 8(2), pp. 135-160.

[81] Bland, J. M., and Altman, D. G., 2007, "Agreement Between Methods of Measurement with Multiple Observations Per Individual," Journal of Biopharmaceutical Statistics, 17(4), pp. 571-582.

[82] 2013, "APDM Movement Monitors," http://apdm.com/Wearable-Sensors/inertial-sensors.

[83] Dejnabadi, H., Jolles, B. M., Casanova, E., Fua, P., and Aminian, K., 2006, "Estimation and visualization of sagittal kinematics of lower limbs orientation using body-fixed sensors," Biomedical Engineering, IEEE Transactions on, 53(7), pp. 1385-1393.

APPENDICES

Appendix A: WMAS Data Collection Checklist

WMAS Data Collection Checklist

Subject ID: _____ **Name:** _____ **Date:** _____

- ❑ **Subject sign informed consent**
- ❑ **Measure and record subject measurements for plug-in gait (see attached measurement sheet)**
- ❑ **Attach Opal Sensors before Vicon markers**
  - ❑ Attach sternum harness with sensor #165
  - ❑ Attach waist sensor #160 on lower back
  - ❑ Right thigh sensor #163
  - ❑ Left thigh sensor #162
  - ❑ Right shank sensor #164
  - ❑ Left shank sensor #161
- ❑ **Attach marker set for plug in gait**

Torso	Pelvis	Right Arm	Left Arm	Left Leg	Right Leg
❑ C7	❑ LASI	❑ RSHO	❑ LSHO	❑ LKNE	❑ RKNE
❑ T10	❑ RASI	❑ RUPA	❑ LUPA	❑ LTHI	❑ RTHI
❑ CLAV	❑ LPSI	❑ RFRA	❑ LFRA	❑ LANK	❑ RANK
❑ STRN	❑ RPSI	❑ RELB	❑ LELB	❑ LTIB	❑ RTIB
❑ RBAK		❑ RWRA	❑ LWRA	❑ LTOE	❑ RTOE
		❑ RWRB	❑ LWRB	❑ LHEE	❑ RHEE
		❑ RFIN	❑ LFIN		

- ❑ **Calibrate Cameras and Force Plates**
- ❑ **Static Trial**

Trials:

Subject will sit in a chair then asked to walk to the end of the walkway turn around, walk back and sit back down in the chair. The trials will be done at normal speed, very slow speed and fast speed.

❑ Normal Speed	❑ Very Slow Speed	❑ Fast Speed
❑ 1	❑ 1	❑ 1
❑ 2	❑ 2	❑ 2
❑ 3	❑ 3	❑ 3
❑ 4	❑ 4	❑ 4
❑ 5	❑ 5	❑ 5

Appendix B: Instructions for WMAS Data Collection

B.1 APDM Instructions

1. Plug access point USB into laptop
2. Plug docking station into outlet using power adapter
3. Connect USB cord into docking station and plug into laptop
4. Go to Programs and open Motion Studio
5. Plug Opal sensors into docking station. The light on each sensor should turn blue
6. Under "Working Directory" specify which folder data will go into
7. Press New at top of Motion Studio
8. It will say “plug in all hardware that you wish to configure” Click Ok
9. It will check the firmware and calibration
10. Choose the “Systems tab”:
    a. Under “Attached hardware” it should show: 1 access point, 6 docking stations and 6 monitors
    b. Under “Recording configuration” it should be Robust Synchronized Streaming, wireless channel 90 and sample rate 128.
11. Choose the “Monitors” tab:

a. Make sure the sensors that you connected are shown in the “Select Monitor” drop down menu

b. Make sure the boxes next to Enable Accelerometer, Enable Gyroscope and Enable Magnetometer are all checked

c. Accelerometer range should be 6g

d. Select Do Nothing for Spin Mode

Appendix B (Continued)

12. Click Configure, it will configure for the channel selected
13. Once its finished it will say Configuration Complete. Click Ok
14. Undock the sensors from the docking station.
15. Put the sensors on the subject (prior to placing the markers on the subject). Make sure the sensor number (located on the back of the sensor case) corresponds accordingly to where the sensors are placed on the subject as specified previously in the "Monitors" tab
16. Attach the sensors with the USB port facing toward the ground
17. Adjust the straps so that they are snug but not uncomfortable on the subject
18. Click the Stream button at the top of the toolbar
19. A window will show up with the strip charts on the right and a list of menu options down the left side.

B.2 Vicon Set Up

1. Place the Plug-in-Gait marker set on the subject
2. Open Workstation on the computer
3. Calibrate the cameras and force plates
4. Create a folder for your data
5. Press the turquoise "New Trial" icon
6. Under Trial Types check mark the Static Trial option
7. Capture a static trial
8. Make sure marker set is Plug in Gait
9. Label the markers and apply autolabel

Appendix B (Continued)

B.3 APDM Sensors Data Collection Steps

1. Click “Stream
    a. Under "Record Duration" choose Indeterminate
    b. Under "Save Options" choose CSV for the file format and the file name should follow the following format: subjectid_typeoftrial_trialnumber
    c. Press Record
    d. Under "Real Time Data Plot" different plot types of each sensor can be picked
    e. Press Stop
    f. Repeat 5 times for each of the 3 trial types
    g. Click Exit
2. Take the sensors off of the subject
3. Dock the Sensors in the docking station
4. Click "Power Off"
5. Undock the Sensors

B.4 Vicon Data Collection Steps

1. Press the turquoise New Trial icon
2. Make sure the Static Trial box is unchecked
3. Capture a trial by pressing Start and Stop

Appendix C: Visual 3D Pipeline

C.1 Joint Angle Calculations

Calculate Right Knee Angle [75]:
Compute_Model_Based_Data
/RESULT_NAME=Right Knee Angle
/FUNCTION=JOINT_ANGLE
/SEGMENT=RSK
/REFERENCE_SEGMENT=RTH
/RESOLUTION_COORDINATE_SYSTEM=
! /USE_CARDAN_SEQUENCE=FALSE
! /NORMALIZATION=FALSE
! /NORMALIZATION_METHOD=
! /NORMALIZATION_METRIC=
/NEGATEX=TRUE
/NEGATEY=TRUE
/NEGATEZ=TRUE
! /AXIS1=X
! /AXIS2=Y
! /AXIS3=Z;

Calculate Left Knee Angle [75]:
Compute_Model_Based_Data
/RESULT_NAME=Left Knee Angle
/FUNCTION=JOINT_ANGLE
/SEGMENT=LSK
/REFERENCE_SEGMENT=LTH
/RESOLUTION_COORDINATE_SYSTEM=
! /USE_CARDAN_SEQUENCE=FALSE
! /NORMALIZATION=FALSE
! /NORMALIZATION_METHOD=
! /NORMALIZATION_METRIC=
/NEGATEX=TRUE
/NEGATEY=TRUE
/NEGATEZ=TRUE
! /AXIS1=X
! /AXIS2=Y
! /AXIS3=Z;

Appendix C (Continued)

C.2 Stride Length Calculations

Calculate the Position of the Right Heel with Respect to the Pelvis [76]:

```
Compute_Model_Based_Data
/RESULT_NAME=RHEEL_WRT_PELVIS
/FUNCTION=TARGET_PATH
/SEGMENT=RHEE
/REFERENCE_SEGMENT=RPV
/RESOLUTION_COORDINATE_SYSTEM=RPV
! /USE_CARDAN_SEQUENCE=FALSE
! /NORMALIZATION=FALSE
! /NORMALIZATION_METHOD=
! /NORMALIZATION_METRIC=
! /NEGATEX=FALSE
! /NEGATEY=FALSE
! /NEGATEZ=FALSE
! /AXIS1=X
! /AXIS2=Y
! /AXIS3=Z;
```

Calculate the Position of the Left Heel with Respect to the Pelvis [76]:

```
Compute_Model_Based_Data
/RESULT_NAME=LHEEL_WRT_PELVIS
/FUNCTION=TARGET_PATH
/SEGMENT=LHEE
/REFERENCE_SEGMENT=RPV
/RESOLUTION_COORDINATE_SYSTEM=RPV
! /USE_CARDAN_SEQUENCE=FALSE
! /NORMALIZATION=FALSE
! /NORMALIZATION_METHOD=
! /NORMALIZATION_METRIC=
! /NEGATEX=FALSE
! /NEGATEY=FALSE
! /NEGATEZ=FALSE
! /AXIS1=X
! /AXIS2=Y
! /AXIS3=Z;
```

Appendix C (Continued)

Calculate the Position of the Right Toe with Respect to the Pelvis [76]:
Compute_Model_Based_Data
/RESULT_NAME=RTOE_WRT_PELVIS
/FUNCTION=TARGET_PATH
/SEGMENT=RTOE
/REFERENCE_SEGMENT=RPV
/RESOLUTION_COORDINATE_SYSTEM=RPV
! /USE_CARDAN_SEQUENCE=FALSE
! /NORMALIZATION=FALSE
! /NORMALIZATION_METHOD=
! /NORMALIZATION_METRIC=
! /NEGATEX=FALSE
! /NEGATEY=FALSE
! /NEGATEZ=FALSE
! /AXIS1=X
! /AXIS2=Y
! /AXIS3=Z;

Calculate the Position of the Left Toe with Respect to the Pelvis [76]:
Compute_Model_Based_Data
/RESULT_NAME=LTOE_WRT_PELVIS
/FUNCTION=TARGET_PATH
/SEGMENT=LTOE
/REFERENCE_SEGMENT=RPV
/RESOLUTION_COORDINATE_SYSTEM=RPV
! /USE_CARDAN_SEQUENCE=FALSE
! /NORMALIZATION=FALSE
! /NORMALIZATION_METHOD=
! /NORMALIZATION_METRIC=
! /NEGATEX=FALSE
! /NEGATEY=FALSE
! /NEGATEZ=FALSE
! /AXIS1=X
! /AXIS2=Y
! /AXIS3=Z;

Appendix C (Continued)

Find the Right Heel Strikes [76]:
Event_Maximum
/SIGNAL_TYPES=LINK_MODEL_BASED
/SIGNAL_NAMES=RHEEL_WRT_PELVIS
! /SIGNAL_FOLDER=ORIGINAL
/EVENT_NAME=RHS
! /SELECT_X=FALSE
/SELECT_Y=TRUE
! /SELECT_Z=FALSE
! /FRAME_WINDOW=8
! /START_AT_EVENT=
! /END_AT_EVENT=
/EVENT_INSTANCE=0;

Find the Left Heel Strikes [76]:
Event_Maximum
/SIGNAL_TYPES=LINK_MODEL_BASED
/SIGNAL_NAMES=LHEEL_WRT_PELVIS
! /SIGNAL_FOLDER=ORIGINAL
/EVENT_NAME=LHS
! /SELECT_X=FALSE
/SELECT_Y=TRUE
! /SELECT_Z=FALSE
! /FRAME_WINDOW=8
! /START_AT_EVENT=
! /END_AT_EVENT=
/EVENT_INSTANCE=0;

Find the Right Toe-offs [76]:
Event_Minimum
/SIGNAL_TYPES=LINK_MODEL_BASED
/SIGNAL_NAMES=RTOE_WRT_PELVIS
! /SIGNAL_FOLDER=ORIGINAL
/EVENT_NAME=RTO
! /SELECT_X=FALSE
/SELECT_Y=TRUE
! /SELECT_Z=FALSE
! /FRAME_WINDOW=8
! /START_AT_EVENT=

Appendix C (Continued)

```
! /END_AT_EVENT=
/EVENT_INSTANCE=0;
```

Find the Left Toe-Offs [76]:

```
Event_Minimum
/SIGNAL_TYPES=LINK_MODEL_BASED
/SIGNAL_NAMES=LTOE_WRT_PELVIS
! /SIGNAL_FOLDER=ORIGINAL
/EVENT_NAME=LTO
! /SELECT_X=FALSE
/SELECT_Y=TRUE
! /SELECT_Z=FALSE
! /FRAME_WINDOW=8
! /START_AT_EVENT=
! /END_AT_EVENT=
/EVENT_INSTANCE=0;
```

Calculate the Right Stride Length [77]:

```
Metric_Vector_Between_Events
/RESULT_METRIC_NAME=RStride
! /RESULT_METRIC_FOLDER=PROCESSED
/GENERATE_VECTOR_LENGTH_METRIC=TRUE
/START_SIGNAL_TYPE=TARGET
/START_SIGNAL_NAME=RHEEL
! /START_SIGNAL_FOLDER=ORIGINAL
/END_SIGNAL_TYPE=TARGET
/END_SIGNAL_NAME=RHEEL
! /END_SIGNAL_FOLDER=ORIGINAL
/EVENT_SEQUENCE=RHS+RTO+RHS
/EXCLUDE_EVENTS=
/GENERATE_MEAN_AND_STDDEV=FALSE
! /APPEND_TO_EXISTING_VALUES=FALSE
! /RETAIN_NO_DATA_VALUES=FALSE;
```

Appendix C (Continued)

Calculate the Left Stride Length [77]:

```
Metric_Vector_Between_Events
/RESULT_METRIC_NAME=LStride
! /RESULT_METRIC_FOLDER=PROCESSED
/GENERATE_VECTOR_LENGTH_METRIC=TRUE
/START_SIGNAL_TYPE=TARGET
/START_SIGNAL_NAME=LHEEL
! /START_SIGNAL_FOLDER=ORIGINAL
/END_SIGNAL_TYPE=TARGET
/END_SIGNAL_NAME=LHEEL
! /END_SIGNAL_FOLDER=ORIGINAL
/EVENT_SEQUENCE=LHS+LTO+LHS
/EXCLUDE_EVENTS=
/GENERATE_MEAN_AND_STDDEV=FALSE
! /APPEND_TO_EXISTING_VALUES=FALSE
! /RETAIN_NO_DATA_VALUES=FALSE;
```

Appendix D: IRB Approval

USF
UNIVERSITY OF SOUTH FLORIDA

DIVISION OF RESEARCH INTEGRITY AND COMPLIANCE
Institutional Review Boards, FWA No. 00001669
12901 Bruce B. Downs Blvd., MDC035 • Tampa, FL 33612-4799
(813) 974-9638 • FAX (813) 974-5613

March 30, 2011

Stephanie Carey
Mechanical Engineering
4202 E. Fowler Ave. ENB 118

RE: **Expedited Approval** for Initial Review
IRB#: Pro00003205
Title: Feasibility of Wearable Sensors to Determine Gait Parameters

Dear Dr. Carey:

On 3/29/2011 the Institutional Review Board (IRB) reviewed and **APPROVED** the above referenced protocol. Please note that your approval for this study will expire on 3/29/2012.

Approved Items:
Protocol Document(s):

Feasibility of Wearble Sensors_Study Protocol.docx	1/12/2011 11:37 AM	0.01

Consent/Assent Documents:

Name	Modified	Version
3205 ICF.docx.pdf	3/30/2011 10:18 AM	0.01

It was the determination of the IRB that your study qualified for expedited review which includes activities that (1) present no more than minimal risk to human subjects, and (2) involve only procedures listed in one or more of the categories outlined below. The IRB may review research through the expedited review procedure authorized by 45CFR46.110 and 21 CFR 56.110. The research proposed in this study is categorized under the following expedited review category:

(6) Collection of data from voice, video, digital, or image recordings made for research purposes.

Please note, the informed consent/assent documents are valid during the period indicated by the official, IRB-Approval stamp located on the form. Valid consent must be documented on a copy of the most recently IRB-approved consent form.

As the principal investigator of this study, it is your responsibility to conduct this study in accordance with IRB policies and procedures and as approved by the IRB. Any changes to the approved research must be submitted to the IRB for review and approval by an amendment.

We appreciate your dedication to the ethical conduct of human subject research at the University of South Florida and your continued commitment to human research protections. If you have any questions regarding this matter, please call 813-974-9343.

Sincerely,

[redacted]

Janelle Perkins, PharmD, Chairperson
USF Institutional Review Board